

**Kentucky Geological Survey**  
James C. Cobb, State Geologist and Director  
University of Kentucky, Lexington

**Classification of Paleochannels and  
their Relationship to Synsedimentary  
Faulting within the Lower Elkhorn  
Coal Zone: Pikeville Formation,  
Breathitt Group, Southeastern  
Kentucky**

**Michael Garry Shultz**

© 2004  
University of Kentucky  
For further information contact:  
Manager, Communications and Technology Transfer  
Kentucky Geological Survey  
228 Mining and Mineral Resources Building  
University of Kentucky  
Lexington, KY 40506-0107

ISSN 0075-5621

**Technical Level**



## **Our Mission**

Our mission is to increase knowledge and understanding of the mineral, energy, and water resources, geologic hazards, and geology of Kentucky for the benefit of the Commonwealth and Nation.

***Earth Resources—Our Common Wealth***

**[www.uky.edu/kgs](http://www.uky.edu/kgs)**



## ABSTRACT OF THESIS

### CLASSIFICATION OF PALEOCHANNELS AND THEIR RELATIONSHIP TO SYNSEDIMENTARY FAULTING WITHIN THE LOWER ELKHORN COAL ZONE, PIKEVILLE FORMATION, BREATHITT GROUP, SOUTHEASTERN KENTUCKY

Paleochannels are a major cause of roof failure in underground coal mines in southeastern Kentucky. Models that predict the location and geometry of paleochannels are essential to assist in mine planning and development.

Data from approximately 506 coal exploration drill holes were subjected to second-order trend-surface analysis to identify stacking or offsetting relationships between sandstone bodies in adjacent stratigraphic intervals. The stacking of sandstone bodies within adjacent intervals suggests the presence of synsedimentary faulting. This model suggests that continued movement along the faults created topographic lows, attracted paleodrainages, and accommodated thick accumulations of sandstone in approximately the same areas through time. Trend-surface residuals analysis successfully located areas of potential synsedimentary faulting within the study area.

An additional 7,189 elevation data points for the top of the Newman Limestone, interpreted from oil and gas records, were utilized to locate sub-Pennsylvanian System faults within the study area. The correlation between faults associated with the coal measures identified using second-order trend-surface analysis and faults affecting the Newman Limestone suggests Pennsylvanian synsedimentary faults were preceded by older Paleozoic fault movement. The greater availability of oil and gas subsurface data makes this relationship an important tool for predicting locations of fault-controlled coal measure paleochannels.

**KEYWORDS:** Lower Elkhorn coal, Newman Limestone, paleochannels, synsedimentary faulting, trend-surface analysis.

Michael Garry Shultz  
April 28, 2003

CLASSIFICATION OF PALEOCHANNELS AND THEIR RELATIONSHIP TO  
SYNSEDIMENTARY FAULTING WITHIN THE LOWER ELKHORN COAL ZONE,  
PIKEVILLE FORMATION, BREATHITT GROUP, SOUTHEASTERN KENTUCKY

By

Michael Garry Shultz

Dr. Gerald A. Weisenfluh  
Co-Director of Thesis

Dr. William A. Thomas  
Co-Director of Thesis

Dr. Alan E. Fryar,  
Director of Graduate Studies

April 28, 2003

## RULES FOR THE USE OF THE THESIS

Unpublished theses submitted for the Masters degree and deposited in the University of Kentucky Library are, as a rule, open for inspection, but are to be used only with due regard to the rights of the authors. Bibliographical references may be noted, but quotations or summaries of parts may be published only with the permission of the author, and with the usual scholarly acknowledgements.

Extensive copying or publication of the thesis in whole, or in part, also requires the consent of the Dean of the Graduate School of the University of Kentucky.

THESIS

Michael Garry Shultz

The Graduate School  
University of Kentucky

2003

CLASSIFICATION OF PALEOCHANNELS AND THEIR RELATIONSHIP TO  
SYNSEDIMENTARY FAULTING WITHIN THE LOWER ELKHORN COAL ZONE,  
PIKEVILLE FORMATION, BREATHITT GROUP, SOUTHEASTERN KENTUCKY

---

THESIS

---

A thesis submitted in partial fulfillment of the  
requirements for the degree of Master of Science in the  
College of Arts and Sciences  
at the University of Kentucky

By

Michael Garry Shultz

Co-Directors: Dr. Gerald A. Weisenfluh, Adjunct Professor of Geology  
and Dr. William A. Thomas, Professor of Geology

Lexington, Kentucky

2003

Copyright © Michael Garry Shultz, 2003

## ACKNOWLEDGEMENTS

I would like to thank everyone who has provided encouragement and support to me throughout the years. Thanks to my parents, who understood my love of geology and encouraged me to follow my dreams. Thanks to Mr. Timothy Miller, a good friend, who provided me with enthusiasm and many skills, which have benefited me throughout the course of my studies. Thanks to Dr. Robert Hook, who didn't mind having me tag along on all those fossil collecting trips. You both have taught me a great deal about geology and life in general. A special thanks to Kelly Sanders, who was very patient throughout the writing of the thesis, and has agreed to be my wife. Her love and support helped make all of this possible.

I am appreciative of my committee members, Dr. Jerry Weisenfluh, Dr. William Thomas, and Dr. Steve Greb, who have given me many ideas and suggestions during the course of this study. I am especially appreciative of Jerry for all of the financial support that he has provided for my research assistantship, as well as all of the learning opportunities that he has given me over the past two years.

I would like to thank the Kentucky Geological Survey for the use of their data, computers, and vehicles. Finally, I would like to thank those who contributed to all aspects of data collection. Thanks to Dr. Jerry Weisenfluh, Dr. Steve Greb, Kieran Hosey, Thomas Becker, and Kelly Sanders. Without you, I would have been alone to do all of the work.

## Table of Contents

Acknowledgements.....	iii
List of Tables .....	vi
List of Figures.....	vii
List of Files.....	x
1.0 Introduction.....	1
1.1 Background.....	1
1.2 Objective of Thesis .....	5
2.0 Location and Geologic Setting.....	7
2.1 Location of Study Area.....	7
2.2 Stratigraphy.....	7
3.0 Data and Methods .....	12
3.1 Data.....	12
3.1.1 Data Type.....	12
3.1.2 Data Sources.....	12
3.2 Methods.....	14
3.2.1 Data Collection and Preparation .....	14
3.2.1.1 Drill Hole Analysis .....	14
3.2.1.2 Data Extraction .....	15
3.2.2 Analysis of Sedimentary Trends .....	15
3.2.2.1 Isolith Maps .....	15
3.2.2.2 Cross Sections and Isolith Profiles .....	15
3.2.2.3 Measured Sections and In-Mine Mapping .....	16
3.2.3 Analysis of Mine Maps .....	17
3.2.4 Deep Structure Analysis of the Newman Limestone .....	17
3.2.5 Relationships between Sedimentary Trends and Structure .....	18
3.2.5.1 Trend-Surface Analysis .....	18
3.2.5.2 Trend-Surface Residual Analysis .....	19
3.2.5.3 Special Remarks on the Use of Trend-Surface Analysis.....	19
4.0 Results.....	22
4.1 Characteristics of Channels within the Study Area .....	22
4.1.1 Background .....	22
4.1.2 Channel types.....	25
4.1.2.1 Regional Incised Sandstone Channels .....	25
4.1.2.2 Local Sandstone Scours .....	28

4.1.2.3 Local Heterolithic Channels .....	29
4.1.2.4 Overbank Deposits.....	31
4.1.3 Coal-Seam Structure and Paleochannel-Related Mining Problems.....	34
4.1.4 Channel Classification Summary .....	40
4.2 Characteristics of the Stratigraphic Intervals.....	41
4.2.1 Background .....	41
4.2.2 Sandstone Geometry Types.....	43
4.2.3 Analysis of Isolith Maps .....	45
4.2.3.1 The Lower Elkhorn/Lower Elkhorn Rider Interval .....	45
4.2.3.2 Lower Elkhorn Rider/Upper Elkhorn No. 2 Interval .....	47
4.2.3.3 Upper Elkhorn No. 2 Split Interval.....	49
4.2.3.4 Upper Elkhorn No. 2/Upper Elkhorn No. 3 Interval .....	50
4.2.3.5 Upper Elkhorn No. 3 Coal Zone Interval.....	52
4.2.3.6 Upper Elkhorn No. 3/Upper Elkhorn No. 3 ½ Interval .....	53
4.2.3.7 Upper Elkhorn No. 3 ½ /Amburgy Interval.....	54
4.2.3.8 Amburgy Split Interval .....	55
4.2.4 Analysis of Isolith Profiles.....	55
4.2.5 Summary of Stratigraphic Intervals .....	60
4.3 Quantitative Comparison of Coal Measure Data to Geologic Structure.....	62
4.3.1 Background .....	62
4.3.2 Map Analysis of Total Sandstone Thickness Residuals.....	66
4.3.3 Map Analysis of Coal Structure Residuals .....	68
4.3.4 Regional Coal Seam Structure .....	72
4.3.5 Summary of Residual Analysis.....	72
4.4 Identification of Structural Lineaments within the Newman Limestone.....	75
4.4.1 Background .....	75
4.4.2 Newman Limestone Structural Lineaments.....	78
4.4.3 Summary of Newman Limestone Structure Analysis.....	89
4.5 A Comparison of Predicted Faults and Upper Elkhorn No. 3 and Lower Elkhorn Paleochannels.....	91
5.0 Discussion and Conclusions .....	99
5.1 Objective and Methodology.....	99
5.2 Channel Types .....	100
5.3 Depositional Setting of the Channel Types .....	104
5.4 Improving the Methods of Identifying Synsedimentary Faults .....	106
Appendices.....	107
Appendix 4.1: Mine and Highway Exposure Location Information.....	108
Appendix 4.2: Isolith Maps of the Defined Stratigraphic Intervals.....	116
Appendix 4.3: Cross Sections and Isolith Profiles.....	131
References .....	138
Vita.....	142

## List of Tables

Table 4.1 Summary table of sandstone body characteristics.....	46
--	----

## List of Figures

Figure 1.1: Offsetting model versus the stacking model for sandstone distribution .....	4
Figure 2.1: Regional location map.....	8
Figure 2.2: Generalized stratigraphic section. ....	9
Figure 2.3: Regional cross section for the Eastern Kentucky Coal Field.....	10
Figure 3.1: Study area.....	13
Figure 4.1: Regional distribution of the Lower Elkhorn coal.....	23
Figure 4.2: Local distribution of regional incised channels.....	26
Figure 4.3: Generalized cross section across the four-quadrangle study area showing the stratigraphy of the Lower Elkhorn coal zone and the presence of regional incised channels and local scours.....	27
Figure 4.4: Sketches of the Beefhide mine portal exposure (a) and Myra Highway exposure (b) showing the characteristics of heterolithic channels. ....	30
Figure 4.5: Stratigraphic columns showing heterolithic overbank facies above the Lower Elkhorn coal at two mine portals. ....	32
Figure 4.6a: Relationship between mining problems and synclines for the Lower Elkhorn coal.....	35
Figure 4.6b: Relationship between mining problems and synclines for the Upper Elkhorn No. 3.....	36
Figure 4.7: Generalized diagram of poor panel development.....	38
Figure 4.8: Structural profiles, showing the four types of synclines identified using coal seam structure maps.....	39
Figure 4.9: Generalized diagram showing the eight stratigraphic intervals and their associated sandstone bodies.....	42
Figure 4.10: Continuum of sandstone geometries. ....	44
Figure 4.11: Isolith map of the total sandstone thickness for the Lower Elkhorn to Lower Elkhorn rider stratigraphic interval. ....	48
Figure 4.12: Locations of cross sections and isolith profiles.....	57
Figure 4.13: Total sandstone thickness isolith profile A-A' .....	58

Figure 4.14: Diagram showing the algebraic method of stacking residual grids.....	64
Figure 4.15: Cumulative second-order residual map for total sandstone thickness .....	67
Figure 4.16: Cumulative residual map of total sandstone thickness showing the location of inferred faults. ....	69
Figure 4.17: Cumulative residual map of coal seam structure.....	70
Figure 4.18: Cumulative residual map of coal seam structure showing the location of inferred faults. ....	71
Figure 4.19: Regional structure map of the Lower Elkhorn coal showing the location of geologic structures.....	73
Figure 4.20: Map showing the relationship between inferred faults identified using total sandstone thickness residuals and coal seam structure residuals. ....	74
Figure 4.21: The location map of Newman Limestone data subsets. ....	77
Figure 4.22: Regional structure contour map of the top of the Mississippian Newman Limestone.....	79
Figure 4.23: Hand-picked Newman Limestone lineaments.....	80
Figure 4.24: Continuous grid of dip for the top of the Newman Limestone for the Q-36 data subset. ....	83
Figure 4.25: Continuous grid for the dip of the Newman Limestone for the Q-12 data subset. ....	84
Figure 4.26a: Continuous grid of dip for the Newman Limestone vs. hand-picked structural lineaments.....	86
Figure 4.26b: Newman Limestone lineaments detected using the continuous grid analysis .....	86
Figure 4.27: Magnitude and direction of displacement associated with the Newman Limestone lineaments.....	87
Figure 4.28: Lower Elkhorn coal seam structure overlain onto the continuous grid of the slope for the top of the Newman Limestone. ....	88
Figure 4.29: Comparison of hand-picked Newman Limestone structural lineaments to faults hand-picked using residual analysis. ....	90
Figure 4.30: Comparison of synclines and paleochannel-related mining problems in Lower Elkhorn coal seam to Newman Limestone inferred faults.....	92

Figure 4.31: Comparison of synclines identified in the Upper Elkhorn No. 3 coal seam structure and paleochannel-related mining problems to inferred faults. ....	93
Figure 4.32: Relationship between sandstone-rich and sandstone-poor areas and inferred faults. ....	96
Figure 4.33: Relationship between the Lower Elkhorn coal seam zero coal thickness isolith contour and Newman Limestone lineaments. ....	97
Figure 4.34: Relationship between sandstone-rich and sandstone-poor areas and Newman Limestone lineaments. ....	98

## List of Files

MGShultz\_Thesis.pdf 2.77 MB

## 1.0 Introduction

### 1.1 Background

The depletion of thick, widespread, and relatively uniform coals in eastern Kentucky has led to the mining of thinner coal seams in more complex situations (i.e., poorer roof conditions, increased depth of mining, etc.) (Weisenfluh et. al, 1998). The increased costs of developing thin coals can be partly mitigated by the use of depositional models relating to coal-measure sediments that aid in the prediction of roof conditions, mineability, and coal quality issues.

One of the factors that limit the development of coal seams relates to impurities and splits within coal seams that result from contemporaneous precursor peat deposit. Contemporaneous sediments may result in higher concentrations of siliciclastic grains (ash content) or siliciclastic partings within the coal. Siliciclastic partings within coal seams typically result from the burial of a mire with sediment from overbank flooding and subsequent development of an overlying peat body (Ferm and Staub, 1984; Guion, 1984; McCabe, 1984). These partings thicken and coarsen toward their trunk channel. Mining terminates where the ratio of rock to coal mined becomes excessive, which limits the total area of coal that can be mined.

Channel-related activity subsequent to peat accumulation can also have a significant effect on roof stability (Ferm and Staub, 1984; Guion, 1984; Greb, 1991; Weisenfluh and Ferm, 1991a; Fulton et. al, 1995; Weisenfluh, 1996). Compaction of lateral or underlying mudstones around sandstone creates inclined, slickensides across bedding within the mudstones, making them prone to roof failure (e.g., Greb, 1991). Rotated slump blocks consisting of intercalated sandstone and shale with inclined or

contorted bedding result from the failure of oversteepened bank deposits along channel margins. This process may also be responsible for localized faulting within coal seams (Greb and Weisenfluh, 1996). Within mixed-lithology channel fills, point-bar facies may be deposited. Point-bar deposits in the roof of mines result in inclined beds of interbedded sandstone and shale from 3 to 25° (Miall, 1992) above the coal seam. If either slumps or point bars exist within mine roof strata, separation planes may form along the inclined or distorted bedding surfaces, resulting in roof failure during mining. Channel deposits may also have laterally associated crevasse-splay sandstones that thin away from the main channel sandstones. Crevasse-splay sandstones can form a tapered wedge of intercalated, weakly bonded sandstone and shale above coal seams known as “stackrock” (e.g., Guion, 1984). Coal and rooted claystone (paleosols) deposited above splays can also result in low-strength strata within the mine roof (e.g., Guion, 1984). Abandonment of channels may lead to local channel fills of interbedded sandstone and shale, mudstone, or coal within a channel belt. Such fine-grained channel-fills may contain weak bedding, which could cause roof failure (e.g., Horne et al., 1978). Coal beneath channel-related sandstone may also be considerably thinner or absent.

Because many paleochannels range from tens to thousands of feet wide, standard drill hole distributions of 2000 feet (609 m) or greater may not be sufficiently dense to detect or define them (Weisenfluh and Ferm, 1991b; Fulton et al., 1995). Channel sinuosity further complicates the detection of these deposits within the roof strata using only drill holes or details gathered from mine mapping. Geologic process models based upon the causal mechanisms of modern channel development can be useful for predicting geometry of ancient channels where detailed data are lacking.

Models that explain mechanisms of channel localization focus on the formation of topographic lows, which can attract potential watercourses. Two sedimentary models, the offset model (Ferm and Cavaroc, 1968) and the stacking model (Horne, 1979), have been used to predict the distribution of siliciclastic bodies within stratigraphic intervals of the Appalachian Basin (Figure 1.1). The offset model infers that differential compaction of fine-grained clastic deposits and peat relative to lateral coarse-grained clastic bodies will result in channels above fine-grained (compactable) deposits. Conversely, the stacking model infers that synsedimentary faulting can maintain topographic lows, such that thick, coarse-grained clastic deposits will vertically stack rather than offset as would happen with differential compaction. Though each model may operate independently, the two may also operate concurrently throughout any given stratigraphic section (Weisenfluh and Ferm, 1991b). If the stacking model can be shown to have been active in a certain area, the location of the synsedimentary faults can be used to predict the distribution of paleochannels, because channels would be oriented parallel to the faults. This model is important to mining because if faults can be identified, then the potential for paleochannels and roof control problems or thin coal areas associated with these deposits can be anticipated along similar trends to the fault.

Synsedimentary fault, penecontemporaneous fault, and growth fault are all terms that have been used to describe a fault that affected the distribution of sedimentation during a period of geologic time. Synsedimentary faults generally show a normal sense of movement, having increased displacement with depth, and may or may not be expressed at the ground surface (Hardin and Hardin, 1961). Many theories have been proposed to explain growth fault formation, which consider gravity or sediment loading: (1) gravity



**Figure 1.1:** Generalized diagram showing the offsetting model (Ferm and Cavaroc, 1968) versus the stacking model (Horne, 1979).

sliding of a sediment “blanket” into a basin (Cloos, 1968) and (2) rapid dewatering of clay-rich sediments (Carver, 1968). Still other theories consider deep-seated structure or tectonic deformation such as (1) flexure of sediment packages over deep-seated, positive structures (i.e., shelf breaks) (Hardin and Hardin, 1961), (2) direct movement of deep basement faults (Shelton, 1968), and (3) gravity sliding on the limbs of growing folds (Thomas, 1968).

Synsedimentary faults have been suggested by a number of studies as a controlling mechanism that affected sedimentation during deposition of the Pennsylvanian System within the Appalachian Basin (Horne, 1979; Weisenfluh, 1982; Weisenfluh and Ferm, 1984; Hook and Ferm, 1988; Weisenfluh and Ferm, 1991; Pashin, 1994; Greb et al., 1999a, b; Liu, 1992; Andrews et al., 1996; Cornett, 2002). Furthermore, synsedimentary faults identified by these authors are thought to be related to deep faults below Pennsylvanian strata that may, in some way, be related to basement faults.

Deep faults similar to those believed to be active within the Appalachian Basin have been attributed to (1) flexural extension due to a tectonic load emplaced on continental crust (Houseknecht, 1986; Bradley and Kidd, 1991), or (2) through reactivation of preexisting basement structures (Root and MacWilliams, 1986; Hook and Ferm, 1988). The orientation of these faults may be parallel or perpendicular to the strike of folds and thrusts within the orogenic belt (Thomas, 1968; Bradley and Kidd, 1991).

## 1.2 Objective of Thesis

The objective of this thesis is to develop models that help predict the location of channel-related mining problems ahead of mining, and in areas with limited data

distribution. Premier Elkhorn Mining, a division of TECO Coal Corporation, has encountered the effects of post-peat deposition of fluvial sediments above the Lower Elkhorn coal in Pike and Letcher Counties, southeastern Kentucky. This property represents one of the few remaining reserves of the economically important Lower Elkhorn coal. A deep mine, developed to access this reserve, has encountered roof-control problems related to paleochannels, which have impeded mining. Premier Elkhorn Mining is concerned about the possibility of encountering similar features as mining progresses, and the subsurface data for this coal have not been adequate for predicting the location of paleochannels ahead of mining.

## **2.0 Location and Geologic Setting**

### **2.1 Location of Study Area**

The study area is a four-quadrangle area encompassing approximately 80 square miles (514 sq. km) within the Eastern Kentucky Coal Field (Figure 2.1). The 7.5-minute quadrangles included within that area are Dorton, Wheelwright, Jenkins West, and Jenkins East.

A second, larger study area consisting of the entire Eastern Kentucky Coal Field was chosen in order to analyze deeper regional structures that appear to have influenced the Mississippian Newman Limestone (“Big Lime”; drillers' term). The larger area was chosen to identify regional structures that may have been active in the smaller four-quadrangle study area.

### **2.2 Stratigraphy**

Stratigraphic units within the study area include, in ascending order, the interval from the lower Pikeville Formation through the lower Hyden Formation of the Breathitt Group (Chesnutt, 1992), Pennsylvanian System (Figure 2.2). This stratigraphic section is bounded below by the Betsie Shale Member and above by the Kendrick Shale Member, (Figure 2.3). The total thickness for this interval, from the Lower Elkhorn coal to the base of the Kendrick Shale, is approximately 520 feet (158 m) within the study area.

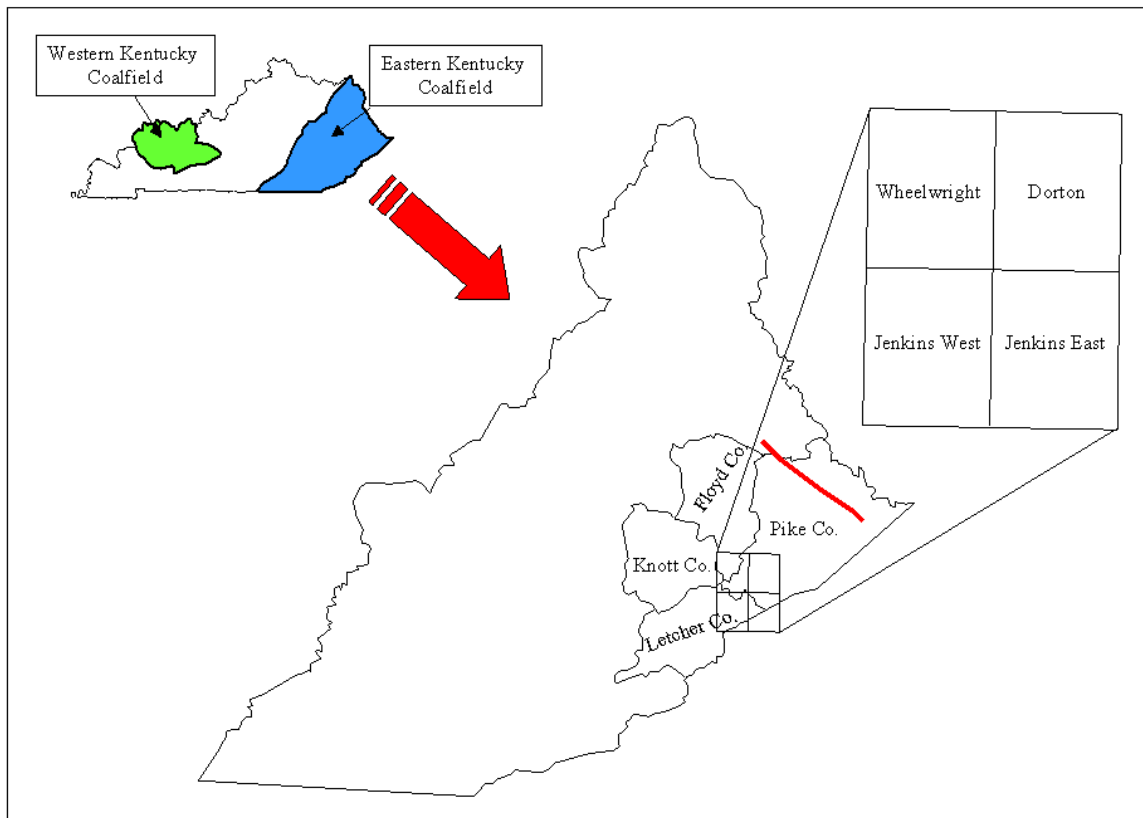


**Figure 2.1:** Map of the Eastern Kentucky Coal Field showing the location of the four-quadrangle study area. The red line marks the location of the cross section in Figure 2.3.

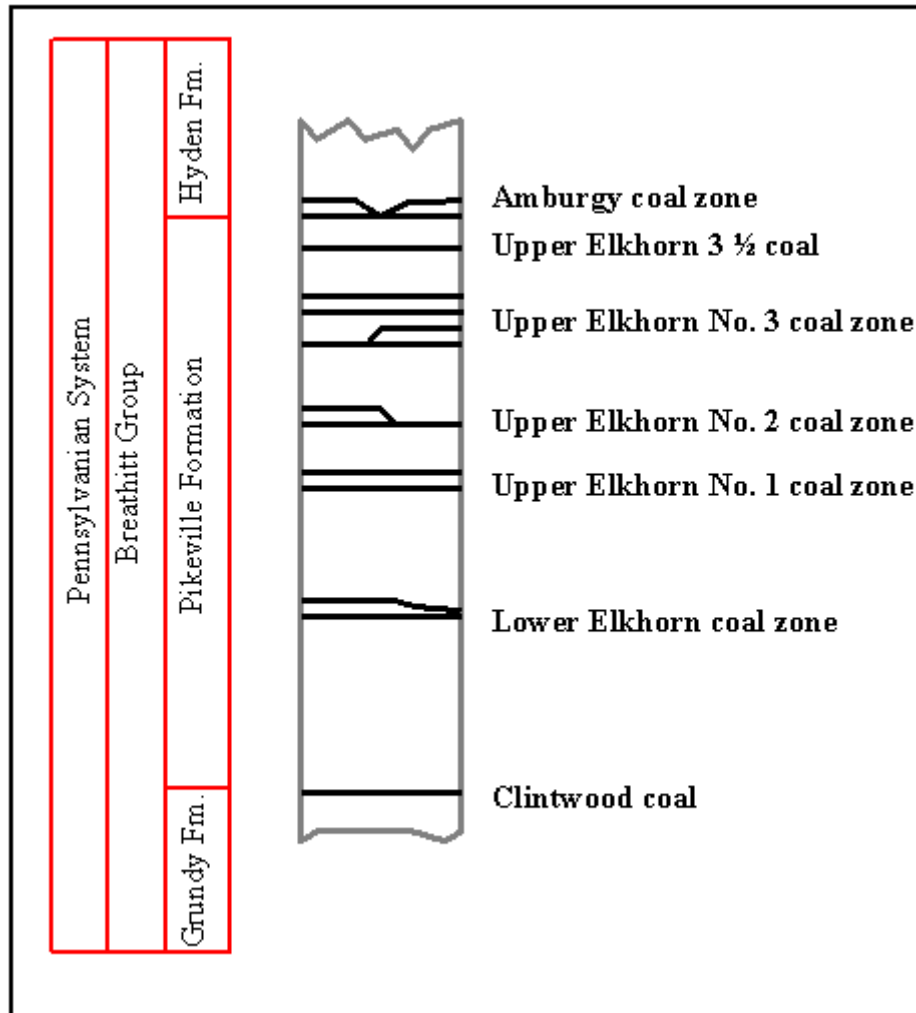


**Figure 2.2:** Generalized stratigraphic section of the study interval.

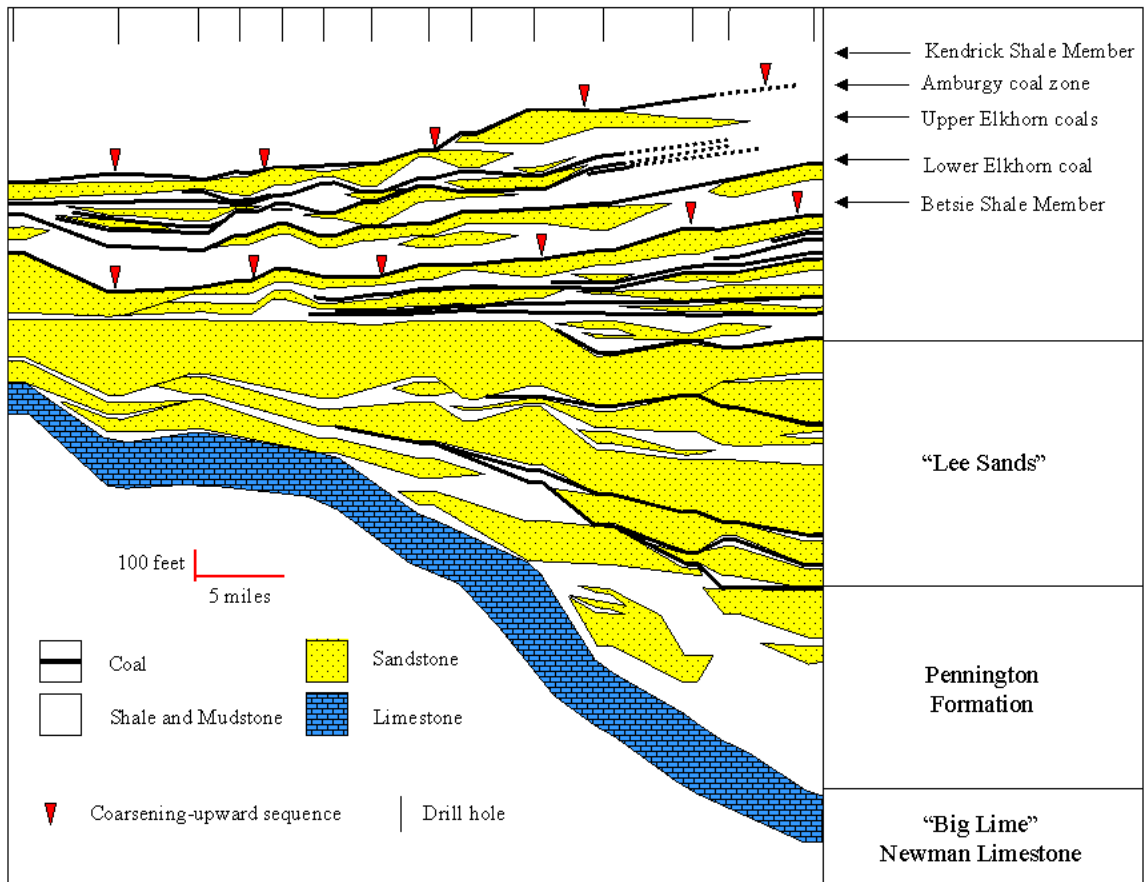


**Figure 2.3:** Regional cross section for the Eastern Kentucky Coal Field, showing the relationship of the study interval to regional stratigraphy of the Mississippian Newman Limestone. The datum for the cross section is the base of the Hagy coal zone.

The major coal beds within the study area are in stratigraphic clusters called coal zones. Rock sequences between coal zones and within coal zones consist of sandstone, shale, and mudstone. The coal zones within this study area, from stratigraphically oldest to youngest, are: Lower Elkhorn, Upper Elkhorn No. 1, Upper Elkhorn No. 2, Upper Elkhorn No. 3, and Amburgy.

## **3.0 Data and Methods**

### 3.1 Data

#### 3.1.1 Data Type

Subsurface data for this study include 7,189 elevation data points, taken from oil and gas wells, for the stratigraphic top of the Mississippian Newman Limestone. In addition to the Newman Limestone data, an additional 524 coal exploration drillholes, eight oil and gas geophysical logs, four measured outcrops, and data from one active Lower Elkhorn mine were utilized for the different parts of this study (Figure 3.1). Information on coal seam structure and mining conditions were obtained from mine maps available for the Lower Elkhorn and Upper Elkhorn No. 3 seams. Finally, roof lithologies associated with the Lower Elkhorn seam were observed and described in one of TECO Coal Company's underground mines.

#### 3.1.2 Data Sources

Data for this thesis were gathered from a variety of sources. The Newman Limestone stratigraphic tops were obtained from the Kentucky Geological Survey's (KGS) oil and gas database. All coal exploration drillholes were obtained from the KGS's drillhole database. To supplement KGS data, TECO Coal Co. and Branham and Baker Coal Co. (AEP) provided additional drillholes. TECO Coal Co. and Branham and Baker Coal Co. also provided mine maps for the Lower Elkhorn seam. Abandoned mine maps for the Upper Elkhorn No. 3 seam were obtained from TECO Coal Co.

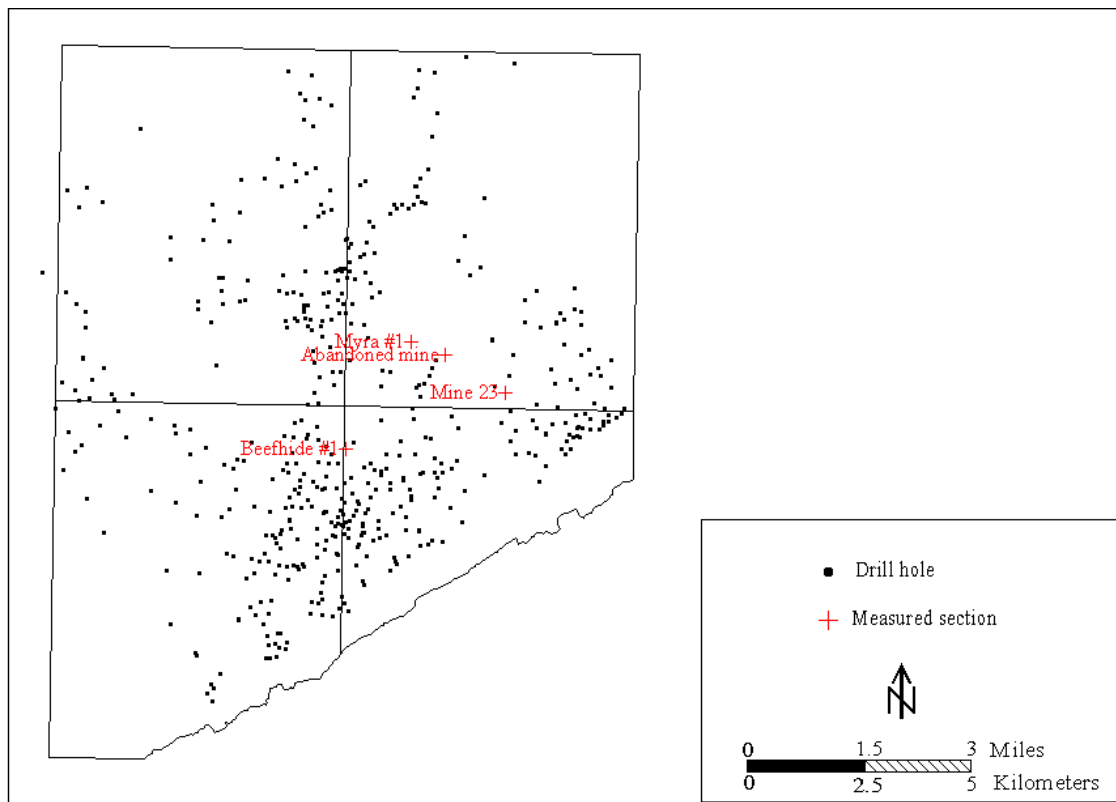


**Figure 3.1:** Map of the four-quadrangle study area showing the distribution of data points.

### 3.1.3 Data Quality

Because of the large size, different sources, and different types of data, the quality of this data set is variable. Geologists picked 3,735 of the stratigraphic tops for the Newman Limestone, while the remaining tops were obtained from drillers' logs. Geologists also described all four measured sections and conducted in-mine mapping. The logging of the coal exploration holes was done by both drillers and geologists. Because these data are drawn from a variety of companies, some of which no longer exist, the exact source of these data cannot be determined. Finally, in-mine mapping and interpretation of active abandoned mine maps for the Lower Elkhorn and Upper Elkhorn No. 3 seams were done by geologists.

## 3.2 Methods

### 3.2.1 Data Collection and Preparation

#### 3.2.1.1 Drillhole Analysis

Approximately 506 of the coal exploration holes were used to show vertical and lateral stratigraphic variation within the four-quadrangle study area. Graphical representations of the drillholes were printed at a vertical scale of 1 inch to 10 feet (3 m), organized into cross sections that traverse the study area, and correlated by aligning the drillholes on a laterally persistent datum. Data between cross sections were utilized to ensure that all bed correlations were consistent among the lines. Correlations were based on coal seam thickness and splitting within coal zones, as well as interburden thickness and lithologic characteristics between coal zones. After correlations were

made, laterally persistent coal seams were tagged and entered into the KGS drillhole database to facilitate data extraction.

#### 3.2.1.2 Data Extraction

Coal seam tags are bounding data used by the computer program CPROCESS (MS-DOS) to define a stratigraphic interval. After the stratigraphic interval is defined, CPROCESS is able to extract information on lithology type and thickness for that interval. Information extracted from drillholes using CPROCESS was imported into ArcView 3.2 or Surfer 8 for analysis and presentation.

### 3.2.2 Analysis of Sedimentary Trends

#### 3.2.2.1 Isolith Maps

Isolith maps were used to show thickness trends of stratigraphic intervals. Stratigraphic intervals, for this study, are intervals bounded by two laterally persistent coal seams or coal horizons. Each pair of coal seams provided an upper and lower stratigraphic boundary necessary for analysis using the computer program CPROCESS. Total sandstone thickness data for eight stratigraphic intervals were extracted and contoured in 10 foot (3 m) intervals.

#### 3.2.2.2 Cross Sections and Isolith Profiles

Cross sections and isolith profiles were created to show lateral and vertical variations in sandstone thickness, sandstone geometry, and coal seam splitting within the four-quadrangle study area. Traditional cross sections were digitally generated at a

vertical scale of 1 inch to 30 feet (9 m) in order to show the lithologic characteristics of the defined intervals. To define sandstone geometry and test stacking versus offsetting relationships between intervals, isolith profiles were made by drawing a line of section on an isolith map, and recording sandstone thickness where isolith contours intersected the line of section. A graph was then made of distance versus total sandstone thickness. Traditional cross sections were compared with the profiles and used to clarify the architecture of the sandstone bodies and thickness trends.

A regional cross section that extends across most of the Eastern Kentucky Coal Field was created to show thickness changes within the coal measures across the coal field (Figure 2.3). This cross section was created from eight oil and gas geophysical logs and nine coal-exploration drillholes. Where neutron-density logs were available, coal seams could be identified and correlated with the coal exploration drillholes. Otherwise, correlation of stratigraphic intervals was done using the major formation-bounding, coarsening-upward sequences (the Betsie Shale Member and Kendrick Shale Member), which are easily identified using gamma-ray signatures, and then comparing the intervening signatures to nearby coal-exploration drillholes. The regional cross section was constructed using a vertical scale of 1 inch = 50 feet (15 m).

### 3.2.2.3 Measured Sections and In-Mine Mapping

Measured sections at mine highwalls and roadcuts and in-mine mapping were done to define channel types, and assess mining problems associated with those channel types within the four-quadrangle study area. Four highway and mine-highwall exposures

were located and described in detail. In addition, TECO Coal Co. provided access to their southernmost Lower Elkhorn mine.

### 3.2.3 Analysis of Mine Maps

Abandoned and active mine maps for the Lower Elkhorn and Upper Elkhorn No. 3 were studied in order to show the relationship between coal seam and channel types, and to understand the geometry of certain types of channels. The mine maps were utilized in two ways. First, base-of-coal structure contours were digitized using ArcView/ArcInfo. On all maps, coal seam elevations were contoured in 5-foot intervals using a data density of one data point every 100 feet (30 m). Second, areas of poor mining conditions were highlighted and digitized using ArcView/ArcInfo. Areas of poor mining conditions are distinguishable by prematurely abandoned panels and/or abandoned entries, which depart from normal panel geometry. Surveyors' notes written on the maps were used to help clarify the mining conditions in those areas.

### 3.2.4 Deep Structure Analysis of the Newman Limestone

Structure and second order derivative (dip) maps for the top of the Mississippian Newman Limestone were created to identify structural features from that horizon. The mapping done for the top of the Newman Limestone was created using a regional data set consisting of 7,189 data points. Two subsets, Q-36 (36 quadrangles; 2,754 data points) and Q-12 (12 quadrangles; 969 data points), were chosen from the regional data set in order to analyze local trends. Using a smaller data set eliminates the smoothing effects

caused by computer contouring of larger, more variable data sets. The Newman Limestone structure maps were created using the normal, point kriging method in the computer program Surfer 8. The structure map was created using a contour interval of 50 feet (15 m).

### 3.2.5 Relationships between Sedimentary Trends and Structure

#### 3.2.5.1 Trend-Surface Analysis

Trend-surface and residual analysis was used in order to compare trends in local and regional stratigraphic and structural data that may not be clear from standard isolith or structural maps. Liu (1992) and Cornett (2002) used trend-surface analysis as a viable method to locate structures that were penecontemporaneous to deposition of the Pennsylvanian System in eastern Kentucky.

Trend-surface analysis is a useful method for identifying and removing regional trends (structural or thickness) to better understand local variations of the data. The geology of any given area contains signals for the distribution of local and regional structural and lithological patterns. To filter out these signals, the process of trend-surface analysis fits a 3-D surface through geographically distributed data. This surface is a best-fit surface through the data set. The surface is either planar (first-order) or geometrically curved (second-order or higher) (Swan and Sandilands, 1995).

This study tested first-, second-, and third-order surfaces over three scales of datasets: (1) single quadrangle, (2) four-quadrangle, and (3) the Eastern Kentucky Coal Field. Testing was done in order to determine which surface best represented the coal exploration drillhole data. The testing of the different methods confirmed Cornett's

(2002) hypothesis that second-order surfaces (one sense of curvature, concave or convex) are the best surfaces to show both local and regional trends. First- and third-order surfaces are also suitable surfaces for geologic data, depending on the nature of the problem (Golden Software, 2002; Swan and Sandilands, 1995). In contrast, surfaces higher than third-order, such as those used by Liu (1992), are said to be less natural, and not as useful for most geologic work (Golden Software, 2002; Swan and Sandilands, 1995).

#### 3.2.5.2 Trend-Surface Residual Analysis

Trend-surface residuals were more important to this study than the trend-surface because the residuals show the departure from the average regional trend (structural or rock thickness). A trend-surface residual is the difference between the trend-surface and each control point z value (any individual elevation or stratigraphic thickness data point), and is a measure of the error of the trend-surface fit through the data (Swan and Sandilands, 1995). If a z-value is above the trend-surface, it is a positive residual, and if the point is below the surface, it is a negative residual. Thus, when the residuals are contoured, highs and lows (i.e., structural high and structural low or thick and thin) are easily shown. Trend-surface residuals were used to confirm or reject the synsedimentary faulting hypothesis that thicker sandstone is isolated in structural lows or thin sandstone is isolated on structural highs.

#### 3.2.5.3 Special Remarks on the Use of Trend-Surface Analysis

During the course of this study, the testing of trend-surface analysis over different-scale data sets (quadrangle and multiple quadrangle) showed that a trend-surface being fit

through a set of geographically distributed data will vary as the size of the area of analysis is changed. A data set consisting of 515 coal exploration holes was analyzed using trend-surface in two different ways. First, the data for total sandstone thickness distributed over the four-quadrangle study area were analyzed using a second-order trend surface. The residuals were calculated, gridded using normal point kriging, and compared with thickness trends shown on isolith maps for total sandstone thickness. Though some of the residual trends are comparable to those shown on the isolith, the match is not precise enough. Next, the 506 exploration holes were separated into individual quadrangles, and a second-order surface was fit through each data set. Residuals were calculated for each of the four-quadrangle data sets. This method resulted in four maps and four sets of residuals. The residuals were combined into one data set and gridded using the normal point kriging method. When this residual map was compared to thickness trends known from isolith maps, the match was more precise.

The reasons that the two methods yield different results, despite using the same data, are because of differences in the variability of the data being analyzed and data density differences. Differences in the variability of the data set are probably the most important factor. The reason for differences is that a large data set has a certain amount of variability, but concentrated sampling of the larger data set generally has less variability than the whole data set. Because of the higher variability of the larger data set, the surface being fit through the whole data set will be exaggerated more to provide a best fit through the data, whereas the surface fit through the less-variable data set will be more smooth. Then, when residuals are extracted for the less-variable data set, the

differences between the best-fit surface and the data points (the residual) will be less, and will more closely match the local thickness trends.

Choosing the scale at which to analyze a data set using trend-surface methods must be considered before doing the analysis. As an example, large structures that extend across multiple quadrangles and gross interval thickness would probably require an analysis incorporating multiple quadrangles of data. In contrast, when looking at thickness variation within sandstone bodies or a narrowly defined stratigraphic interval, a single quadrangle analysis may be more useful.

## 4.0 Results

### 4.1 Characteristics of Channels within the Study Area

#### 4.1.1 Background

The focus of this thesis is to predict the location of channel-related mining problems within the Lower Elkhorn interval ahead of active mining operations, and in areas with limited data distribution. The main Lower Elkhorn (Pond Creek) coal body is found almost exclusively within Pike County, and is “L”-shaped in geometry (Figure 4.1). The northern projection of the coal body extends approximately 32 miles (51 km) to the northwest from the Kentucky/Virginia border. The southern projection of the coal body extends approximately 40 miles (64 km) to the southwest from the Kentucky/West Virginia border.

The Lower Elkhorn coal body is part of a coal zone that contains persistent upper and lower coal benches and rider seams (Figure 4.1 inset). Throughout most of the Lower Elkhorn coal body in eastern Pike County, the upper and lower benches merge to form a single, thick coal seam. These areas have been the major focus of Lower Elkhorn mining operations in eastern Kentucky. A split between the upper and lower benches produces a reduction in coal thickness at the edge of the core coal body. Outside the split line (shown by the red lines on Figure 4.1), only the upper bench is mineable. In some areas, an overlying rider seam joins the upper bench to form a thick (greater than 42 inches [ $> 106$  cm]) seam, indicated by the blue lines on Figure 4.1. This combination of benches has also been locally mined. There are also several thin, local riders between the Lower Elkhorn and main rider seam in eastern Kentucky.

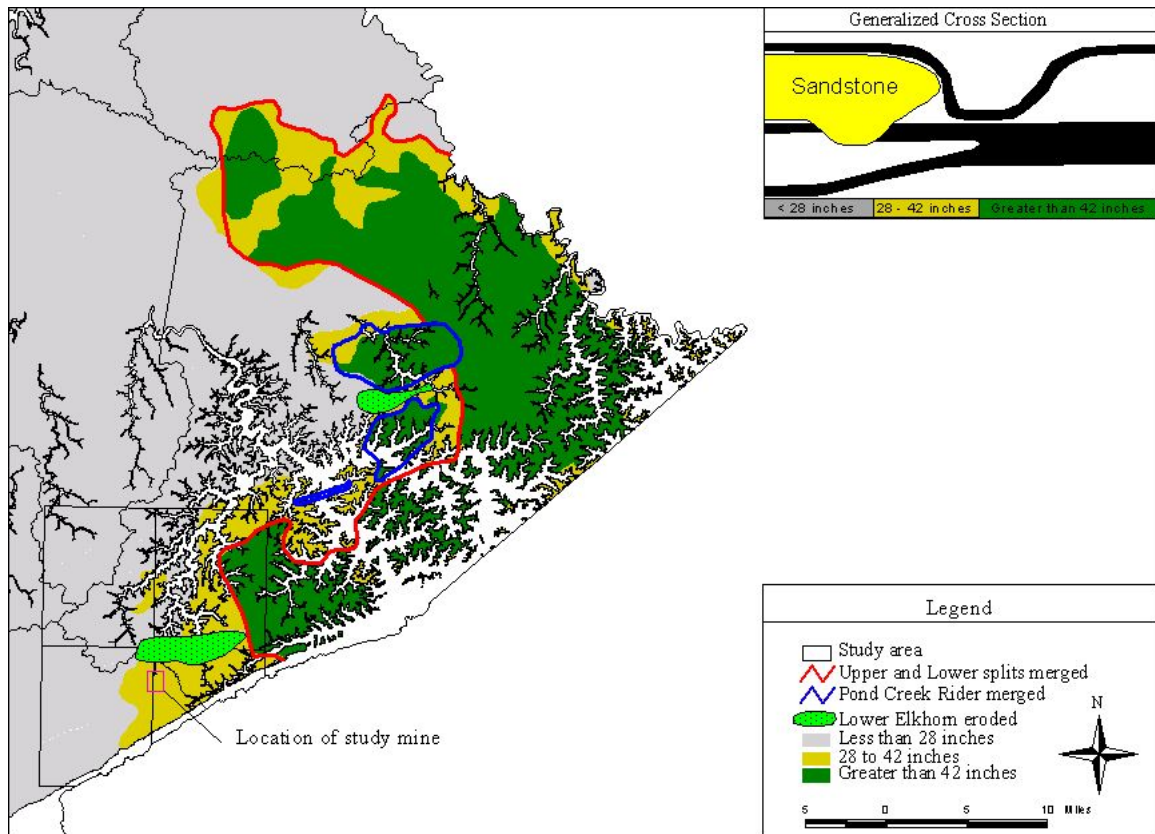


**Figure 4.1:** Regional distribution of the Lower Elkhorn coal (modified from Thacker et. al, 1998).

With the depletion of the thick (greater than 42 inches) Lower Elkhorn coal reserves throughout eastern Kentucky, attention is now being paid to thinner reserves of 28 inches to 42 inches (71 to 106 cm) along the margin of the coal body (Figure 4.1). One of these reserves is found in the southern half of the four-quadrangle study area. This area of coal represents one of the few remaining economically important reserves of Lower Elkhorn coal.

Within the southern half of the four-quadrangle study area, the mineable Lower Elkhorn reserves are comprised of only the upper coal bench (Figure 4.1). Premier Elkhorn Mining, a division of TECO Coal Corporation, has developed two deep mines within these Lower Elkhorn reserves. Premier Elkhorn's southernmost deep mine (Figure 4.1) has encountered roof-control problems related to paleochannels, which have impeded mining. Premier Elkhorn Mining is concerned about the possibility of encountering similar features as mining progresses. To date, the spacing of subsurface data for this coal has not been sufficient to predict the extent of channel-related problems ahead of mining.

To develop models for predicting possible locations of channels, field data, drill-holes, and mine maps for the Lower Elkhorn and adjacent strata were examined to determine the character, dimensions, and orientations of known paleochannels. The result of this process has led to the classification of three channel types, which are informally defined herein according to the nature and magnitude of incision or the lithologic nature of the channel fill.

## 4.1.2 Channel Types

### 4.1.2.1 Regional Incised Sandstone Channels

Regional incised sandstone channels are identified from drillholes that show zero coal thickness along a linear trend, indicating significant reduction or complete removal of the underlying coal seam across a broad area (Figure 4.1). These channels were detected during the course of a basinwide coal resource assessment (Thacker et al., 1998).

Regional incised channels were formed at the base of a sandstone body, 40 feet (12 m) or greater in thickness, that separates the main Lower Elkhorn seam from the Lower Elkhorn rider seams. Identified regional incised channels trend east–west, and are on average 1.2 miles (2 km) wide by 4.6 miles (8 km) long, and intersect the major coal body at approximately right angles to the main split line (Thacker et al., 1998). Locations of two incised channels are shown on Figure 4.1. Areas where the coal has been completely removed by the regional incised channel in the four-quadrangle study area have been defined in more detail during the course of this study. A map was created showing those areas where the Lower Elkhorn has been completely removed (Figure 4.2). Though the map shows narrow bands of zero coal thickness, the area affected by the regional incised channel is much larger.

Mining operations that have encountered regional incised sandstone channels in other areas of the coal field were terminated because of the complete removal of the coal over a large area (Greb et. al, 1991, 1999a). Where sandstone-filled channels have scoured through fine-grained roof strata, slickensides form in the fine-grained rock that result in weak roof conditions (Figure 4.3). Typically, roof-control problems associated with

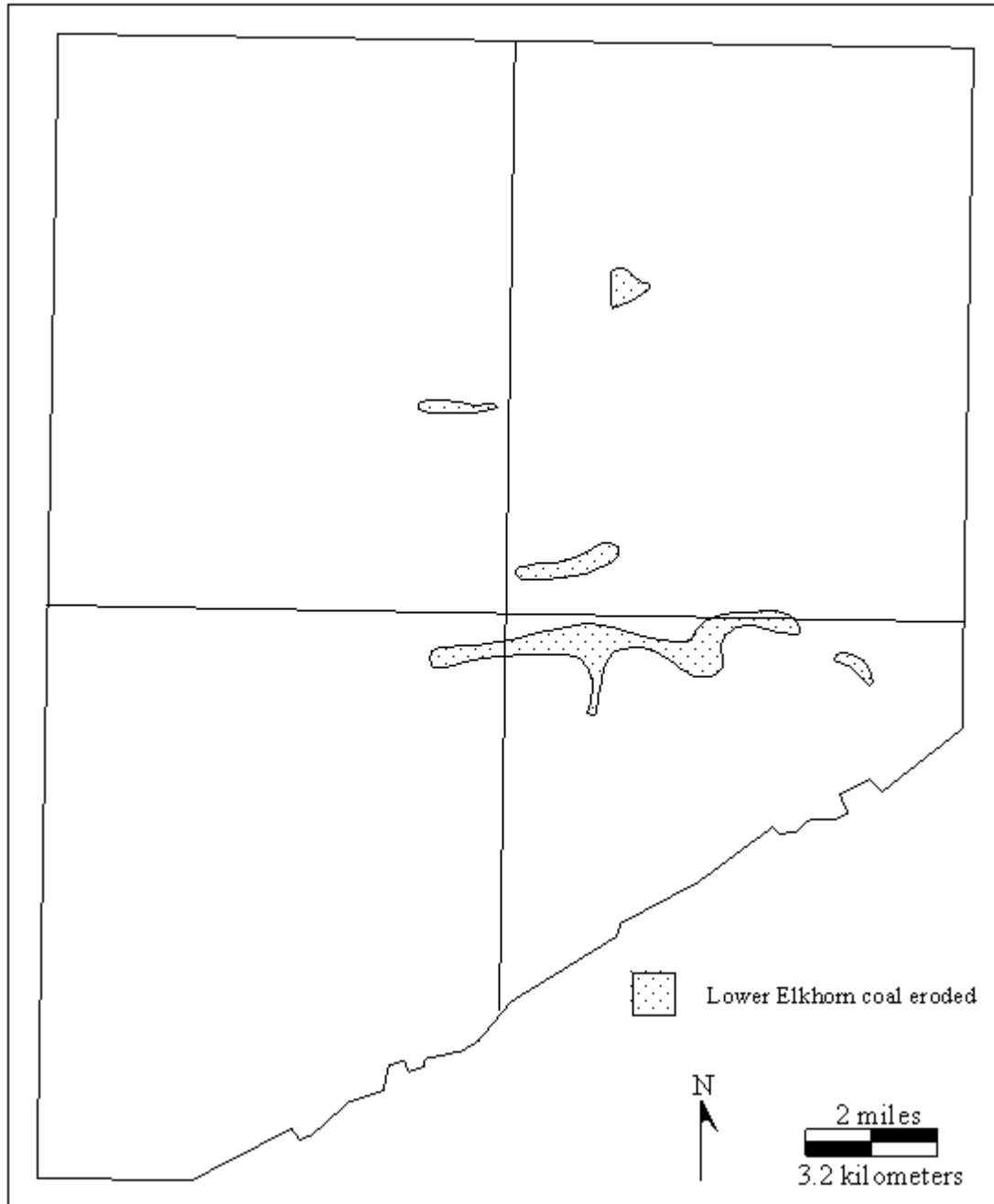


**Figure 4.2:** Map of the four-quadrangle area showing locations where the Lower Elkhorn coal has been removed due to erosion by regional incised channels.

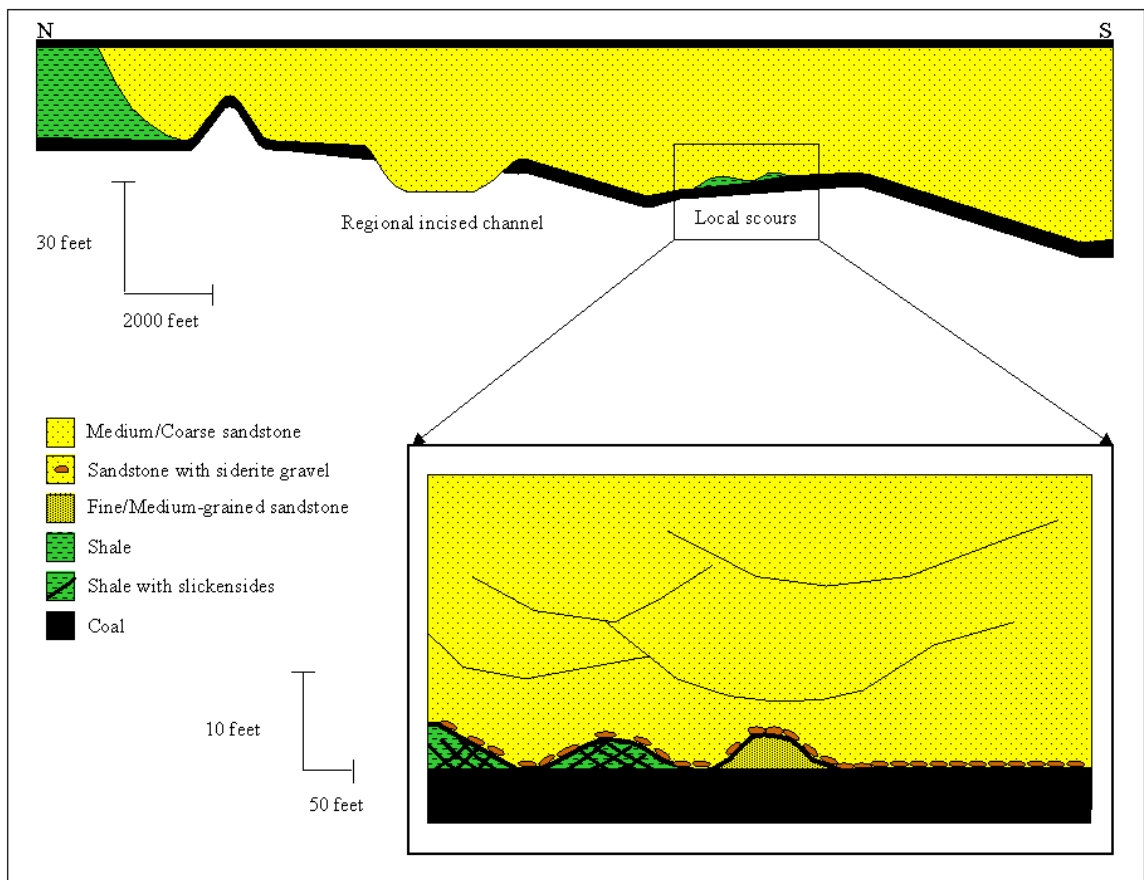


**Figure 4.3:** Generalized cross section across the four-quadrangle study area showing the stratigraphy of the Lower Elkhorn coal zone and the presence of regional incised channels and local scours.

slickensides are common with incised channel sandstones (Greb, 1991; Weisenfluh and Ferm, 1991a). Incised channels are large-scale features that are easily detected during exploration drilling with typical spacing of drillholes at 2000 feet (609 m).

#### 4.1.2.2 Local Sandstone Scours

Local sandstone scours are erosional features that locally remove adjacent roof rocks across small areas. Local sandstone scours are in areas where the overlying sandstone scours into roof rocks, leaving erosional remnants of sandstone or slickensided shale between scours (Figure 4.3). Local scours generally do not reduce coal thickness. In the Lower Elkhorn study mine, local scours are characterized by overlying coarse-grained sandstone that incises into dark gray shale with siderite nodules or a fine- to medium-grained crossbedded sandstone. Scour surfaces are overlain by siderite-pebble conglomerate, log fossils, and fossilized plant fragments. The depths of incision of scours into underlying lithologies are approximately 5 feet, but complete in-mine exposures are not common. The true depth of incision is difficult to determine because of the presence of numerous overlying amalgamation surfaces, as well as a lack of surface exposure where profiles can be observed. Within the mine, these incisions are approximately 50 feet (15 m) wide or less. Similar types of incisions in nearby highway exposures, in a different stratigraphic interval, are as wide as 300 feet (91 m). The length of these scours cannot be determined from the available data, but mine exposures suggest a maximum of 100 to 200 feet (30 to 61 m).

Roof falls and spalling associated with local scours result from compactional slips in underlying fine-grained rock. Falls are associated with sandstone to sandstone

contacts along inclined bedding related to an erosional surface, and abrupt grain-size changes with plant fossils above and below the scour surface. These roof falls are minor, however, and appear to have had relatively little effect on mining. Because of the small areas affected by local scours, they do not generally appear on mine maps. Also, in contrast to incised channels, local scours are very small-scale features that are impossible to detect with a drilling program using 2000 foot (609 m) spacing.

#### 4.1.2.3 Local Heterolithic Channels

The third type of paleochannel in the study area consists of mixed sandstone and interbedded shale above a sharp, erosional, basal contact (Figures 4.4a and 4.4b). This channel type is termed heterolithic. Heterolithic channels vary in the ratio of sandstone to shale. Channel fills are composed of dark gray shale with siderite concretions, coal spars, fossilized plant fragments, epsilon crossbedding, lateral accretion surfaces, and rotated slump blocks (Figure 4.4 a and 4.4 b). Heterolithic channels also cut into horizontally bedded heterolithic overbank deposits (Figure 4.4 b). Mining problems that have been encountered by TECO Coal Co. are related to the heterolithic channel type with rotated slump blocks. Slump blocks observed within the study mine consist of inclined dark gray shale and siltstone that are bounded by slickensided surfaces. These slump blocks occurred in a zone 570 feet (174 m) wide and 3000 feet (914 m) long. Slump deposits were encountered in three nonparallel mains, implying an arcuate trend to the channel. The slump deposits were not directly observed during the course of this study, but reports indicate that the direction of slumping is dominantly to the northeast, with a minor southwestern component into the main paleochannel (Greb,

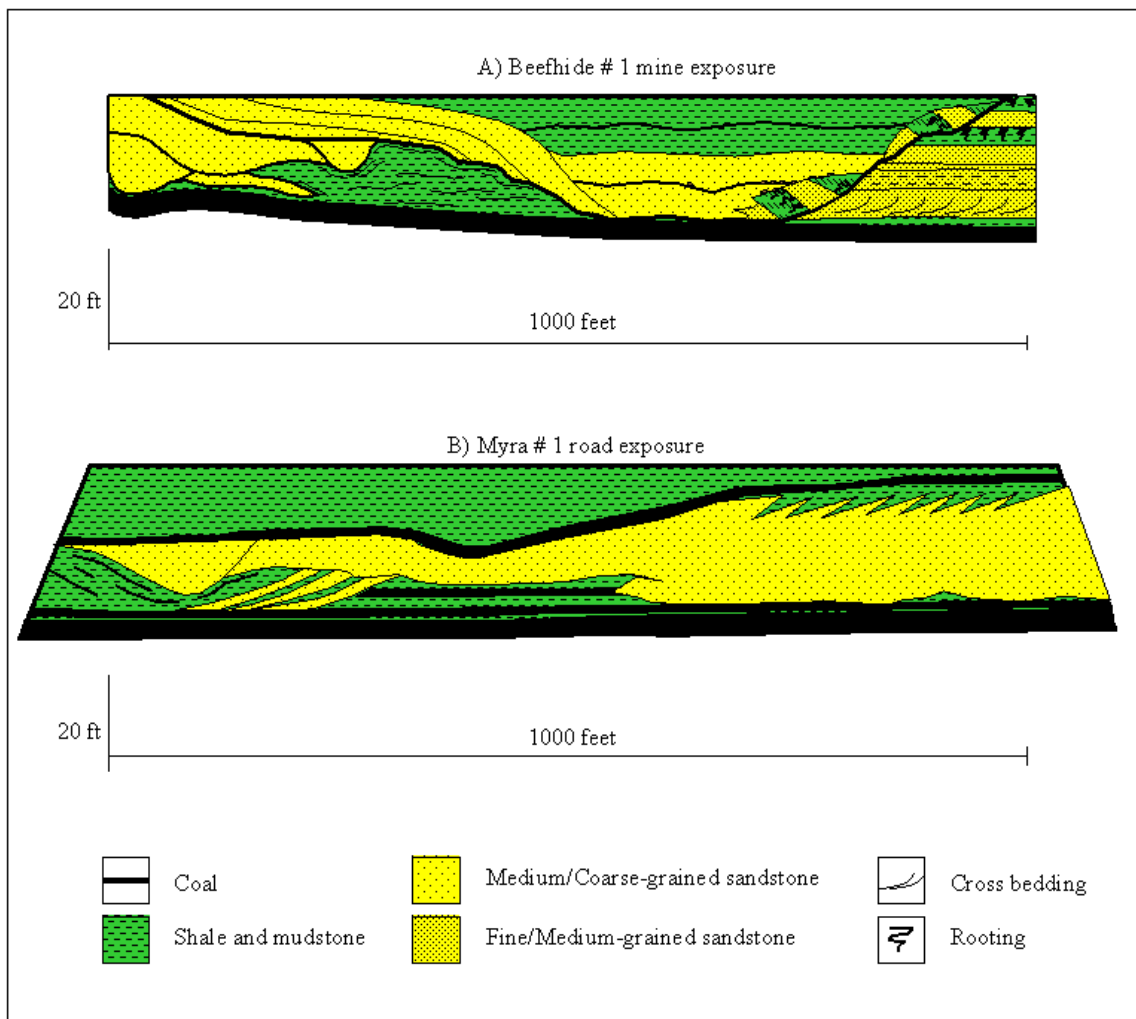


**Figure 4.4:** Sketches of the Beefhide Mine portal exposure (a) and Myra Highway exposure (b), showing the characteristics of heterolithic channels.

pers. comm., 2002). In addition to the observed slump-related problems, mining problems associated with heterolithic channels could also consist of roof falls that propagate along separation planes between interbedded sandstone and shale, or between the coal and shale within the channel fills (Greb, 1991).

Heterolithic channels are intermediate in scale between incised channels and local scours. Much like local scours, however, heterolithic channels are hard to detect in a drilling program with 2000 foot (609 m) spacing between drillholes. Heterolithic channels are easier to detect than local scours because heterolithic channels are probably as much as 1000 feet (300 m) wide. Average lengths of this channel type could not be determined because of poor in-mine and highway exposures.

Heterolithic channels are potentially hazardous to mining operations because of the weak nature of their associated strata, and potential for local removal of the coal seam. Moreover, these channels are very difficult to predict in the subsurface because of the lack of closely spaced drillholes required to accurately map the distribution.

#### 4.1.2.4 Overbank Deposits

Overbank deposits were identified in two measured sections adjacent to mine portals. These sections consist of horizontally bedded, heterolithic sandstone and shale sequences (Figure 4.5). Sandstone units are fine- to medium-grained, are partly rooted, and generally taper in one direction. Associated interbedded shale is clay- to silt-rich, dark gray, with siderite nodules and whole or fragmentary plant remains and scattered rooting. In some places, thin bone coal seams are also present.

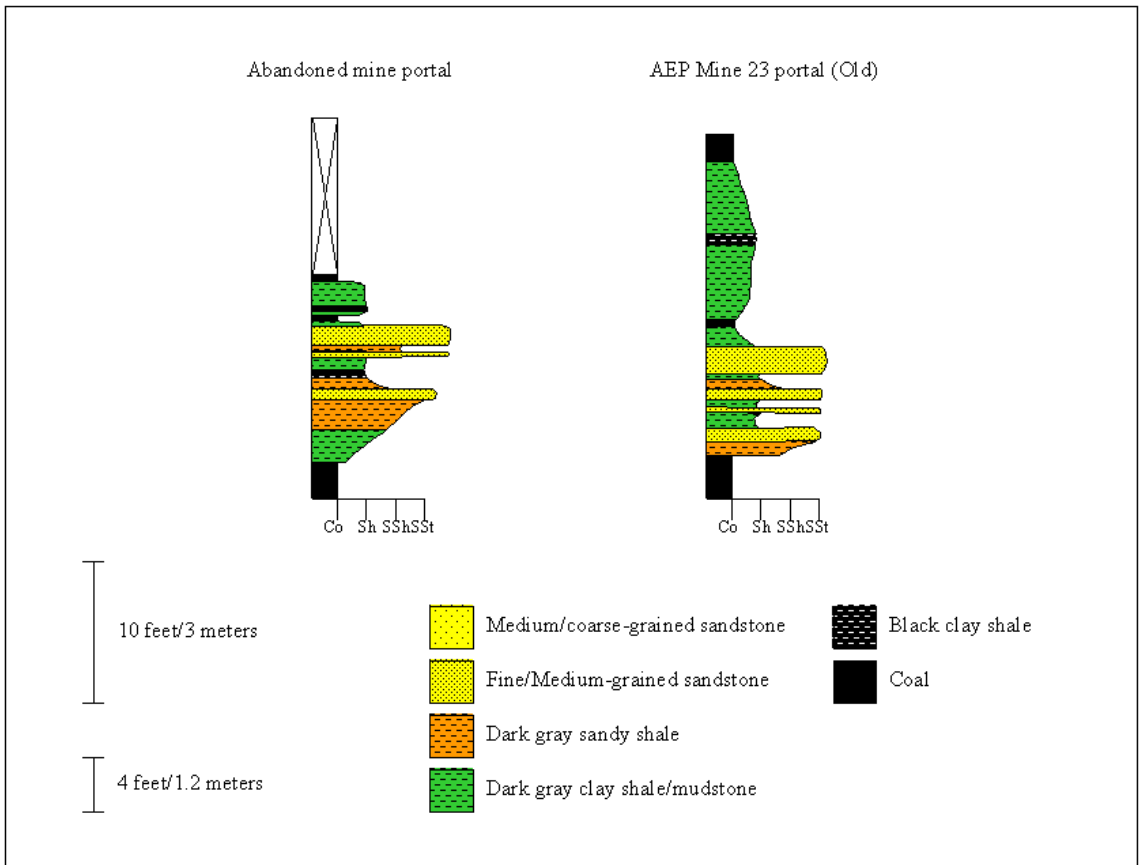


**Figure 4.5:** Stratigraphic columns showing heterolithic overbank facies above the Lower Elkhorn coal at two mine portals. Co = coal, Sh = shale, SSh = sandy shale, SSt = sandstone.

Mining conditions in active Branham and Baker mines, as well as an abandoned mine, that contain overbank deposits within the roof strata vary from mine to mine. A heterolithic overbank sequence described at the portal of an abandoned mine consists of interbedded sandstone and shale sequences with abundant rooting horizons, thin rider coal seams, and tapering sandstone bodies. Mine-map analysis of this mine revealed severe roof problems, which probably terminated mining operations prematurely. Roof falls in this mine were not directly observed, but likely occurred along separation planes between interbedded strata and within lithologies such as coal and rooted horizons. Heterolithic sequences were also observed at another nearby mine portal. The roof strata at this mine contain sandstone bodies that are uniform in thickness, with no rider seams or rooting horizons. On the basis of mine-map observations and interviews with engineers, roof problems were not a serious issue at this mine.

Lithologic characteristics associated with the heterolithic overbank deposits, such as rooting and interbedded rider coals seams, are easy to detect in core drilling. The lateral gradient of lithologic change in overbank sequences, however, is such that a drilling spacing of 2000 feet (609 m) or more may not be sufficient to detect and predict the extent of potential mining problems associated with these sequences or to predict lateral rates of lithologic change.

Of the three types of channels, heterolithic channels pose the greatest potential for hazardous mining conditions. Furthermore, because of poor exposure and limited distribution, their predictability is more uncertain. Thus, in order to understand the geometry of heterolithic channels and coal seam structure, abandoned mine maps were analyzed. Because heterolithic channels are often in close proximity to coal seams, and

create hazardous roof conditions, it was assumed that they might be indicated on abandoned mine maps by areas of poor panel development across areas similar to those identified in the Lower Elkhorn study mine. The overlying Upper Elkhorn No. 3 was chosen for this analysis because of the availability of mine maps that cover a large continuous area above the study mine.

#### 4.1.3 Coal-Seam Structure and Paleochannel-Related Mining Problems

Abandoned and active mine maps for the Lower Elkhorn and Upper Elkhorn No. 3 seams were examined to understand the orientation and geometry of heterolithic channels, and to see if there is a relationship between channel-related mining problems and coal seam structure. Base-of-coal structure maps, obtained from TECO Coal Co., were generated from in-mine elevation surveys using data at a density of approximately one point every 100 feet (30 m). Structure maps were contoured in 5 foot (1.5 m) intervals. In addition to surveyed elevations, notes on mining conditions were shown on the Upper Elkhorn No. 3 maps. These notes helped clarify whether areas of poor panel development were related to paleochannels. Mine-map coverage for the Lower Elkhorn coal seam showing coal seam structure and mining problems comes from the study mine (Figure 4.6a). The Upper Elkhorn No. 3 mine map also shows coal seam structure and mining problems, but covers a continuous area of approximately 24 square miles (62 sq. km) (Figure 4.6b).

Mining problems associated with the Lower Elkhorn and Upper Elkhorn No. 3 seams are highlighted on mine maps by areas of poor panel development. Mining

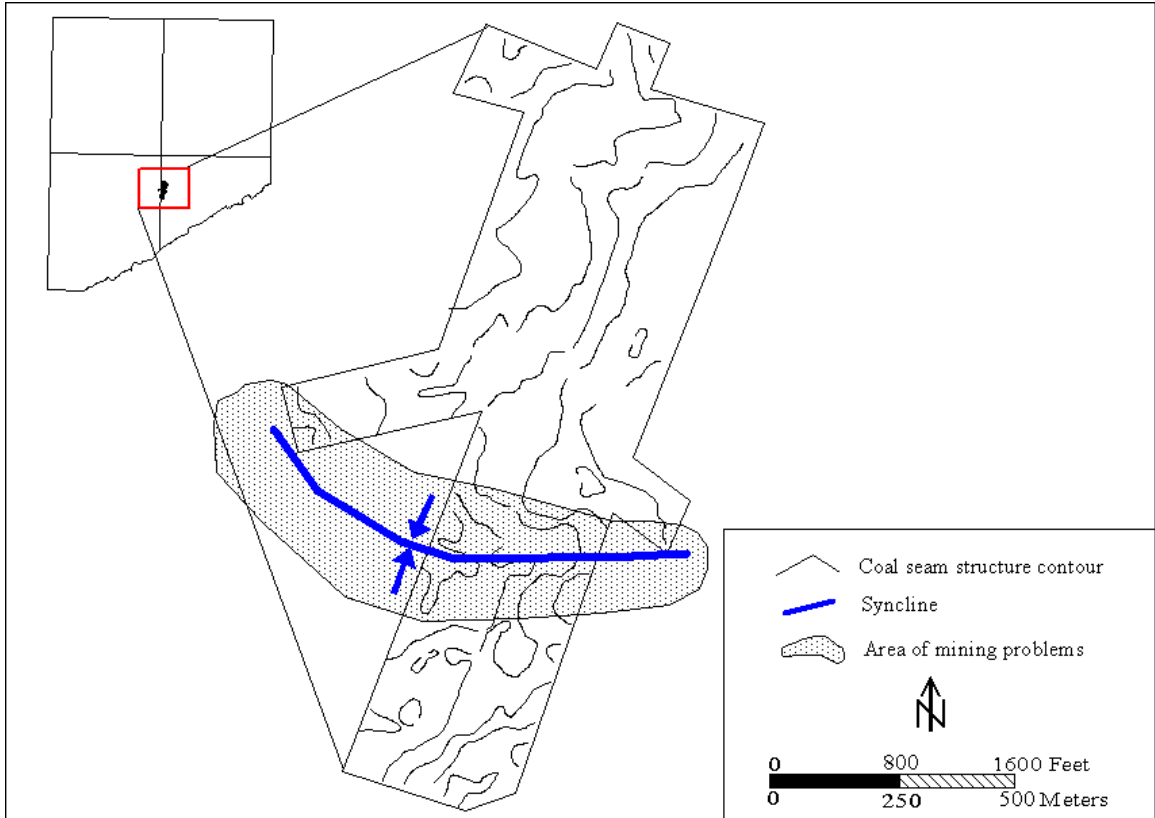


**Figure 4.6a:** Relationship between mining problems and synclines for the Lower Elkhorn coal.

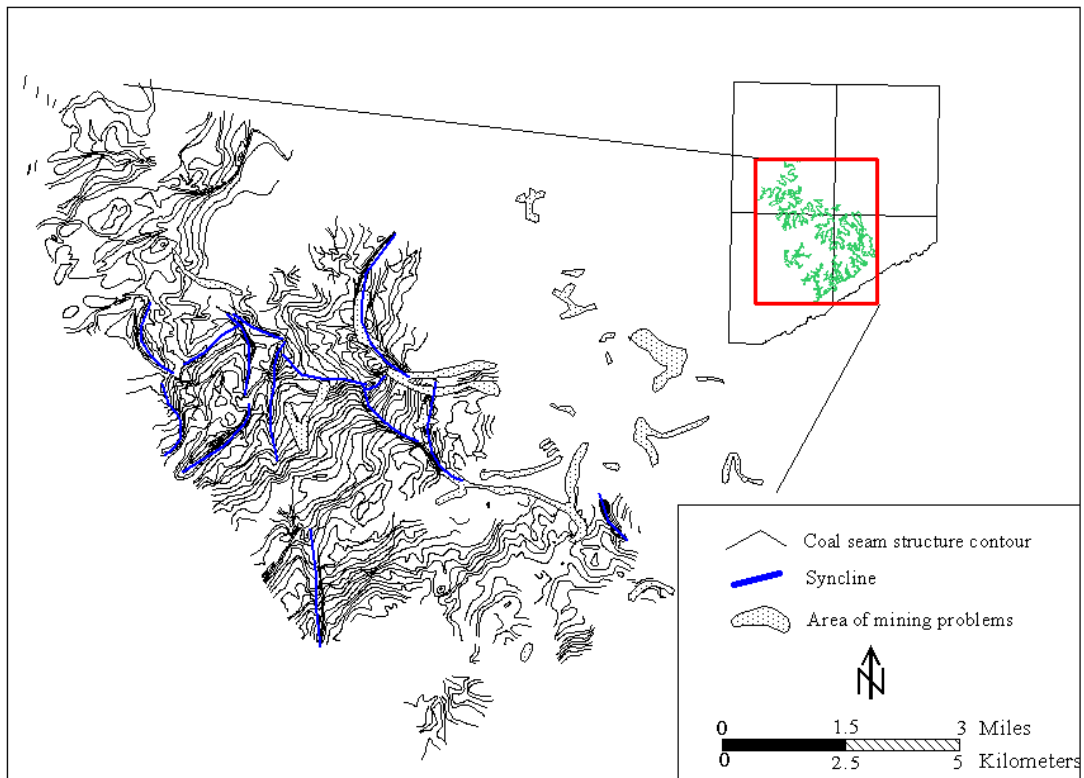


**Figure 4.6b:** Relationship between mining problems and synclines for the Upper Elkhorn No. 3 seam. The extent of Upper Elkhorn No. 3 mines is shown by the green outline.

problems for both seams are recognized as narrow linear, locally bifurcating zones where entries or panels were abandoned prematurely or where no mining occurred (Figure 4.7).

The dimensions of the linear zones may be as much as 500 feet wide and 3000 feet (0.6 mi; 0.9 km) long for the Lower Elkhorn seam, and 250 feet wide (76 m) and 11,000 feet (2.0 mi; 3.3 km) long for the Upper Elkhorn No. 3. Surveyors' notes on the Upper Elkhorn No. 3 mine maps indicated a thinning of the coal within some of these linear areas. On the basis of their linear nature, thinning of the coal seam, and dimensions, these areas were determined to likely represent areas of poor mining conditions resulting from heterolithic channels.

Analysis of the structural contours revealed prominent monoclines, anticlines, and synclines for both the Lower Elkhorn and Upper Elkhorn No. 3 coal seams. Overall, the structural dip of the coals is to the northwest. Synclines are the most predominant structural feature on the maps and have approximately 20 feet (6 m) of relief. In some parts of the mines, inferred heterolithic channels coincide with synclines. Not all synclines are associated with paleochannels, however. Synclines for both seams were closely studied and are categorized into four types: (1) steep-sided, symmetrical, (2) steep-sided, asymmetrical, (3) broad, symmetrical (4) broad, asymmetrical (Figure 4.8).

Comparison of the base-of-coal structure map to the distribution of mining problems reveals a correlation between mining problems related to inferred heterolithic channels and synclines. Greb and Popp (1999) also recognized this relationship in the Lower Elkhorn coal zone, but in a different part of the coal field. The geometry of a syncline, however, does not appear to be associated with paleochannel occurrence. For example, paleochannel-related mining problems within the Lower Elkhorn study mine are

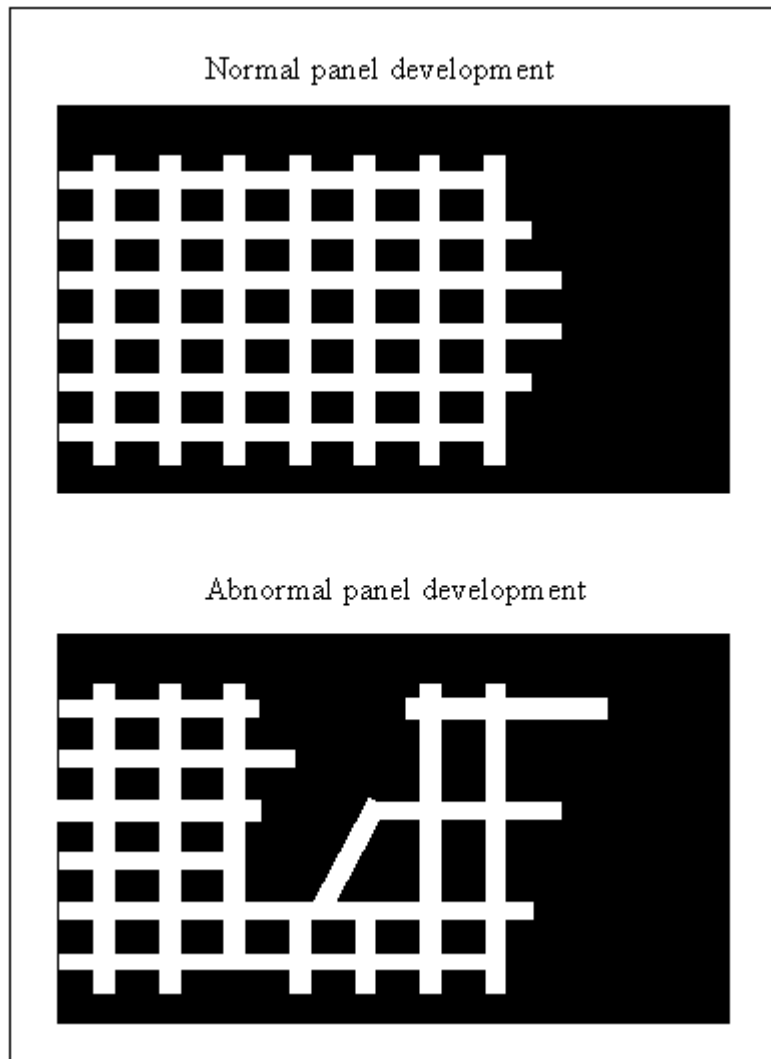


**Figure 4.7:** Generalized diagram showing an example of poor panel development.

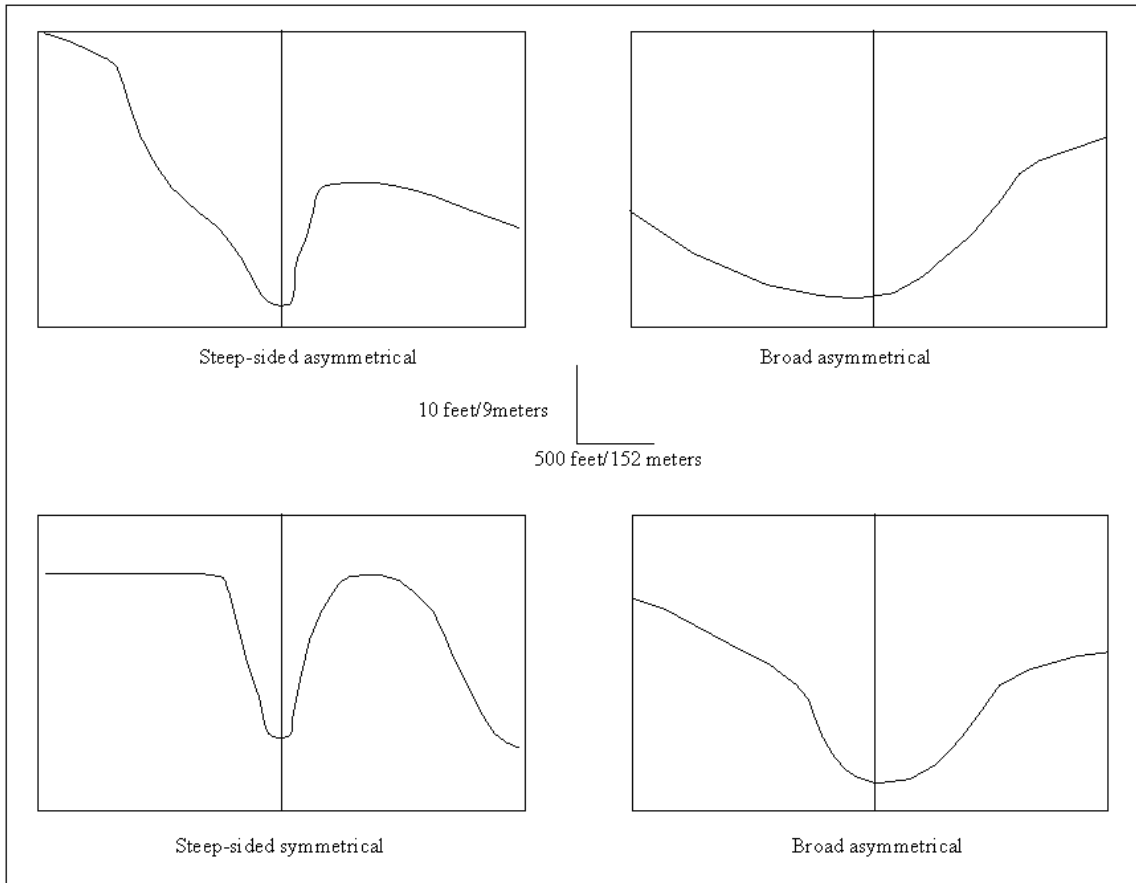


**Figure 4.8:** Structural profiles, showing the four types of synclines, taken from the base-of-coal structure map for the Upper Elkhorn No. 3.

associated within a broad symmetrical syncline. In contrast, mining problems associated with the Upper Elkhorn No. 3 are associated with steep-sided symmetrical and asymmetrical synclines. Three very prominent steep-sided synclines coincide with paleochannel-related mining problems, on the eastern side of the map. These synclines and paleochannels show an overall northwest–southeast trend, but the northern two are strongly curvilinear to the northeast.

The synclines described herein may be true structural features or may represent abandoned scours that predated deposition of the peat (now coal) (Greb et al., 2001). The formation of the scours, however, could have been structurally influenced. The different geometries of the synclines may result from the curvature of the channel that formed the scour, as well as weathering or slope modification of the scour prior to and during peat accumulation.

#### 4.1.4 Channel Classification Summary

Field work, drill-hole information, and mine map data show three principal types of channels within the study area: (1) regional incised sandstone channels, (2) local sandstone scours, and (3) heterolithic channels. Of the three recognized channel types, heterolithic channels appear to be the most hazardous to mining because of their unpredictable nature and weak lithologies. Based on mine map information, these channels appear to be most closely related to narrow synclines, as shown by the base-of-coal structure. None of the four types of synclines identified, however, appear to be the most likely to have associated, overlying paleochannel deposits.

Two of the three channel types (regional incised channels and local scours) associated with the Lower Elkhorn coal are clearly related to large sandstone bodies in the interval between the Lower Elkhorn and Lower Elkhorn rider seams (Figure 4.3). The relationship between heterolithic channels to overlying sandstone bodies is not as clear. Analysis of the thickness variation of these sandstone bodies may lead to more defining relationships between all channel types that could be used to predict locations or orientations of the three channel types. Moreover, comparison of sandstone geometries in the context of a wider stratigraphic interval could result in defining process models that would be useful for predicting channel locations in areas of sparse data. Intervals between the Lower Elkhorn and Amburgy coals were chosen for this analysis.

## 4.2 Characteristics of the Stratigraphic Intervals

### 4.2.1 Background

Eight stratigraphic intervals that contain sandstone bodies are defined between the Lower Elkhorn coal zone and the Amburgy coal zone (Figure 4.9). A laterally persistent coal bed defines the base of each stratigraphic interval. The upper boundary of each interval is chosen as the next, stratigraphically higher coal seam that has lateral continuity throughout the study area. It was necessary to combine some adjacent intervals into a composite interval, because bounding coal beds have insufficient continuity to be used as reliable datums (e.g., Lower Elkhorn rider/Upper Elkhorn No. 2 interval, Figure 4.9). For these intervals, total sandstone thickness was calculated for the combined interval, but characteristics of individual sandstone bodies can be observed on cross sections.

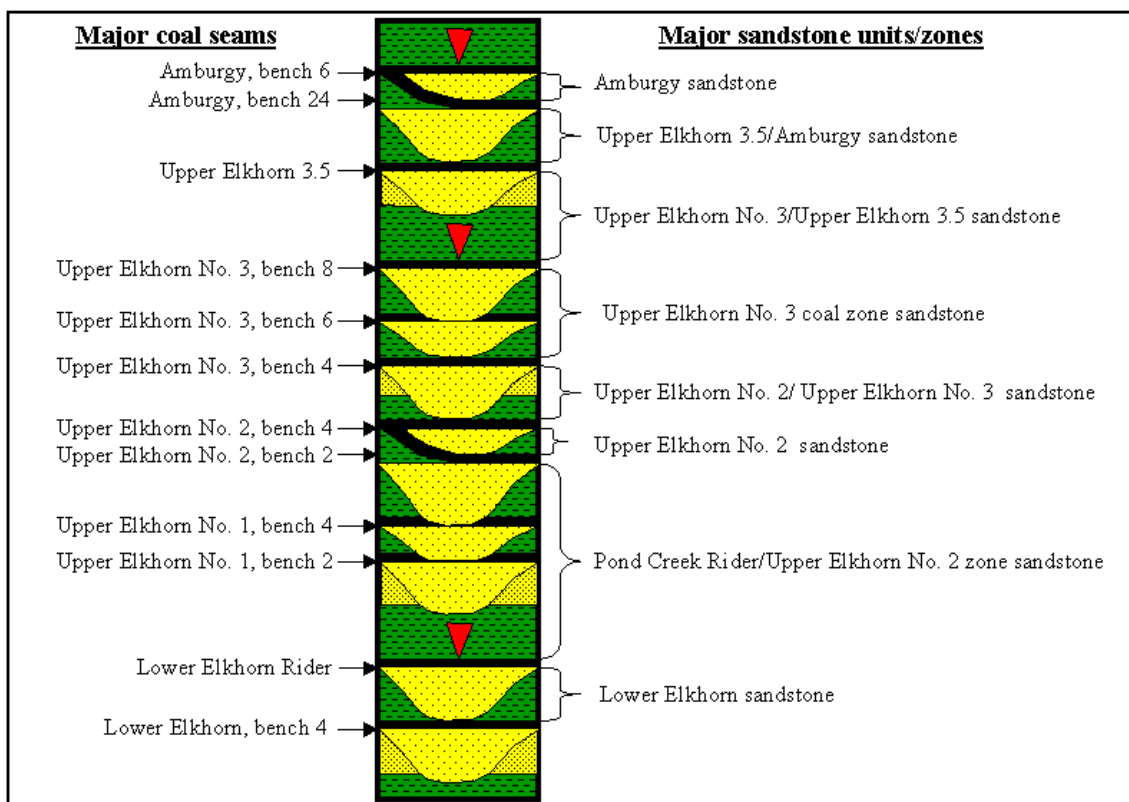


**Figure 4.9:** Generalized diagram showing the eight stratigraphic intervals and their associated sandstone bodies.

Isolith maps and profiles (simplified cross sections) are used to show the thickness trends, define sandstone geometries, and better characterize the vertical relationship between sandstone bodies within and between the stratigraphic intervals. From the isolith maps and profiles, four sandstone geometries are recognized, and are defined by the extent of the sandstone-rich areas and their relationship to sandstone-poor areas.

#### 4.2.2 Sandstone Geometry Types

Analysis of isolith maps of total sandstone thickness results in the characterization of sandstone geometry, primarily on the basis of the extent of sandstone-poor areas. The threshold contour that defines the sandstone-poor areas was arbitrarily chosen as the 10 foot (3 m) total sandstone isolith contour for all intervals. The threshold contour for sandstone-rich areas varies from interval to interval. When the relationships between sandstone-rich areas and sandstone-poor areas are considered, sandstone body geometries can be defined. Two end members, sheet and isolated, are shown in Figure 4.10. Sheet sandstone bodies extend across the entire study area, whereas isolated sandstone bodies are solitary and bounded by extensive sandstone-poor areas. Other intervals show a belt-like geometry, which includes a continuum between the two end members. Across this continuum, from sheet to isolated, the sandstone-poor areas increase in size, restricting the distribution of sandstone-rich areas (Figure 4.10). Some sandstone bodies are classified as composite, where two or more intervals have been combined because of nonpersistent bounding horizons. Composite sandstone bodies may be two or more stacked sandstones separated by fine-grained rock. More commonly, adjacent sandstone

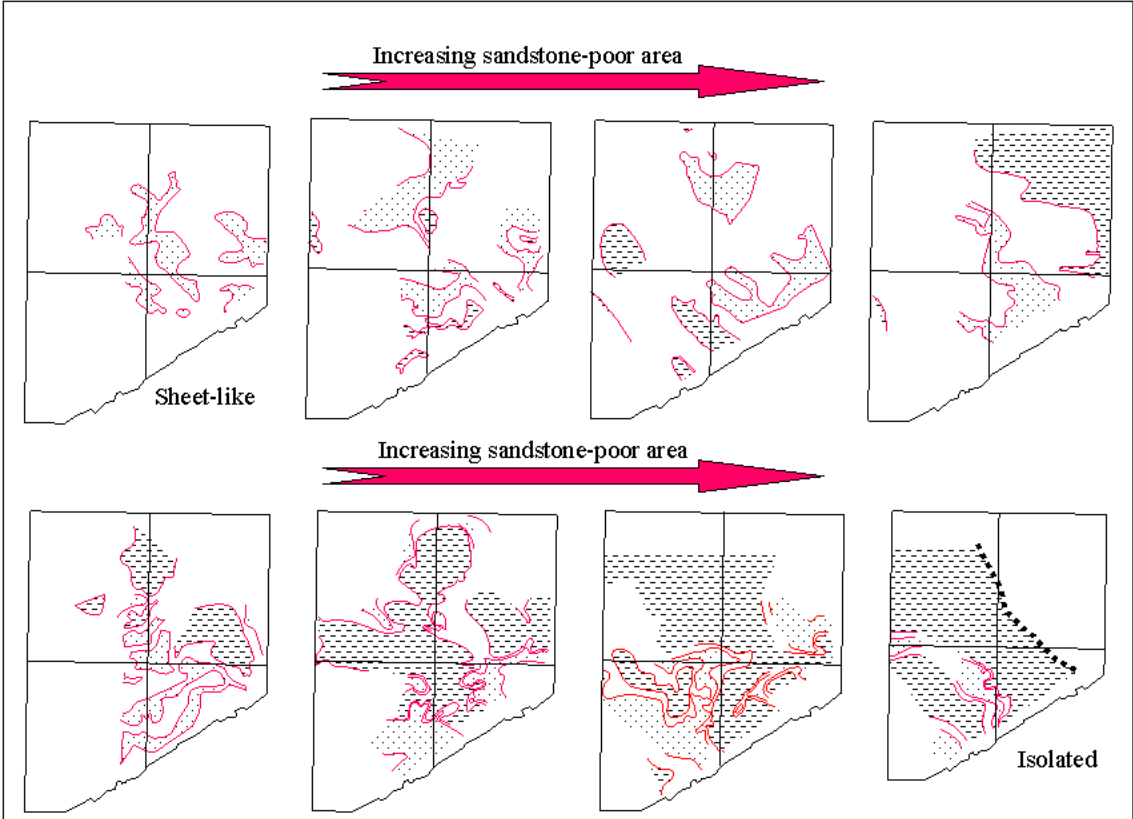


**Figure 4.10:** Continuum of sandstone geometries identified for the eight stratigraphic intervals.

bodies are amalgamated because of scouring, and this is the reason the bounding horizons are absent. By using cross sections, sheet, belt, and isolated sandstone geometries can be identified within a composite interval. A summary table of sandstone geometry, dimensions of sandstone body geometries, and sandstone thickness trends for each stratigraphic interval is given in Table 4.1.

In order to identify controlling mechanisms for sandstone distribution, sandstone geometries were compared among the adjacent stratigraphic intervals. Areas that persist as sandstone-poor or sandstone-rich through time define a vertical stacking relationship, which can be attributed to syndimentary faulting. Conversely, where sandstone-rich areas are offset from interval to interval, the controlling mechanism of sandstone body distribution is differential compaction.

The way in which trends are compared varies with the type of geometry. Comparisons are relatively easy between intervals that contain belt-like or isolated sandstone bodies. Where the sandstone body is sheet-like, however, comparisons of thickness variation must be made using linear thickness trends within the sheet, such as the axes of thickest sandstone-rich areas, rather than distribution of nonsandstone lithologies (sandstone-poor areas).

#### 4.2.3 Analysis of Isolith Maps

##### 4.2.3.1 The Lower Elkhorn/Lower Elkhorn Rider Interval

The Lower Elkhorn/Lower Elkhorn rider interval is the stratigraphically lowest interval (Figure 4.9). The top of the interval is defined as the base of the Lower Elkhorn rider, and the base of the interval is defined as the base of the upper bench of the Lower

Interval	Geometry	Width of belt or isolated sandstone	Defining isopach contour	Linear trends, minimum width	Linear trends, maximum width	Direction of trends
Lower Elkhorn/Lower Elkhorn Rider	Belt-like, locally composite	Over 22,000 ft or 4 mi; 6.7 km	40 ft; 12 m	1,000 ft; 304 m	6,200 ft or 1.2 mi; 1.9 km	NE/SW; E/W
Lower Elkhorn Rider/Upper Elkhorn No. 2	Sheet-like, regionally composite	Not applicable	50 ft; 15 m	1,800 ft; 548 m	10,000 ft or 2 mi; 3 km	NWSE
Upper Elkhorn No. 2 split	Isolated	Over 14,784 ft or 2.8 mi; 4.5 km	20 ft; 6 m	1,200 ft; 366m	11,000 ft or 2.0 mi; 3.2 km	NWSE
Upper Elkhorn No. 2/Upper Elkhorn No. 3	Belt-like, regionally Composite	Over 30,773 ft or 5.8 mi;; 9.4 km	60 ft; 18 m	1,500 ft; 457 m	15,000 ft or 2.8 mi; 4.5 km	NWSE; NE/SW in southeastern portion of study area
Upper Elkhorn No. 3 zone	Belt-like, regionally composite	Over 30,000 ft or 5.7 mi; 9.2 km	60 ft; 18 m	1,100 ft; 335 m	12,600 ft or 2.4 mi; 3.8 km	NE/SW; E/W
Upper Elkhorn No. 3/Upper Elkhorn 3.5	Belt-like	Over 22,176 ft or 4.2 mi; 6.8 km	Variable	6,700 ft or 1.3 mi; 3.0 km	16,000 ft or 3.1 mi; 4.9 km	NWSE
Upper Elkhorn 3.5/Amburgy	Belt-like	Not applicable	50 ft; 15 m	5,400 ft or 1.02 mi; 1.6 km	16,000 ft or 3 mi; 4.8 km	NWSE
Amburgy split	Belt-like	Over 10,000 ft or 1.9 mi; 3 km	30 ft; 9 m	945 ft; 288 m	9,400 ft or 1.8 mi; 2.9 km	NE/SW; E/W

**Table 4.1:** Summary table of sandstone body characteristics for the eight stratigraphic intervals.

Elkhorn coal. Total sandstone thickness for this interval ranges from zero to more than 50 feet (15 m) thick, and is locally more than 70 feet (21 m) thick (Figure 4.11). The interval has a dominantly belt-like geometry, containing local areas of storied (composite) sandstone bodies.

The isolith map of total sandstone thickness for the Lower Elkhorn/Lower Elkhorn rider interval shows that sandstone-rich areas within this interval are dominantly oriented northeast–southwest to east–west across the study area (Figure 4.11). The map in Figure 4.11 shows a number of abrupt angular changes in the orientation of isolith contours in the southern half of the study area. Along these angular changes, the sandstone-rich areas take on a northeast–southwest orientation. In the northern half of the study area, the contours are oriented east–west to slightly northwest–southeast.

#### 4.2.3.2 Lower Elkhorn Rider/Upper Elkhorn No. 2 Interval

The Lower Elkhorn rider/Upper Elkhorn No. 2 interval overlies the Lower Elkhorn/Lower Elkhorn rider interval (Figure 4.9). The top of this interval is defined as the base of the Upper Elkhorn No. 2 (lower bench) coal, and the base of the interval is defined as the base of the Lower Elkhorn rider seam. The interval includes the Upper Elkhorn No. 1 coal horizon. The boundaries are chosen because there were no continuous coal seams within the Upper Elkhorn No. 1 coal zone that could be used to define a reliable datum. Total sandstone thickness for the Lower Elkhorn rider/Upper Elkhorn No. 2 interval ranges from 30 feet (9 m) to more than 100 feet (30 m) (Appendix 4.2.1). This interval has a composite sandstone geometry because sandstone bodies stratigraphically higher in the interval erode the Upper Elkhorn No. 1 coal zone and

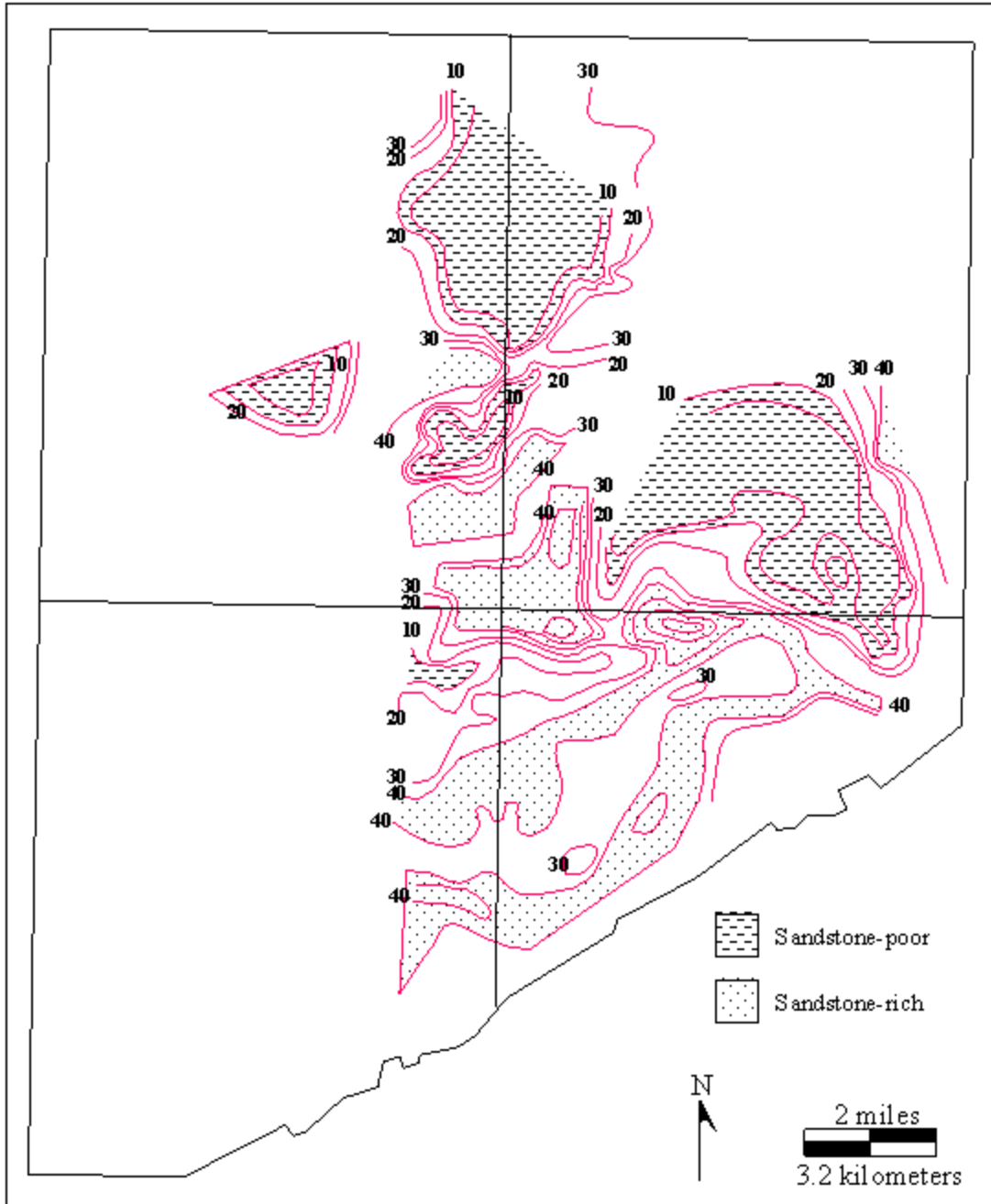


**Figure 4.11:** Isolith map of the total sandstone thickness for the Lower Elkhorn to Lower Elkhorn rider stratigraphic interval. Contour interval equals 10 feet (3 m).

amalgamate into the underlying sandstone. On the basis of cross sections, sheet, belt, and isolated sandstone geometries can be recognized within this composite sandstone interval. Also, cross-section data show that sandstone-rich areas, on the extreme eastern side of the map in Appendix 4.2.1, are the result of increasing amalgamation of different sandstone bodies within the composite interval. Overall, though, the composite sandstone body has a sheet geometry because it extends across the entire study area with no sandstone-poor areas.

The isolith map for the Lower Elkhorn rider/Upper Elkhorn No. 2 interval shows strong northwest–southeast orientations of sandstone-rich areas with little variation in orientation (Appendix 4.2.1). Other trends within the interval may be obscured because the interval is composite.

The comparison of thickness trends between the Lower Elkhorn rider/Upper Elkhorn No. 2 and the Lower Elkhorn/Lower Elkhorn rider interval shows some comparable relationships between the axes of the sandstone-rich areas in the two intervals (Appendix 4.2.2). Thickness trends for both intervals are perpendicular and offset on the western side of the map. In contrast, the two intervals are parallel and offset along the eastern side of the map.

#### 4.2.3.3 Upper Elkhorn No. 2 Split Interval

The Upper Elkhorn No. 2 split interval overlies the Lower Elkhorn rider/Upper Elkhorn No. 2 interval (Figure 4.9). This interval is defined above and below by the upper and lower benches of the Upper Elkhorn No. 2, and hence is laterally equivalent to a rock parting that separates the two main benches of the coal. Total sandstone thickness

for the Upper Elkhorn No. 2 split interval ranges from zero to more than 30 feet (9 m) (Appendix 4.2.3). The Upper Elkhorn No. 2 coal seam splits to the west along a line oriented northwest–southeast through the center of the study area (Appendix 4.2.3). Because of this splitting relationship, the sandstone body is restricted to the western half of the study area. The sandstone geometry is best defined as an isolated geometry, because laterally continuous, sandstone-poor areas border sandstone-rich areas (Appendix 4.2.3).

The isolith map shows that sandstone-rich areas for this stratigraphic interval are dominantly northwest–southeast with little variation, and closely parallel the split line for the Upper Elkhorn No. 2 coal (Appendix 4.2.3). The exception is where the northwest–southeast trend turns due west along the western side of the study area.

A comparison between the sandstone thickness trends in the Upper Elkhorn No. 2 split interval and the Lower Elkhorn rider/Upper Elkhorn No. 2 interval shows parallelism, but no other obvious stacking or offsetting relationships between the axes of the sandstone-rich areas in the two intervals (Appendix 4.2.4). Overall, the thickness trends for the two intervals are nearly parallel.

#### 4.2.3.4 Upper Elkhorn No. 2/Upper Elkhorn No. 3 Interval

The Upper Elkhorn No. 2/Upper Elkhorn No. 3 interval overlies the Upper Elkhorn No. 2 split interval (Figure 4.9). The base of this interval is defined as the top of the Upper Elkhorn No. 2 coal zone. This lower boundary is the base of the main Upper Elkhorn No. 2 seam (upper and lower benches merged), or the base of the upper bench in the areas where the coal seam is split. The top of the interval is defined as the base of the Upper Elkhorn No. 3A seam. The Upper Elkhorn No. 3A seam consists of an upper and

lower bench. Because the lower bench is laterally discontinuous, it was not chosen as the upper datum. Instead, where the two benches are separated, the upper datum is placed at the base of the upper bench. The Upper Elkhorn No. 2/Upper Elkhorn No. 3 sandstone interval ranges from zero to greater than 80 feet (24 m) in thickness (Appendix 4.2.5). This interval is composite in nature, and overall has a belt-like geometry. As with other composite intervals, different geometries can be identified within the composite section. On the basis of cross-section data, the stratigraphically lower sandstone, between the top of the Upper Elkhorn No. 2 and the true base of the No. 3, can be defined as a belt-like sandstone with isolated pods of sandstone-poor areas. The stratigraphically higher sandstone, between the two benches of the Upper Elkhorn 3A, has an isolated geometry.

The isolith map for the Upper Elkhorn No. 2/Upper Elkhorn No. 3 interval shows that sandstone-rich areas for the composite interval are dominantly oriented to the northwest–southeast, with an important variation (Appendix 4.2.5). This variation is shown along the southeastern margin of the map in Appendix 4.2.5, where a substantial sandstone-rich area is oriented northeast–southwest. The orientation of this trend turns abruptly to the northwest in two places along the south-central border of the study area.

A comparison between the Upper Elkhorn No. 2/Upper Elkhorn No. 3 interval with the Upper Elkhorn No. 2 split interval shows few relationships between the axes of the sandstone-rich areas in the two intervals (Appendix 4.2.6). On the south-central part of the map in Appendix 4.2.6 there is a parallel offset relationship between the two intervals. Otherwise, no other trends are apparent between the two sandstone bodies. In general, the thickness trends for the two intervals are parallel.

#### 4.2.3.5 Upper Elkhorn No. 3 Coal Zone Interval

The Upper Elkhorn No. 3 zone interval overlies the Upper Elkhorn No. 2/Upper Elkhorn No. 3 interval (Figure 4.9). The top of the Upper Elkhorn No. 3 zone interval is defined as the base of the uppermost bench of the Upper Elkhorn No. 3 coal zone, and the base of the interval is defined as the base of the Upper Elkhorn No. 3A seam. The middle bench of the Upper Elkhorn No. 3 coal zone, the Upper Elkhorn 3B bench, is not laterally continuous over the study area, and does not provide a suitable bounding datum.

Sandstone thickness for the Upper Elkhorn No. 3 zone interval ranges from zero to greater than 80 feet (24 m) in thickness (Appendix 4.2.7). This sandstone interval is composite and consists of numerous, unrelated sandstone bodies. The composite interval as a whole, though, has a belt-like geometry with isolated pod-shaped, sandstone-poor areas.

Isolith maps for the Upper Elkhorn No. 3 zone interval shows sandstone-rich areas with northeast–southwest, northwest–southeast, and east–west orientations (Appendix 4.2.7). A very prominent change in orientation is found near the east-central to south-central part of the map in Appendix 4.2.7, where a northwest–southeast trend abruptly changes in orientation to northeast–southwest. In addition, in the southeastern corner of the study area, there is a poorly defined northeast–southwest trend.

A comparison of the Upper Elkhorn No. 3 zone interval with the underlying Upper Elkhorn No. 2/Upper Elkhorn No. 3 interval shows some similarities between the axes of the sandstone-rich areas between the two intervals (Appendix 4.2.8). A strong parallel and stacked relationship is shown near the center of the map in Appendix 4.2.8, as well as a weaker example of this relationship in the north-central part of the map.

There is also a parallel and offset relationship on the eastern side of the map in Appendix 4.2.8, but this relationship is unclear because the sandstone-rich areas are broad and nearly perpendicular. Overall, the thickness trends for the two intervals are perpendicular to each other.

#### 4.2.3.6 Upper Elkhorn No. 3/Upper Elkhorn No. 3 ½ Interval

The Upper Elkhorn No. 3/Upper Elkhorn No. 3 ½ interval overlies the Upper Elkhorn No. 3 zone interval (Figure 4.9). The top of the interval is defined as the base of the Upper Elkhorn No. 3 ½ coal seam, and the base of the interval is defined as the base of the uppermost bench of the Upper Elkhorn No. 3 coal zone. The Upper Elkhorn No. 3 coal zone/Upper Elkhorn No. 3 ½ interval ranges in thickness from zero to greater than 80 feet (24 m) (Appendix 4.2.9). The isolith map shows that the interval has a more isolated geometry bounded by laterally continuous sandstone-poor areas.

The sandstone-rich areas in this interval are oriented to the northwest–southeast, with little variation (Appendix 4.2.11). One exception is along the eastern side of the map, where a northwest–southeast trend abruptly changes orientation to northeast–southwest.

A comparison between the Upper Elkhorn No. 3/Upper Elkhorn No. 3 ½ interval and Upper Elkhorn No. 3 zone interval shows some similarity between the axes of the sandstone-rich areas in the two intervals (Appendix 4.2.10). A parallel and stacked relationship is shown near the center of the map in Appendix 4.2.10, and near the north-central part of the figure. In other areas, the trends are perpendicular, or cover too broad an area to make a comparison. Overall, the thickness trends for these two intervals are nearly parallel.

#### 4.2.3.7 Upper Elkhorn No. 3 ½ /Amburgy Interval

The Upper Elkhorn No. 3 ½ /Amburgy interval overlies the Upper Elkhorn No. 3/Upper Elkhorn No. 3 ½ interval (Figure 4.9). The top of this interval is defined as the base of the Amburgy A coal, and the base of this interval is defined as the base of the Upper Elkhorn No. 3 ½ coal. The Upper Elkhorn No. 3 ½ /Amburgy sandstone interval ranges in thickness from zero to 90 feet (Appendix 4.2.11). This interval has a sheet-like geometry overall, even though the isolith map for this interval shows a poorly defined zero isolith contour in the northeastern quarter of the study area. This interval may be an example of a scale-dependent belt geometry, where the belt extends beyond the study area.

Sandstone-rich areas in the Upper Elkhorn 3 ½ /Amburgy interval are oriented to the northwest–southeast, with little variation (Appendix 4.2.11). One feature to note is that the dominant sandstone-rich area bifurcates in the south-central part of the study area, where the eastern fork extends to the northwest through the remainder of the study area.

A comparison between the Upper Elkhorn 3 ½ /Amburgy and the Upper Elkhorn No. 3/Upper Elkhorn 3 ½ interval shows two important relationships between the axes of the sandstone-rich areas in both intervals (Appendix 4.2.12). On the southeastern quarter, along the southwestern edge, and on the north-central part of the map in Appendix 4.2.12, there is a parallel and stacking relationship between the two intervals. In addition, on the south-central part of the map in Appendix 4.2.12 there is a parallel and offsetting relationship between the two intervals. Overall, thickness trends within this interval tend to parallel the thickness trends for the underlying interval.

#### 4.2.3.8 Amburgy Split Interval

The Amburgy split interval overlies the Upper Elkhorn 3 ½ /Amburgy interval (Figure 4.9). This interval is defined above and below by the upper and lower benches of Amburgy coal, and hence is laterally equivalent to a rock parting that separates the two main benches of the coal body. The Amburgy split sandstone interval ranges in thickness from zero to greater than 70 feet (21 m) (Appendix 4.2.13). This sandstone interval has a belt-like geometry.

The isolith map for the Amburgy split interval shows that sandstone-rich areas for the interval are dominantly oriented northeast–southwest and east–west (Appendix 4.2.13). The exceptions to these trends are found in the southwestern and northeastern quarters of the map in Appendix 4.2.13. In these areas, two separate thickness trends are northwest–southeast, perpendicular to the average trend. Also of note is an abrupt change in the orientation of the thickness trends from northeast–southwest to east–west near the center of Appendix 4.2.13.

A comparison of the Amburgy split interval and Upper Elkhorn 3.5/Amburgy interval shows that there are no clear similarities between the axes of sandstone-rich areas in the two intervals (Appendix 4.2.14). Some stacking occurs in the central, southeast quarter and southwestern quarter of the map in Appendix 4.2.14. In general, the trends between the two maps are perpendicular or oblique in some way.

#### 4.2.4 Analysis of Isolith Profiles

Isolith profiles were used to compare total sandstone thickness between intervals to better characterize stacking and offsetting relationships between intervals, which may be obscured on isolith maps and traditional cross sections. Five profiles and two cross

sections were created for the four-quadrangle study area (Figure 4.12). These profiles were chosen and drawn through areas of the greatest data density, and areas chosen from isolith maps that were thought to show stacking and offsetting relationships. In order to compare the difference between isolith profiles and cross sections, two traditional cross sections were made parallel to the lines of section for the A-A' and B-B' profiles (Appendix 4.3.1 and 4.3.2).

Thickness trends along profile A-A' (Figure 4.13) show some stacking relationships between most intervals, at the northeast end of the line of section. The exception is the Upper Elkhorn 3 1/2/Amburgy interval, which is offset and thickens to the southwest, especially toward the middle of the profile. This central thickening matches a similar trend in the underlying Upper Elkhorn No. 2/Upper Elkhorn No. 3 and Upper Elkhorn No. 3 zones, as well as in the Amburgy split interval. Thickness trends on the southwestern side of the profile appear to be dominantly offset in all intervals.

The relationships shown along profile B-B' (Appendix 4.3.3) are largely unclear because the profiles show fairly uniform sandstone thickness across all the intervals. There is, however, a stacking relationship between the Lower Elkhorn/Lower Elkhorn rider and Lower Elkhorn/Upper Elkhorn No. 2, Upper Elkhorn No. 2/Upper Elkhorn No. 3, and Upper Elkhorn 3 1/2/Amburgy intervals in the northwestern end of the profile. The Upper Elkhorn No. 3 interval is offset to this trend and thickens to the south. There is a stacked relationship between the Upper Elkhorn No. 3, Upper Elkhorn No. 3/Upper Elkhorn 3 1/2, Upper Elkhorn 3 1/2/Amburgy, and Amburgy split intervals on the southeastern side of the profile.

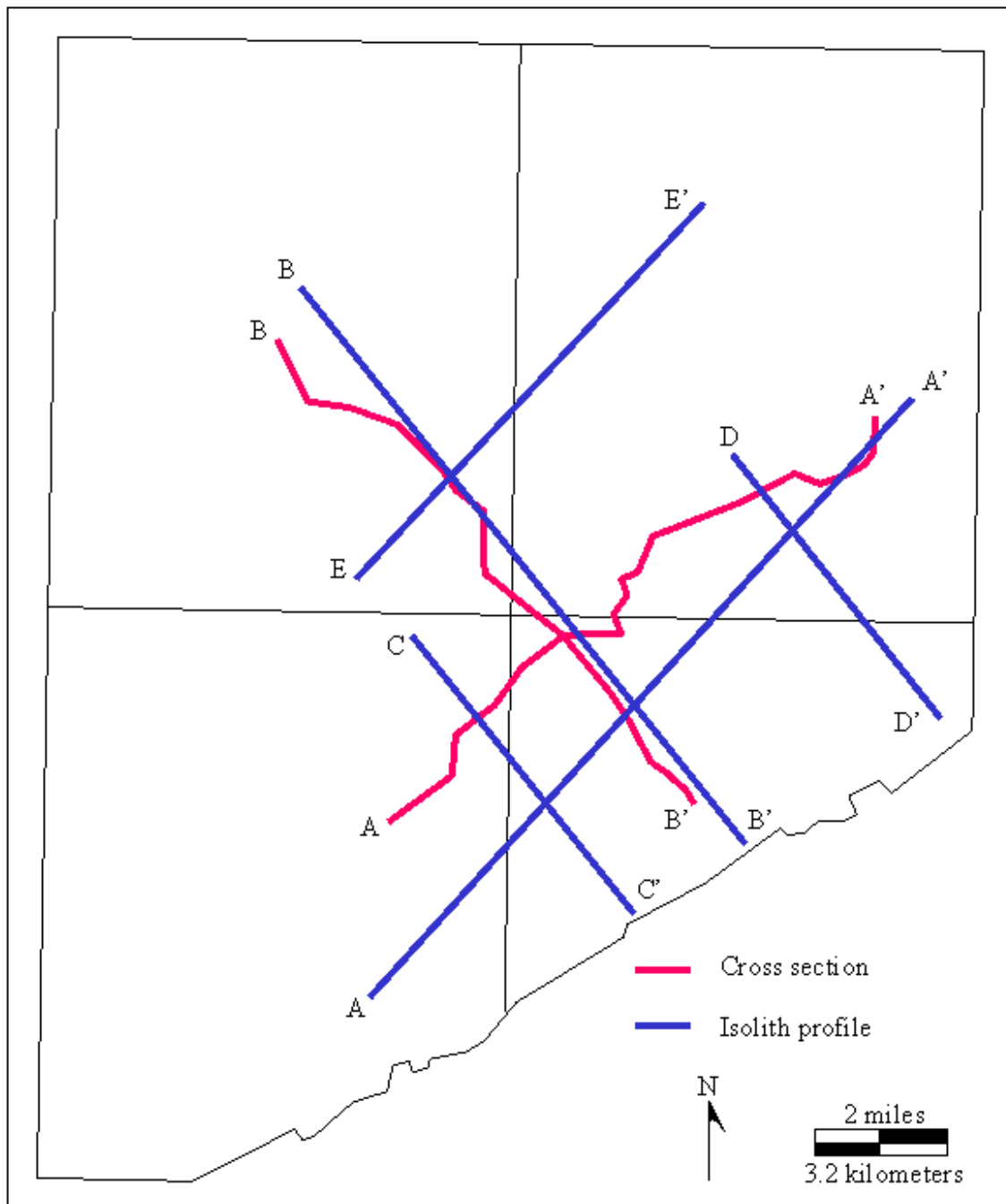


**Figure 4.12:** Locations of cross sections (red) and isolith profiles (blue) within the four-quadrangle study area.

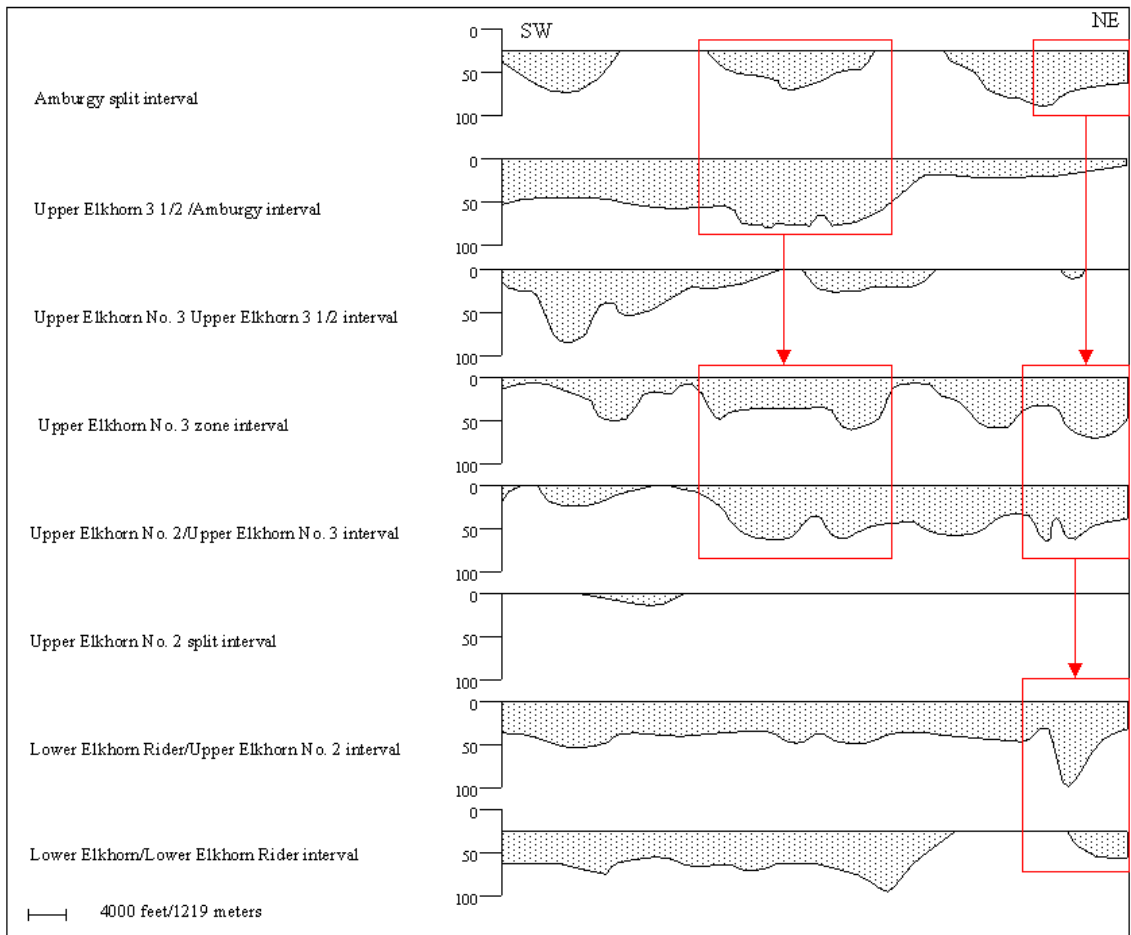


**Figure 4.13:** Total sandstone thickness isolith profile A-A'. Stacking relationships shown by the red boxes. Thickness values are in feet (e.g., 0 ft, 50 ft, 100 ft).

The relationships shown along profile C-C' are mixed (Appendix 4.3.4). The Lower Elkhorn/Lower Elkhorn rider and Lower Elkhorn rider/Upper Elkhorn No. 2 intervals show a stacking relationship along the profile to the southeast. There is also a stacked relationship for the Upper Elkhorn No. 2/Upper Elkhorn No. 3, Upper Elkhorn No. 3 zone, and Amburgy split intervals, but these intervals are stacked to the northeast. The Upper Elkhorn No. 3/Upper Elkhorn 3 ½ interval also shows a stacked relationship to these groups. The Upper Elkhorn 3/Upper Elkhorn 3 ½ and Upper Elkhorn 3 ½/Amburgy intervals show a thickening to the southeast, which may correspond to a stacked relationship to the latter groups. The Upper Elkhorn No. 2 split interval is too thin to show a clear stacked or offset relationship to any of the intervals.

The relationships shown along profile D-D' are mixed (Appendix 4.3.5). The Lower Elkhorn/Lower Elkhorn rider intervals appear to be stacked toward the southern end of the profile. This part of the profile is incomplete due to a lack of data. The Upper Elkhorn No. 2/Upper Elkhorn No. 3 and Upper Elkhorn No. 3 zone intervals offset to one another. The Upper Elkhorn No. 3 zone shows stacked relationships to the Upper Elkhorn 3 ½ /Amburgy and Amburgy split intervals, and an offset relationship between the Upper Elkhorn No. 3/Upper Elkhorn 3 ½ interval.

The relationships shown along profile E-E' differ from the previous profiles (Appendix 4.3.6). The Lower Elkhorn/Lower Elkhorn rider and Lower Elkhorn rider/Upper Elkhorn No. 2 intervals are offset in the center of the profile. The relationship between the Upper Elkhorn No. 2/Upper Elkhorn No. 3 and Upper Elkhorn No. 3 zone is unclear, but the latter is clearly offset to the Upper Elkhorn No. 3/Upper

Elkhorn No. 3 ½ zone. The relationships between the Upper Elkhorn No. 3/Upper Elkhorn No. 3 ½ and Amburgy split interval to other intervals are unclear.

#### 4.2.5 Summary of Stratigraphic Intervals

Isolith maps, profiles, and cross sections were used to characterize the geometries of sandstone bodies within defined stratigraphic intervals overlying and including the Lower Elkhorn coal. Using all available data, four sandstone body geometries were identified: (1) sheet, (2) belt, (3) isolated, and (4) composite. Sheet, belt, and isolated sandstone geometries correspond to individual sandstone bodies, whereas composite sandstone bodies correspond to an arbitrary grouping of adjacent sandstone bodies that are, at least in some of the area, separated by fine-grained, nonsandstone lithologies.

Isolith maps were used to show general thickness trends of total sandstone thickness for each stratigraphic interval. Most isolith maps show a strong northwest–southeast orientation of sandstone-rich areas. Some parts of the maps deviate from this trend and are oriented northeast–southwest. The linear nature of sandstone-rich areas and character of adjoining strata imply deposition in a channel setting. In addition, a dominant northwestward orientation of sandstone-rich areas suggests a northwest paleoslope or structural trend controlling these fluvial systems. The paleoslope concept is supported by regional, northwestward dip of all coal beds within the study area as well as previous investigations (Davis and Ehrlich, 1974; Ferm, 1974). Deviations from the northwest–southeast trend may have resulted from structural control, which captured and diverted paleochannels to a northeast or southwest orientation. Furthermore, some sandstone-rich areas for many intervals show a parallel stacked relationship or a parallel offset relationship. These relationships are important when

identifying the controlling mechanism of sandstone distribution. Stacked relationships imply structural control, whereas offsetting relationships imply differential compaction controls.

Isolith profiles can be used to demonstrate stacking and offsetting relationships. The results of the profiles for this study, however, returned mixed results. For example, some intervals show stacking in almost all profiles, such as the Lower Elkhorn/Lower Elkhorn rider and Lower Elkhorn rider/Upper Elkhorn No. 2 interval. On the other hand, the profile shown in Figure 4.13 shows stacking on one side of the profile between almost all intervals, but offsetting relationships on the opposite side. Furthermore, relationships are harder yet to determine in profiles that traverse areas with uniform sandstone thickness, like the profile shown in Appendix 4.3.3.

Comparing the thickness trends for adjacent intervals is important to show stacking or offsetting relationships. Comparing two or more isolith maps is difficult because it is hard to differentiate between the many trends (thick and thin sandstone) within successive intervals. Summarizing the isolith maps by highlighting the axes of sandstone-rich areas can help clarify the linear thickness trends, but comparing more than two intervals using this method can create very confusing maps. Trend-surface residual analysis was used to clarify sandstone thickness trends. Trend-surface residuals are useful because residual maps show only those areas that deviate from an average trend such as thick or thin sandstone.

## 4.3 Quantitative Comparison of Coal Measure Data to Geologic Structure

### 4.3.1 Background

The distribution, orientation, and character of paleochannels in southeastern Kentucky may be influenced by a number of factors: (1) drainage alignments parallel to regional paleoslope, (2) restriction by laterally adjacent coal bodies, (3) differential compaction and offsetting of sequential sandstone bodies, and (4) diversion from regional drainage patterns by synsedimentary faulting. Pervasive northwest trends of sandstone bodies in the study area are likely caused by a regional northwest paleoslope. Other orientations could be related to either of the two other mechanisms. If synsedimentary faults were continuously reactivated during deposition of the coal-bearing sequences, it would be expected that greater thickness of sandstone would be localized on downthrown fault blocks and that this would be repeated over time. In order to test this hypothesis, trend-surface residual analysis was used to quantitatively measure sandstone distribution relative to geologic structure for successive stratigraphic intervals.

Trend-surface residual analysis was used in order to better characterize sandstone thickness trends, and to show stacking and offsetting relationships between adjacent intervals within the study area. By testing first-, second-, and third-order trend surfaces against the coal exploration data it was decided that a second-order trend surface best represents the thickness trends for all intervals, which agrees with a similar study done by Cornett (2002). Second-order trend surfaces were calculated for total sandstone thickness in all intervals except the Upper Elkhorn No. 2 split interval. Positive and negative residuals from the trend surface for each data point were derived and contoured.

The Upper Elkhorn No. 2 split interval was excluded because of limitations in the methodology, which will be discussed later.

Residuals for each interval were compared to those of the overlying interval using logical grid algebraic functions. Stacking relationships, positive or negative, should continually overlap from interval to interval, indicating that structural control is likely the controlling mechanism of sandstone distribution. The residual data for each interval was gridded using regular point kriging. Grid dimensions, the maximum direction of X and Y axes, were defined on the basis of maximum extent of data. The same grid dimensions were used for each interval so that they could be analyzed using the grid|math tool in Surfer 8. Next, after all grids were generated, they were mathematically analyzed to show only those areas of overlap between like residuals. This analysis was done using the conditional statement:

$$C = \text{if } (A < 0 \text{ AND } B < 0, A + B, 0) \text{ OR if } (A > 0 \text{ AND } B > 0, A + B, 0),$$

where C is the resulting grid, A is the underlying residual grid, and B is the overlying residual grid. The statement requires that the two grids will be algebraically summed only if a grid node in the underlying grid and corresponding grid node in the overlying grid have stacked positive or stacked negative values (Figure 4.14). If the residuals for the two grids have opposite signs (offset relationship), those areas of the resulting grid will be assigned a value of zero. This method removes offsetting relationships and sums stacked relationships.

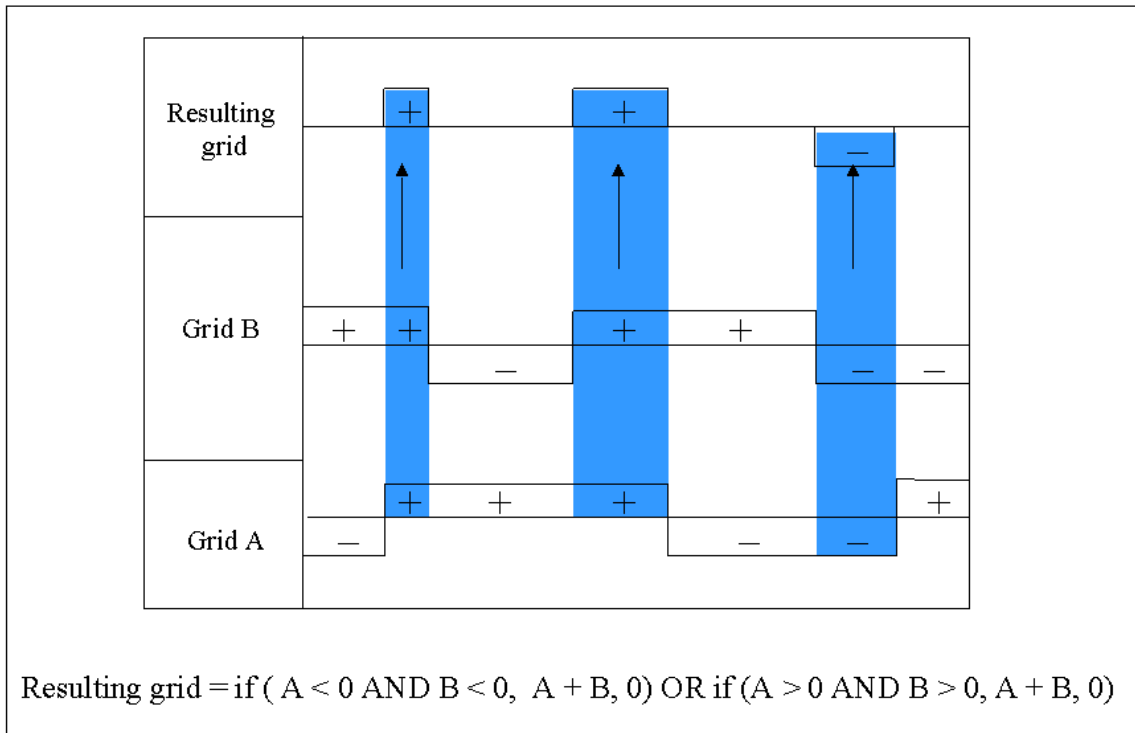


**Figure 4.14:** Diagram showing the algebraic method of stacking residual grids for comparison of stratigraphic intervals. Like values are recorded in the resulting grid. That resulting grid is then compared to the next stratigraphically younger grid horizon, and a new resulting grid is calculated. This method is continued to the top of the stratigraphic profile studied so that there is one remaining resulting grid for the study interval.

Using this methodology, the Upper Elkhorn No. 2 split interval had to be excluded from the analysis. First, the sandstone body for this interval is not present in all quadrangles resulting in zero thickness for two of the four quadrangles, which equals no trend. Thus, a trend-surface analysis could not be done in the same manner that was done for previous intervals. Second, if a trend-surface analysis had been done only for those quadrangles that did contain the sandstone body, the grid could not have been mathematically stacked with other grids because all grids must have the same extent in order to be analyzed with the algebraic function defined above.

Adding grids based on a conditional statement differs from the method used by Liu (1992) and Cornett (2002). Their method algebraically adds two residual grids together using the function:

$$C = (A + B),$$

where A and B are residual grids for two different intervals and C is the resulting grid. When adjacent grids are added in this manner, instead of considering only overlapping values, the stacking versus offsetting relationship on the resulting map is less definitive. The problem arises from the fact that if a negative grid node in one grid is much smaller than the corresponding positive node in the second grid, the end result is a positive value for the grid node, or vice versa. Thus, using this method may give false indications of stacked positive and negative residuals.

The method of using stacking relationships of sandstone bodies between stratigraphic intervals to locate faults is imperfect because any offsetting relationships

would mask the identification of overlying stacking trends when the maps are compared using the conditional statement method. In order to overcome this methodological problem, coal-seam structure was analyzed using trend-surface residuals. Coal-seam structure was used because if an underlying structure was active at any time during deposition of the study intervals, or subsequently, the expression of the underlying structure should be manifested in all coal seams between those intervals.

Trend-surface residual analysis for the base-of-coal structure was performed using the same methodology used for the total sandstone thickness. Base-of-coal structure was considered only for the most laterally persistent coal seams or coal horizons. The laterally persistent coal seams are: the Lower Elkhorn, Lower Elkhorn rider, Upper Elkhorn No. 2, Upper Elkhorn No. 3A, Upper Elkhorn 3 ½, and Amburgy A coal seams.

#### 4.3.2 Map Analysis of Total Sandstone Thickness Residuals

All intervals were stacked and analyzed for overlap. During the course of this analysis it was determined that the total sandstone thickness residuals for two intervals, the Lower Elkhorn rider/Upper Elkhorn No. 2 and Upper Elkhorn 3 ½ and Amburgy intervals, do not stack with the other intervals, but show an offsetting relationship to them. Thus, the map shown in Figure 4.15 is the cumulative overlap for all other intervals, excluding the Lower Elkhorn rider/Upper Elkhorn No. 2 and Upper Elkhorn 3 ½ /Amburgy intervals (Figure 4.9).

The results of the stacked total sandstone residual map are a scattered distribution of positive and negative cumulative residuals (Figure 4.15). At first, the distribution appears to be random, but using the stacking model, which assumes structural control,

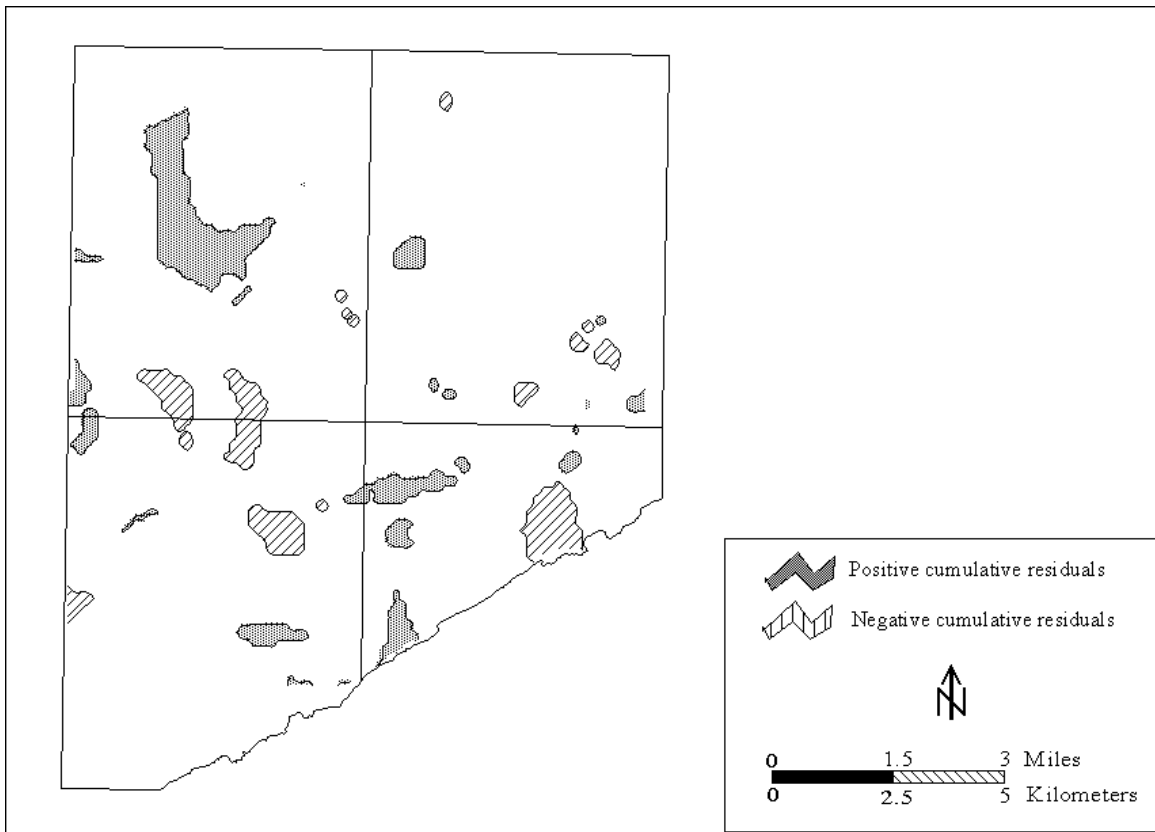


**Figure 4.15:** Cumulative second-order residual map for total sandstone thickness for all intervals except the Lower Elkhorn rider/Upper Elkhorn No. 2, and Upper Elkhorn No. 3/Upper Elkhorn 3 ½ intervals.

lines were subjectively placed on the map showing the position of possible faults (Figure 4.16). Cumulative negative residuals (sandstone-poor areas) were considered to be the upthrown side of the fault, and cumulative positive residuals (sandstone-rich areas) were considered to be the downthrown side. The inferred faults have two trends, either to the northeast–southwest or northwest–southeast, and show a down-to-the-south or southeast sense of movement. The orientation of these trends corresponds to total sandstone thickness trends for the stratigraphic intervals defined in the previous section.

#### 4.3.3 Map Analysis of Coal Structure Residuals

The cumulative stacked coal-seam structural residual map (Figure 4.17) shows similar trends as the total sandstone thickness map. The coal-seam structure residual map shows scattered, but more extensive, stacked positive and negative residuals. Again, lines were placed on the map to delineate trends in the distribution of residuals (Figure 4.18). These lines were considered to be the location of possible faults. For the coal seam structure, positive residuals — areas that are structurally higher than the regional trend — are considered to be the upthrown side of a fault. Negative residuals — areas that are structurally lower than the regional trend — are considered to be the downthrown side. These inferred faults have similar northeast–southwest and northwest–southeast orientations and down-to-the-south sense of movement. These fault orientations and sense of movement are similar to those identified using total sandstone thickness residuals (Figure 4.16).

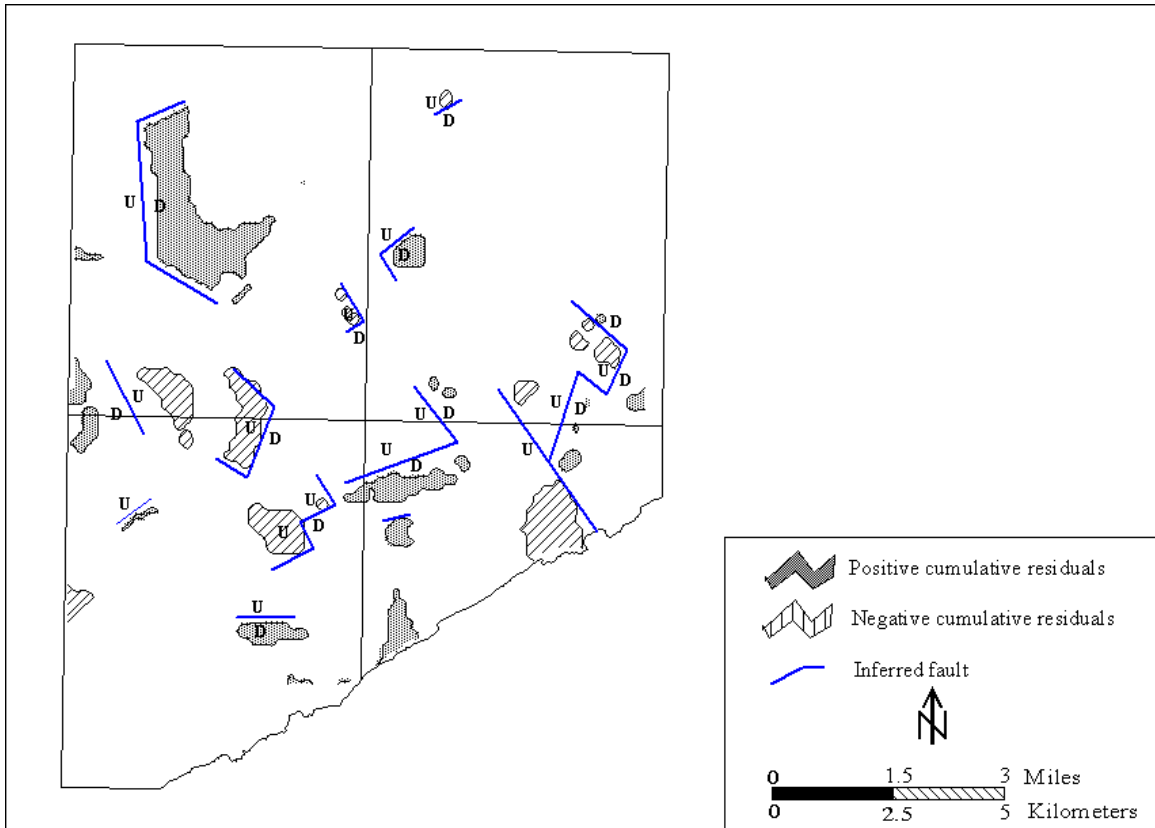


**Figure 4.16:** Cumulative residual map of total sandstone thickness showing the location of inferred faults.

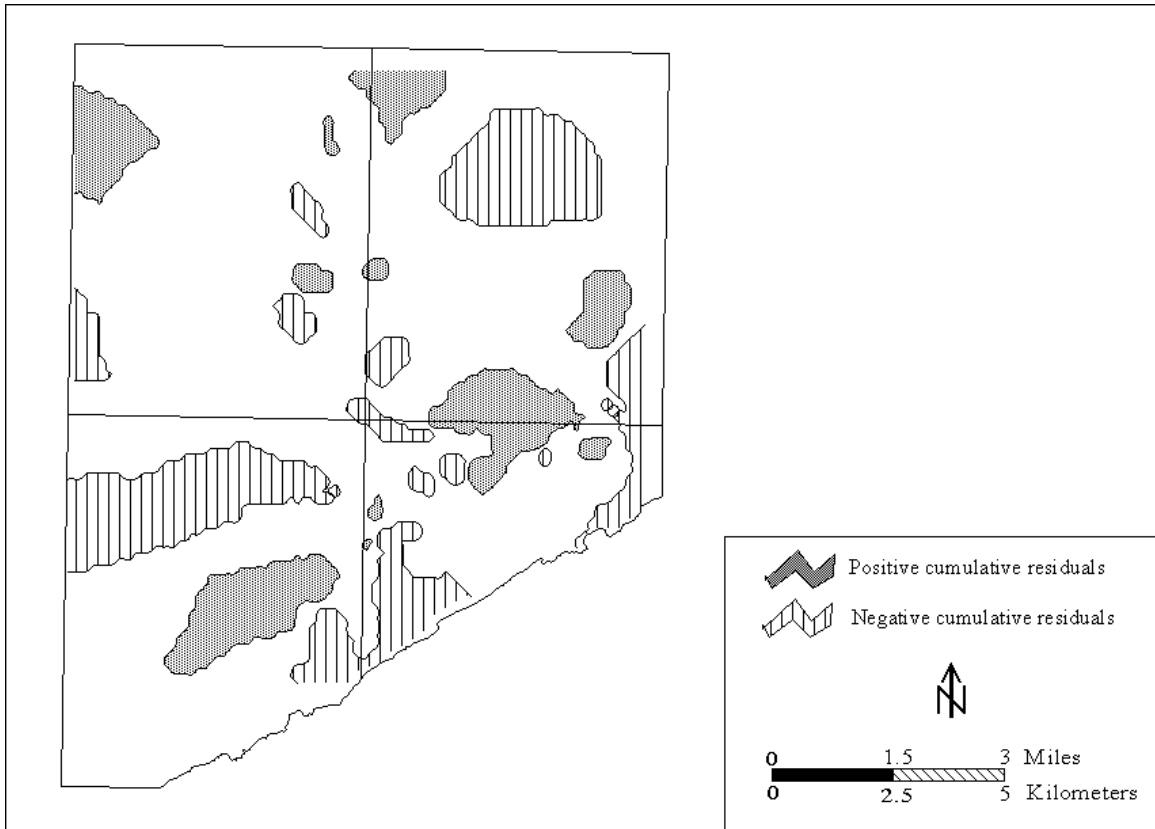


**Figure 4.17:** Cumulative residual map of coal-seam structure for laterally persistent coal horizons.

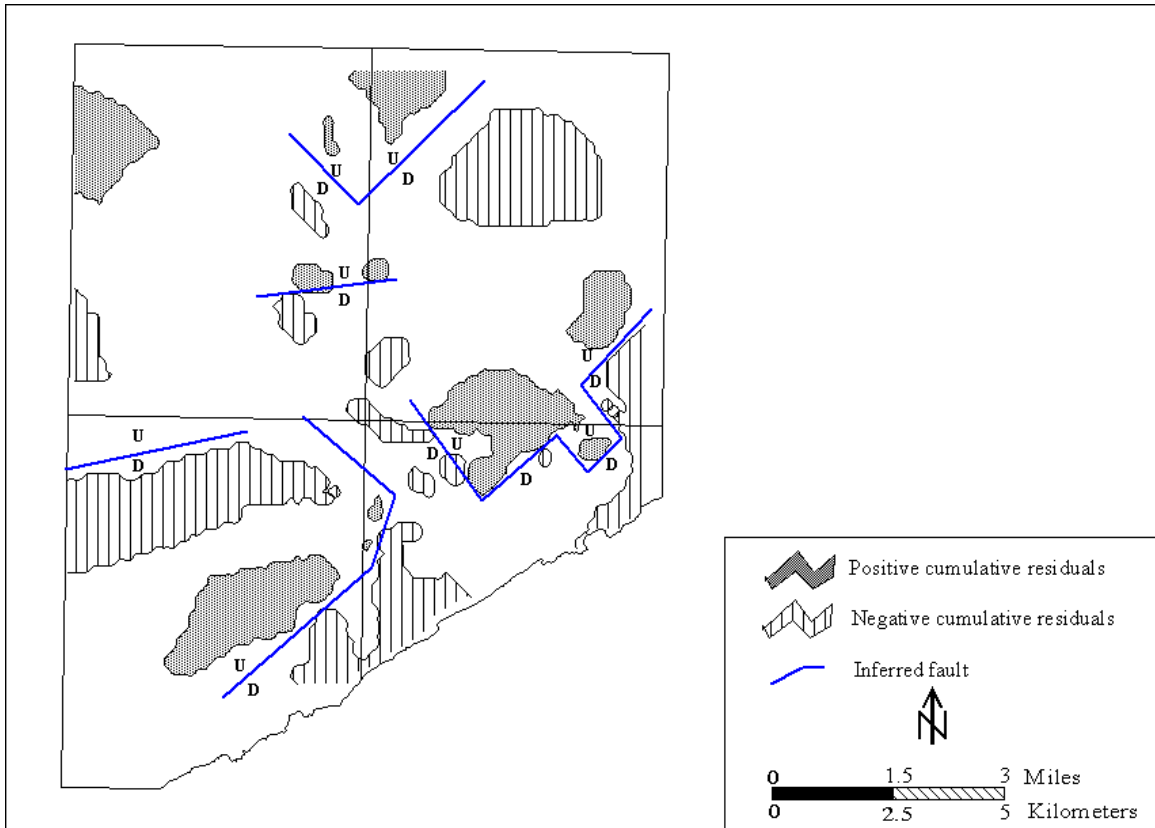


**Figure 4.18:** Cumulative residual map of coal-seam structure showing the location of inferred faults.

#### 4.3.4 Regional Coal-Seam Structure

The Lower Elkhorn coal-seam structure for the Eastern Kentucky Coal Field was studied in order to identify regional structures and relate them to those structures identified within the study area. Coal seam structure for the Lower Elkhorn coal (Thacker et al., 1998) shows a large regional syncline (the Eastern Kentucky Syncline), along with a number of smaller antiform/synform pairs along its southeastern limb (Figure 4.19). Some of these latter structures have been given names such as the Belfry Anticline, whereas others have not been named, but are equally as prominent. The orientation of these structures is dominantly northeast–southwest, which is parallel to those structures identified within the study area using trend-surface analysis. Furthermore, the southwestern end of the Belfry Anticline, along with an associated, unnamed structure to the north, project into the four-quadrangle study area.

#### 4.3.5 Summary of Residual Analysis

The analysis of total sandstone and coal-seam structure defined northeast–southwest- and northwest–southeast-oriented structures with a down-to-the-south or southeast sense of movement. When Figures 4.16 and 4.18 are overlain, the faults on both maps parallel or intersect with adjacent faults with similar orientations and movement (Figure 4.20). The map shown in Figure 4.20 shows faults that are discontinuous on individual maps (Figures 4.16 and 4.18), but combine to form more laterally continuous structures. An example of this is shown along the southeastern side of the study area (Figure 4.20). Also, smaller, more independent structures are shown in the north-central, south-central, and northeastern parts of the map.

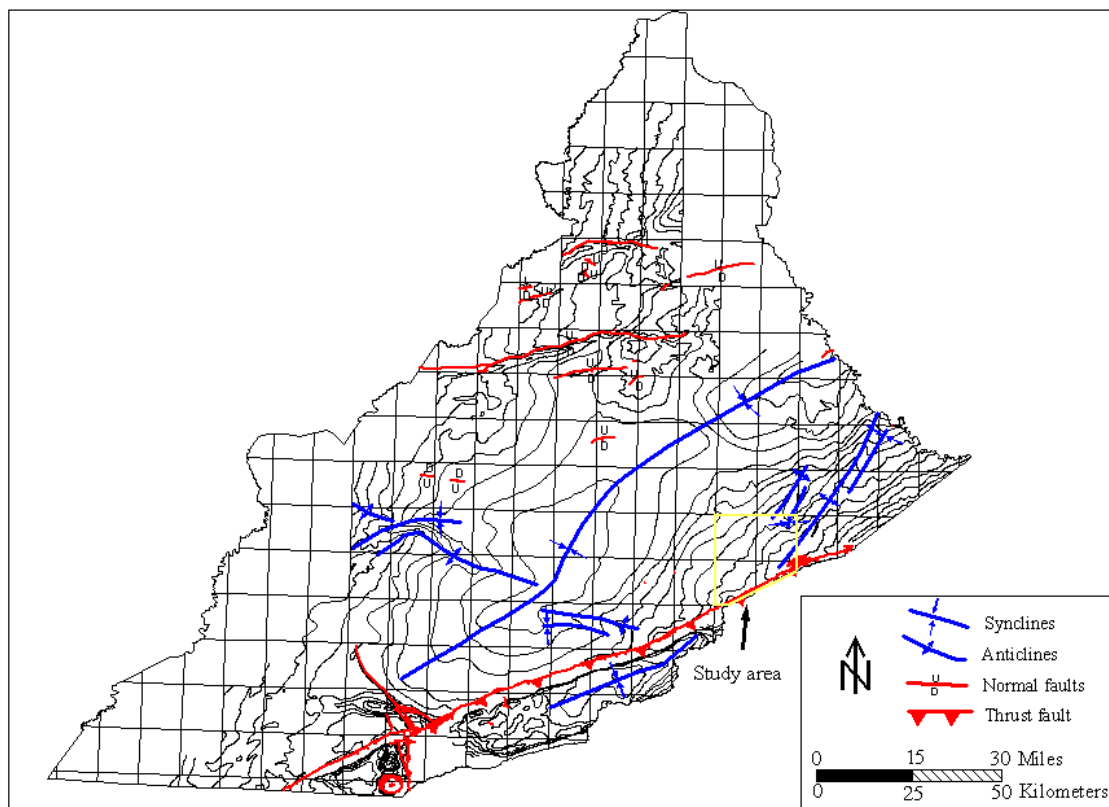


**Figure 4.19:** Regional structure map of the Lower Elkhorn coal showing the location of geologic structures. The four-quadrangle study area is highlighted in yellow.

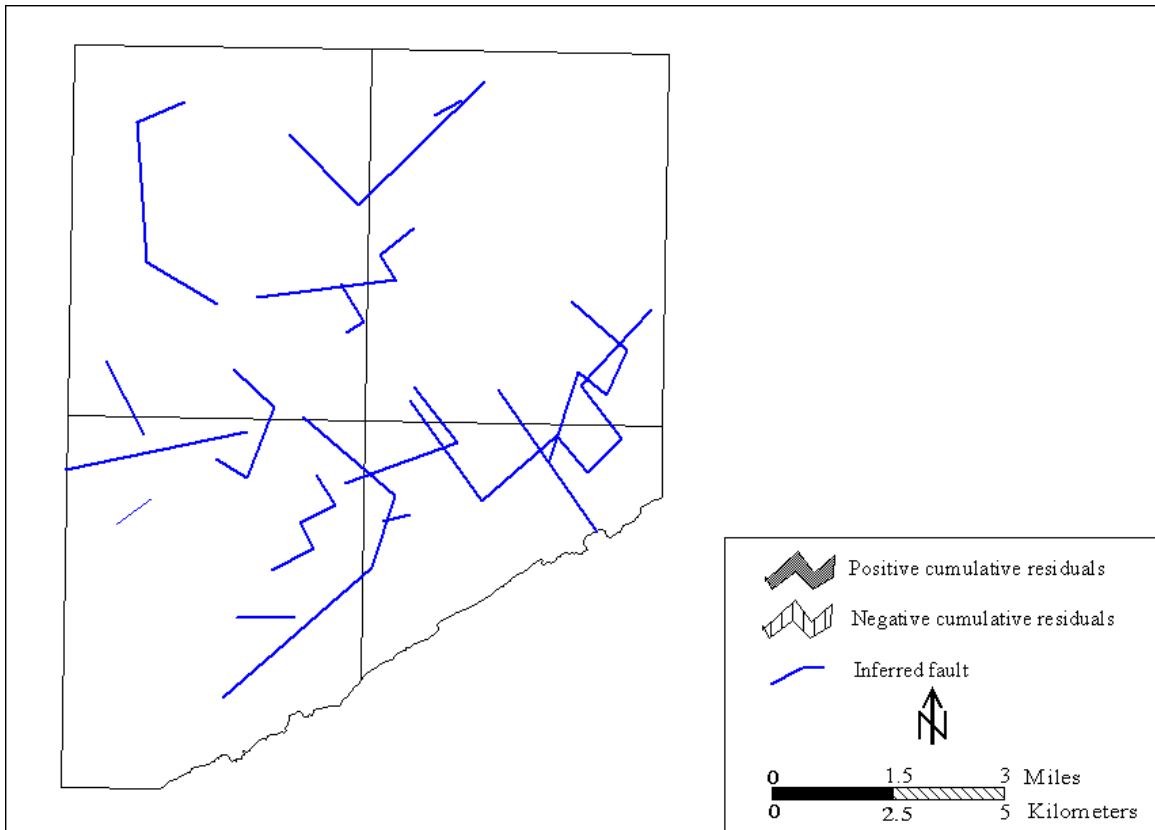


**Figure 4.20:** Map showing the relationship between inferred faults identified using total sandstone thickness residuals and coal-seam structure residuals.

The scale and regional extent of structures expressed on the regional Lower Elkhorn coal seam structure map suggest that their development may have been controlled by a deeper structure. In addition, some previous workers have attributed structures, such as the Belfry Anticline, to faults in the Mississippian System or deeper-seated basement faults (Raione et al., 1991; Hower et al., 1991). This trend is parallel to the D'Invilliers Basement Fault (Drahovzal and Noger, 1995).

A stratigraphic horizon below the Pennsylvanian System was chosen for structural analysis in order to identify deep faults that may be related to faults identified using residual analysis, and structures observed on the Lower Elkhorn coal seam structure map. If structures found during residual analysis are related to deeper structures, they should show up in the deeper strata. The stratigraphic top of the Mississippian Newman Limestone was chosen for analysis because of the large amount of elevation data available for this horizon, and because it is below the Pennsylvanian section. The objective of this analysis is to identify older faults that may have affected deposition of the Pennsylvanian System, and to use the trace of those faults to help predict channel-related mining problems ahead of mining.

#### 4.4 Identification of Structural Lineaments within the Newman Limestone

##### 4.4.1 Background

The upper Mississippian Newman Limestone is a prominent rock unit that is easily identified on oil and gas geophysical logs; it was studied to detect the presence of geologic structures that underlie the Pennsylvanian System. The vertical difference between the Newman Limestone and the Lower Elkhorn coal (base of the study section)

varies from 600 feet (183 m) in the north to more than 2,000 feet (609 m) in the south (Figure 2.3). A structure contour map was made for the top of the Newman Limestone across the Eastern Kentucky Coal Field using 7,189 data points (regional data set) in order to show the general structural trends for that horizon (Figure 4.21). The elevation data were contoured using the normal point kriging method and contoured with 50-foot (15-m) intervals.

Two subsets of the original 7,189 data points were selected and gridded independently in order to remove the effects of regional structural trends. The first subset was selected to show regional structures and consists of approximately 2,754 data points (subset Q-36; 36 quadrangles) selected from the regional data set (7,189 data points) (Figure 4.21). The second subset was chosen to analyze regional structures identified using subset Q-36 in more detail. This second subset consisted of 969 data points (subset Q-12; 12 quadrangles) chosen from the Q-36 data, for the four-quadrangle study area and surrounding eight quadrangles (Figure 4.21). A structure map was prepared only for the Q-12 data subset because this data set is the most critical to the four-quadrangle study area and surrounding quadrangles. The Q-12 data set was contoured using the normal point kriging method with 50-foot (15-m) intervals.

Second-order derivative maps of the top of the limestone were calculated to show areas of high dip. These maps were prepared for both subsets Q-36 and Q-12 in order to locate areas of increased dip and identify the location of lineaments, which are inferred to be potential faults. Dip maps are shown as continuous grids (referred to as image maps by Surfer 8) classified by degrees of dip, and displayed using a color ramp scale.

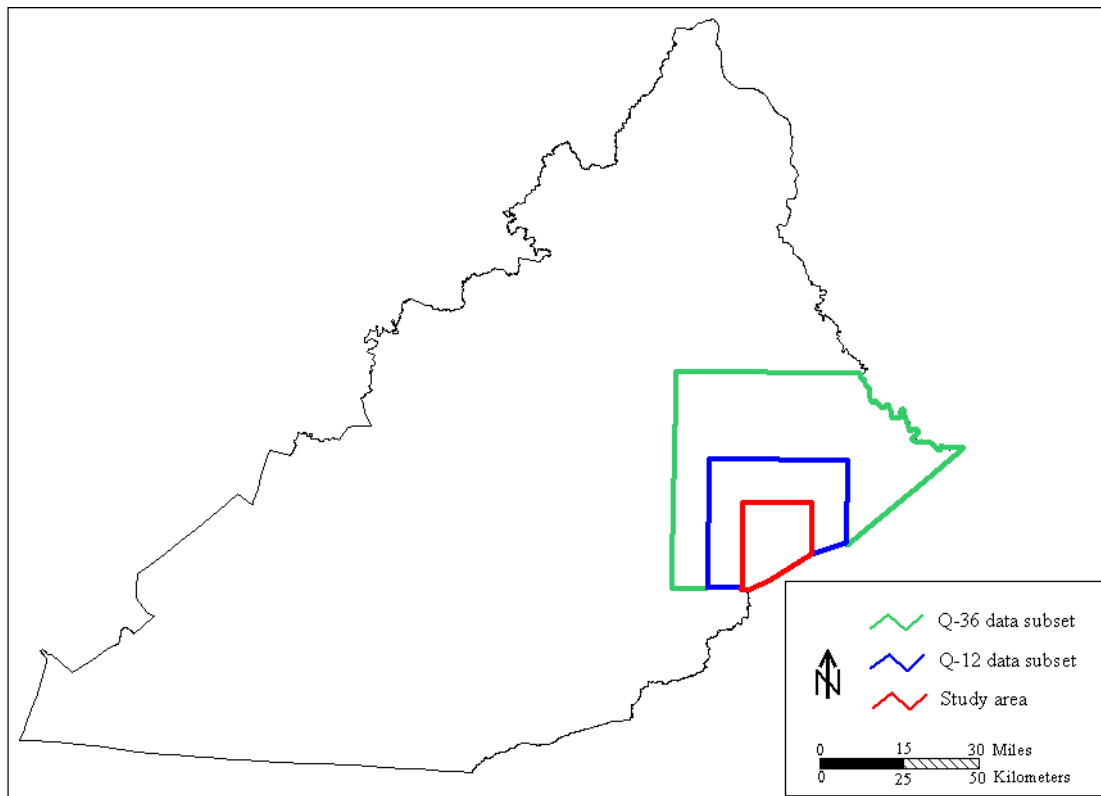


**Figure 4.21:** The location of data subsets within the context of the Eastern Kentucky Coal Field.

#### 4.4.2 Newman Limestone Structural Lineaments

The regional structure map (Eastern Kentucky Coal Field) for the Newman Limestone shows that structural dip is consistently to the south and southeast (Figure 4.22), unlike structural dips for the Lower Elkhorn coal, which reflect a synclinal structure that dips to the northwest along its southern limb. The structural relief shown on the Newman Limestone structure map is more than 2,800 feet (853 m) from the northwestern edge of the map to the Virginia border. The trends of structure contours shown on the map indicate that the structural strike for the top of the Newman Limestone has northeast–southwest and northwest–southeast orientations (Figure 4.22). In places, contours show areas of increased dip and/or northeast–southwest strike orientations abruptly changing to northwest–southeast orientations.

A structure contour map was created for the local subset Q-12 (969 data points) in order to identify structural lineaments (possible faults) in the Newman Limestone within the four-quadrangle study area and surrounding quadrangles (Figure 4.23). Analysis of Figure 4.23 shows that the orientations of structural contours are similar to the regional map (Figure 4.22), but the contours show local structural trends in greater detail. After the general orientations of the structural trends were assessed, structural contours were visually analyzed for significant changes in elevation over a short horizontal distance (increased dip) or abrupt changes in the orientation of structural contours. Any structural contours that showed increased dip or changes in orientation were noted and compared with the surrounding data points. If the selected structural contours and data points indicated a decrease in structural elevation equal to or greater than 50 feet (15 m) per mile (1.6 km), a line was drawn parallel to that trend defining a Newman Limestone

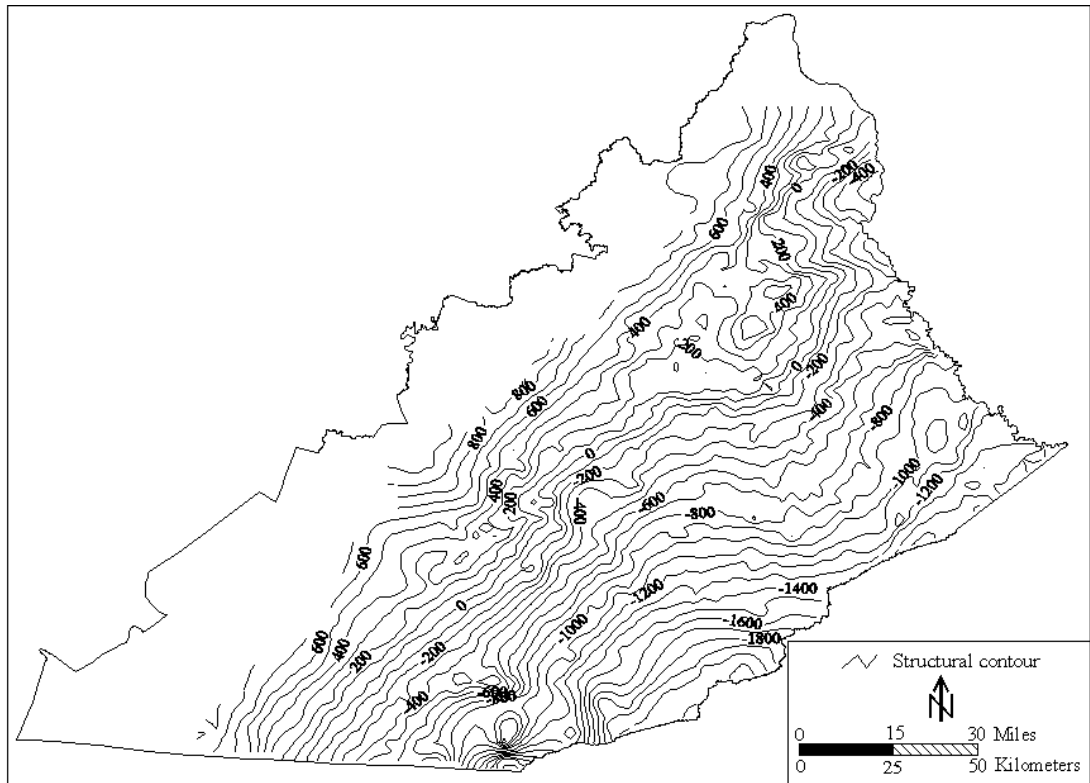


**Figure 4.22:** Regional structure contour map of the top of the Mississippian Newman Limestone. Contour interval equals 50 feet.

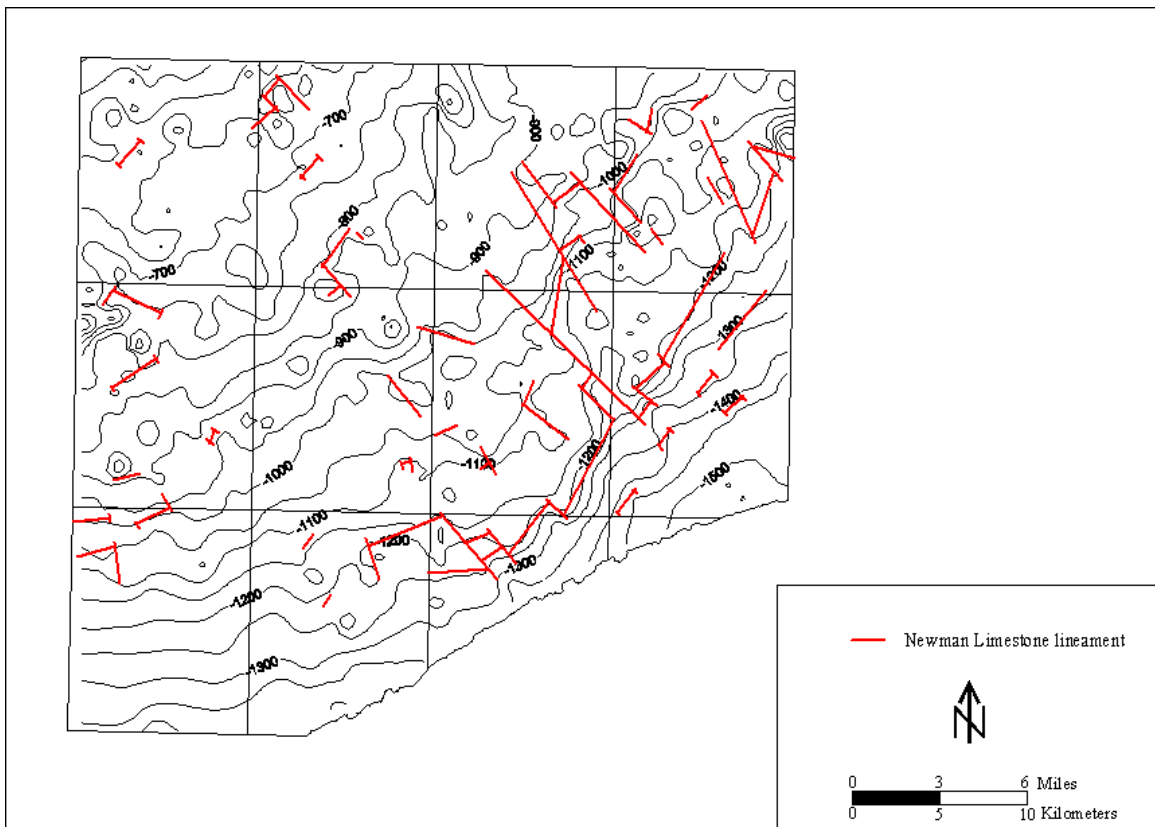


**Figure 4.23:** Location of Newman Limestone lineaments identified using structural contour analysis.

structural lineament (Figure 4.23). In addition, a line was drawn along any trend for structural contours that showed a change in orientation of 45 degrees or more that carried through two or more successive contours. These areas of persistent deflection in structural contours were also recorded as Newman Limestone structural lineaments (Figure 4.23).

Analysis of the structural contours and individual elevation data points for the Newman Limestone reveal both large-scale, interconnected structural lineaments that extend across most of the study area, and individual, relatively isolated lineaments (Figure 4.23). In general, the orientations of structural lineaments are dominantly northeast–southwest and appear to be offset by northwest–southeast-oriented lineaments. The most significant set of lineaments is along the southeastern and south-central part of the map, which are oriented northeast–southwest. To the north of this set is another set of northeast–southwest lineaments. At the easternmost edge of the four-quadrangle study area, the northern set terminates against a northwest–southeast lineament. The southern set is more extensive, and terminates in the southwestern part of the four-quadrangle study area. In addition, to the north, several smaller, isolated lineaments appear to be separate from the more extensive sets of lineaments (Figure 4.23).

Continuous grids of dip were created to compare a computer-generated interpretation of areas of increased dip to Newman Limestone structural lineaments that were defined using structural contours and elevation data points. Two continuous grids were created for the dip of the top of the Newman Limestone in order to determine the best scale to show the structural trends. The first map was created using the Q-36 subset

(2,754 data points), and is ideal for clearly showing the general trend of regional structures (Figure 4.24). The most significant dip trends are on the eastern side of the 36-quadrangle area and trend northeast–southwest. These dip trends consist of a southern, more extensive trend that projects into the 12-quadrangle area. A smaller, northern trend is limited to the 12-quadrangle area and parallels the more extensive southern trend. Furthermore, the southwestern end of this northern trend abruptly turns to the south and appears to merge with the southern trend near the eastern margin of the four-quadrangle study area (Figure 4.24). The second map was made using the Q-12 subset (969 data points) (Figure 4.25). This was the same data set used to identify potential geologic structures by visually analyzing structure contours and individual data points. The trends revealed using the Q-12 data set better define the actual geometry of regional structures identified using the Q-36 data set. Analysis of Figure 4.25 shows that the two regional linear northeast–southwest dip trends, in the northeastern part of the 12-quadrangle area, are actually northeast–southwest increased-dip trends that appear to be offset by northwest–southeast trends. The two linear dip trends (northern and southern) merge along the eastern margin of the four-quadrangle study area, and continue to the southwest, where the trend terminates in the southwestern part of the four-quadrangle study area (Figure 4.25). There is also a set of isolated linear dip trends to the north of the more extensive southern trends (Figure 4.25).

The Newman Limestone lineaments identified using structural contours and elevation data points (Q-12 subset) were overlain on the continuous grid for dip

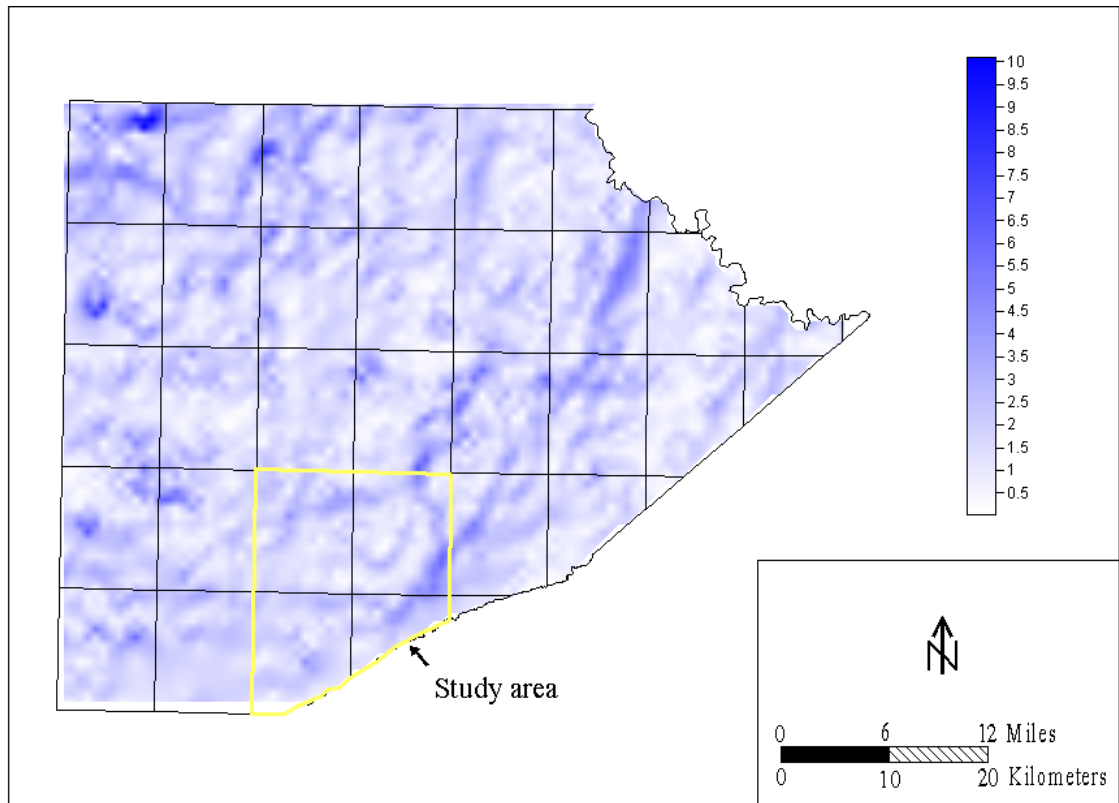


**Figure 4.24:** Continuous grid showing the dip for the top of the Newman Limestone for the Q-36 data subset. Scale bar is calibrated in degrees of dip.

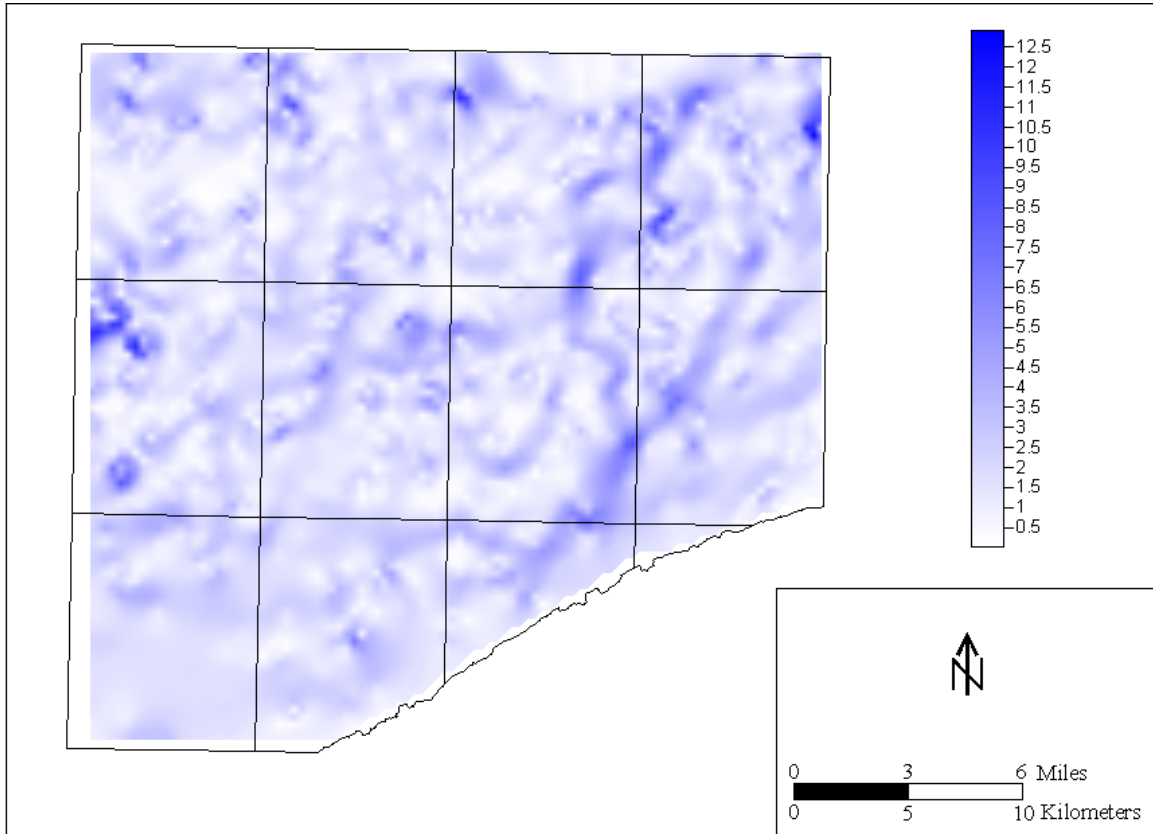


**Figure 4.25:** Continuous grid for the dip of the Newman Limestone for the Q-12 data subset. Scale bar calibrated in degrees of dip.

(Q-12 subset) in order to compare the two methods. The relationships of the areas of increased dip shown on the continuous grids are nearly identical to the lineaments that were defined using structural contour analysis (Figure 4.26a). Though the match between the two maps is not perfect, by using the continuous grid of dip, a more accurate map can be created by adding, subtracting, or shortening previously defined lineaments to match dip trends (Figure 4.26b). After the structural lineaments were refined, structural contours were used to show direction and magnitude of displacement along the lineaments (Figure 4.27).

#### 4.4.3 Comparison of Newman Limestone Lineaments to Coal Measure Data

Lineaments identified for the Newman Limestone are inferred to be faults with 50 feet (12 m) of minimum displacement that is dominantly down-to-the-southeast. A comparison of Figure 4.24 with the Lower Elkhorn coal seam structure shows a correlation between several of the more extensive northeast–southwest inferred faults and structures such as the Belfry Anticline and a nearby unnamed anticline north of the Belfry Anticline (Figure 4.28). Because the Lower Elkhorn coal seam structure is contoured in 100-foot intervals, smaller faults may not be expressed by the structure contours.

Inferred faults within the Newman Limestone are also associated with the regional Lower Elkhorn coal-seam structure, as well as local (four-quadrangle structure) coal-seam structure and sandstone distribution. A comparison of the inferred faults defined by analyzing structure for the Mississippian Newman Limestone data to those lineaments defined using the trend-surface

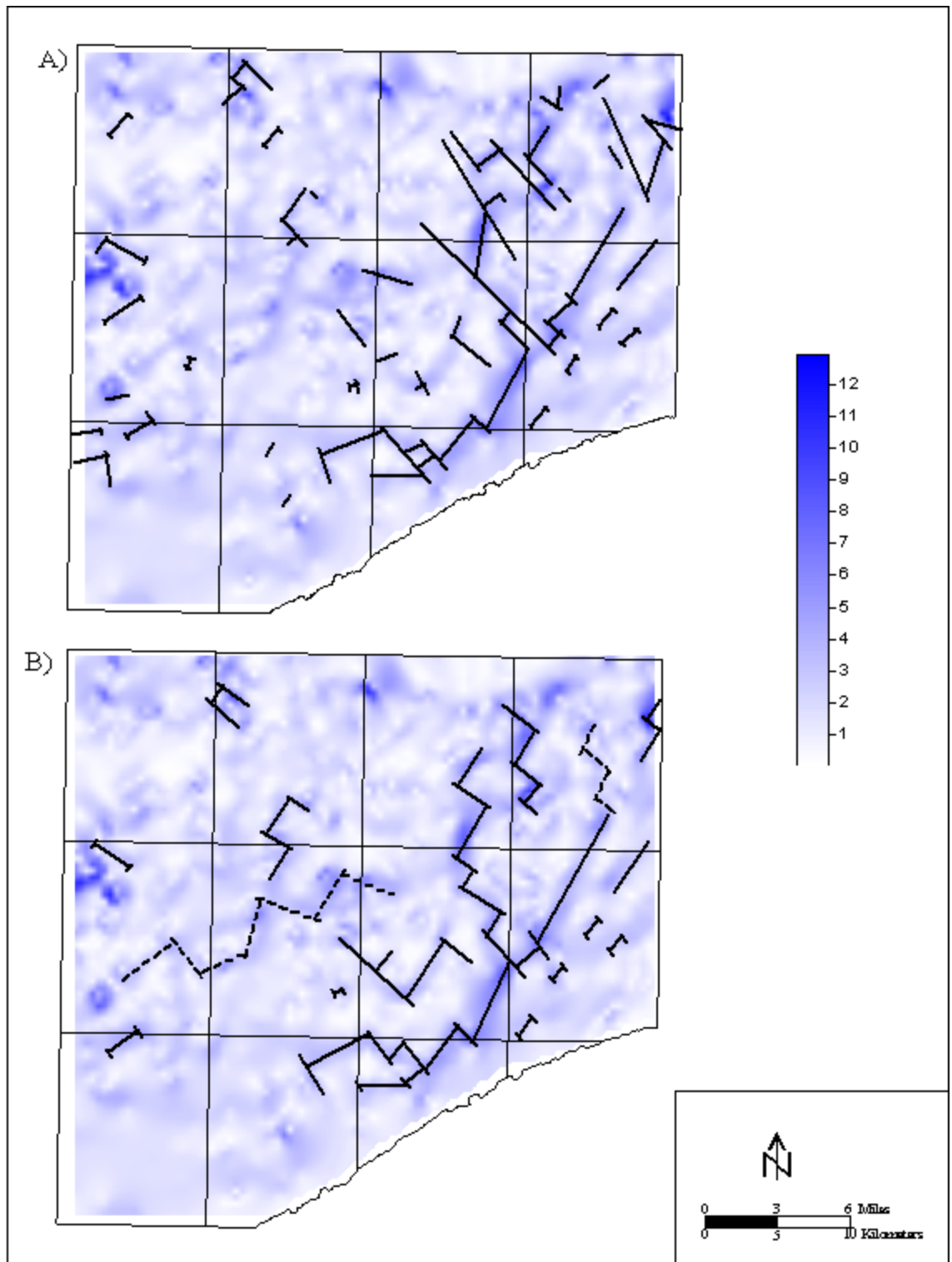


**Figure 4.26:** Continuous grid of dip for the Newman Limestone showing (a) structural lineaments picked using structural contour analysis and (b) Newman Limestone structural lineaments detected using the continuous grid analysis. Scale bar calibrated in degrees of dip.

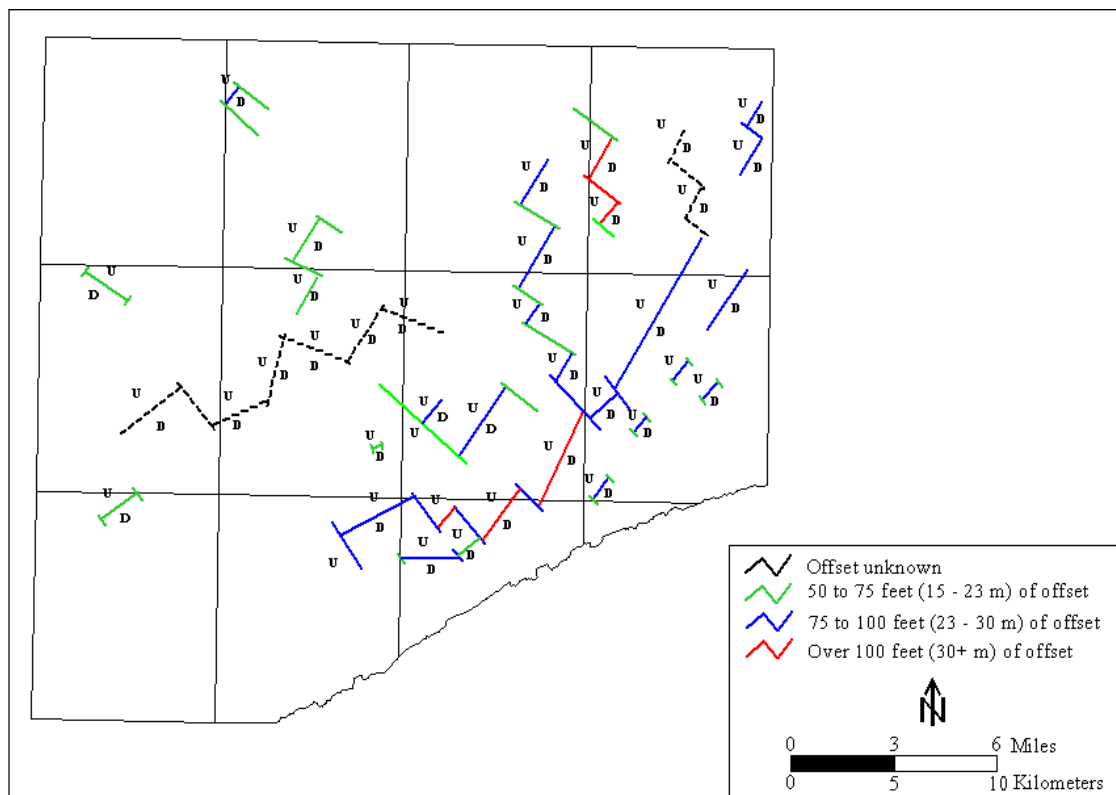


**Figure 4.27:** Magnitude and direction of displacement associated with the Newman Limestone structural lineaments.

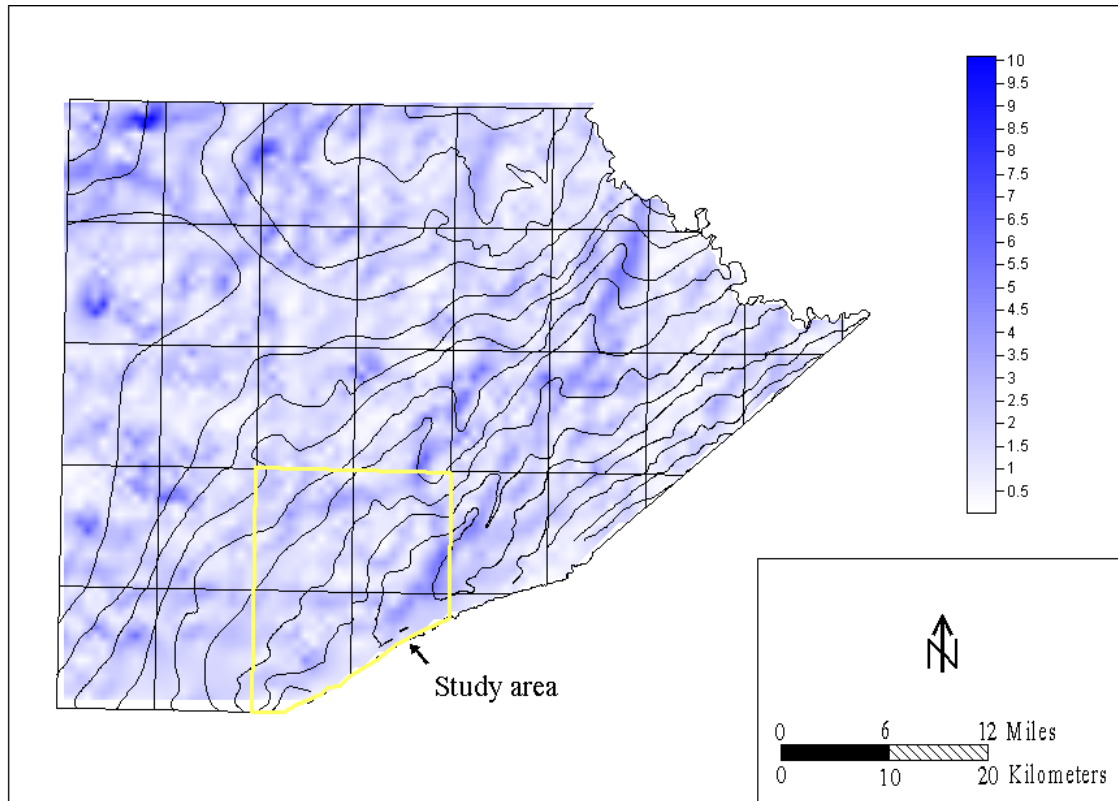


**Figure 4.28:** Lower Elkhorn coal seam structure overlain onto the continuous grid of the slope for the top of the Newman Limestone. Note the correspondence between geological structures identified in the coal seam structure and areas of increased slope. The structural dip on the base of the Lower Elkhorn coal is to the northwest.

residual analysis also reveals a strong correlation between the two horizons (Figure 4.29). Most notable is the correlation between the extensive interconnected faults across the southern part of the four-quadrangle study area on both maps. Some of the northern, isolated faults also show an association on both maps. Though the maps are very similar, it is important to note that the geometry of the faults identified during residual analysis is much more general than those identified using continuous grids of dip and structure maps for the Newman Limestone.

#### 4.4.3 Summary of Newman Limestone Structure Analysis

The analysis of the structure of the top of the Newman Limestone yielded important information on the location of structural lineaments, which likely represent subsurface faults. By using continuous grids and structure maps, and analysis of dip derived from structure maps, the location of these inferred faults can be confirmed and modified to provide a clear picture of faults that could have potentially affected the distribution of younger paleochannels during deposition of the Pennsylvanian System. Furthermore, a comparison of faults identified using trend-surface residual analysis to faults identified using the Newman Limestone data shows a close match between the two. If the faults predicted using trend-surface analysis match those faults used by analyzing the Newman Limestone match, the relationship suggests that the faults within the Newman Limestone were active during the deposition of the study interval and could have affected the distribution of paleochannels and trends of coal-seam structure.

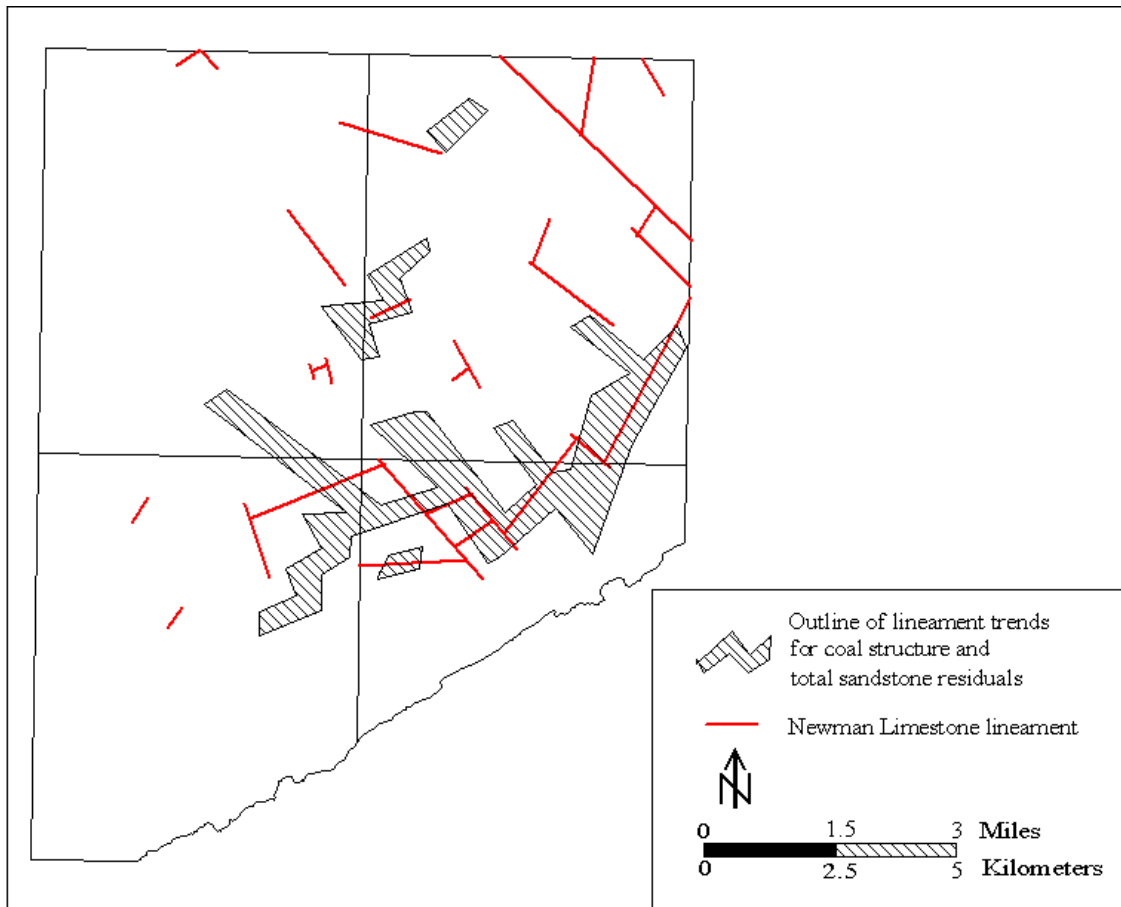


**Figure 4.29:** Comparison of hand-picked Newman Limestone structural lineaments to faults hand-picked using residual analysis.

#### 4.5 A Comparison of Predicted Faults and Upper Elkhorn No. 3 and Lower Elkhorn Paleochannels

The recognition of deep faults and their association with near-surface structure and the distribution of sandstone bodies suggests that the projections of faults may help predict paleochannel-related mining problems ahead of active operations or in areas of poor data distribution. When predicted faults are compared to mining problems within the Upper Elkhorn No. 3 and Lower Elkhorn horizons, some parallelism is shown to exist between the orientation of the faults and the orientation of some synclines and heterolithic channel-related mining problems. Mining problems and the associated broad syncline within the Lower Elkhorn study mine are found on the downthrown side of the predicted fault (Figure 4.30). The mining problems within the Lower Elkhorn mine have an arcuate trend, which corresponds to the edge of the predicted fault block. In the Upper Elkhorn No. 3 horizon, the westernmost arcuate paleochannel trend and synclines (Figure 4.31) closely match the western arcuate paleochannel trend observed in the Lower Elkhorn mine (shown on Figure 4.30) and parallels the downthrown side of the inferred fault. The arcuate nature of this trend closely matches the geometry of the fault block superimposed nearly 300 feet (90 m) above the Lower Elkhorn paleochannels. The two other paleochannel trends also parallel the downthrown side of predicted faults. The remaining paleochannels and most synclines, however, do not follow the structural trends and are arcuate. Rather, the paleochannels and synclines intersect possible faults at 90 degrees or show no relationship at all (Figure 4.31). The association of mining problems to predicted faults within the two coal horizons suggests a structural control on the location of these channels. Therefore, the relationship between the location of faults and mining

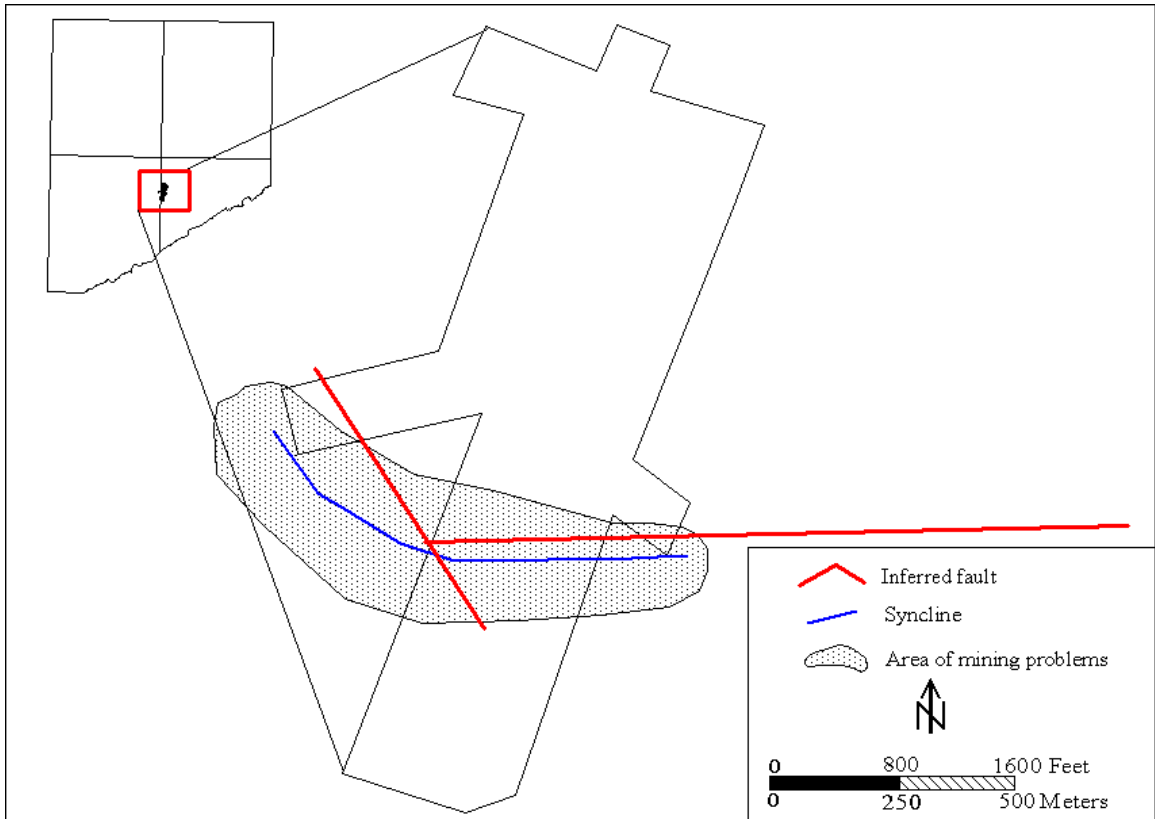


**Figure 4.30:** Comparison of synclines identified in Lower Elkhorn coal seam structure (a) and locations of paleochannel-related mining problems (b) to inferred faults.

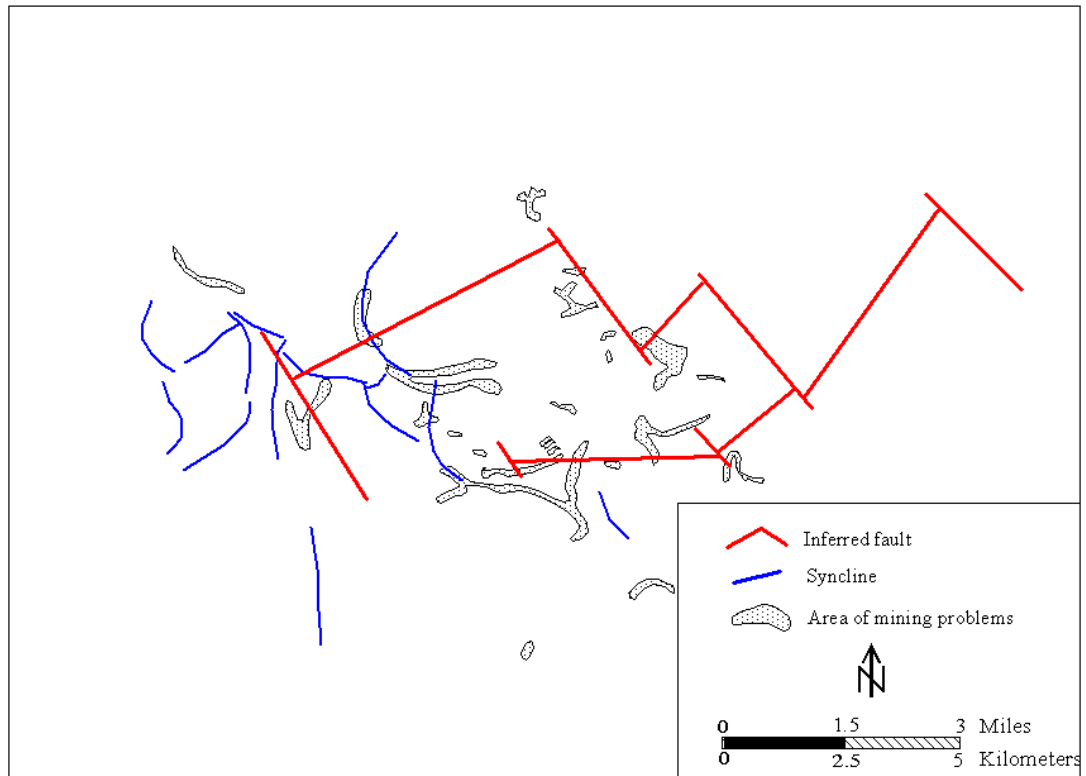


**Figure 4.31:** Comparison of synclines identified in Upper Elkhorn No. 3 coal seam structure (a) and paleochannel-related mining problems to inferred faults.

problems suggests that the projections of faults may be useful in predicting areas with greater probability of containing heterolithic channels.

Sandstone-rich areas in the Lower Elkhorn/Lower Elkhorn rider interval and the location of regional incised channels show a relationship to predicted faults. Sandstone-rich areas, for the Lower Elkhorn interval (Figure 4.32), are oriented northeast–southwest in the southern part of the study area. These sandstone-rich areas parallel the downthrown side of the southern set of interconnected faults. Sandstone-poor areas in the central part of the study area all appear to be on the upthrown sides of the faults. The northernmost sandstone-poor area, however, appears to be on the downthrown side of all nearby faults, suggesting structural control may not have been active in that area. Finally, a large regional incised channel in the southern half of the study area follows the geometry of predicted faults, though it does not always coincide with the downthrown side of the faults (Figure 4.33). This relationship may result from (1) error in the placement of faults, (2) the angular manifestation of the faults into overlying sediments, (3) a change in the throw of the fault during later reactivation, or (4) channels cutting across faulted areas as the alluvial belt widened or avulsed with time.

Sandstone-rich areas for the Upper Elkhorn No. 3 zone are also parallel to the downthrown sides of predicted faults (Figure 4.34). Furthermore, sandstone-rich areas in the Upper Elkhorn No. 3 zone overlie and parallel sandstone-rich areas in the Lower Elkhorn interval. In the southern half of the study area, sandstone-rich areas parallel predicted faults. In addition, sandstone poor areas along the eastern and north-central parts of the study area are found on the upthrown sides of the faults. Sandstone-poor areas in the eastern and north-central parts of the study area correspond to the upthrown

sides of faults. Other sandstone-poor areas along the southernmost faults and along the western side of the study area, however, parallel the downthrown side of the faults, which suggests no structural control. The sandstone-poor area in the north-central part of the study area is nearly identical in location to a sandstone-poor area in the Lower Elkhorn interval.

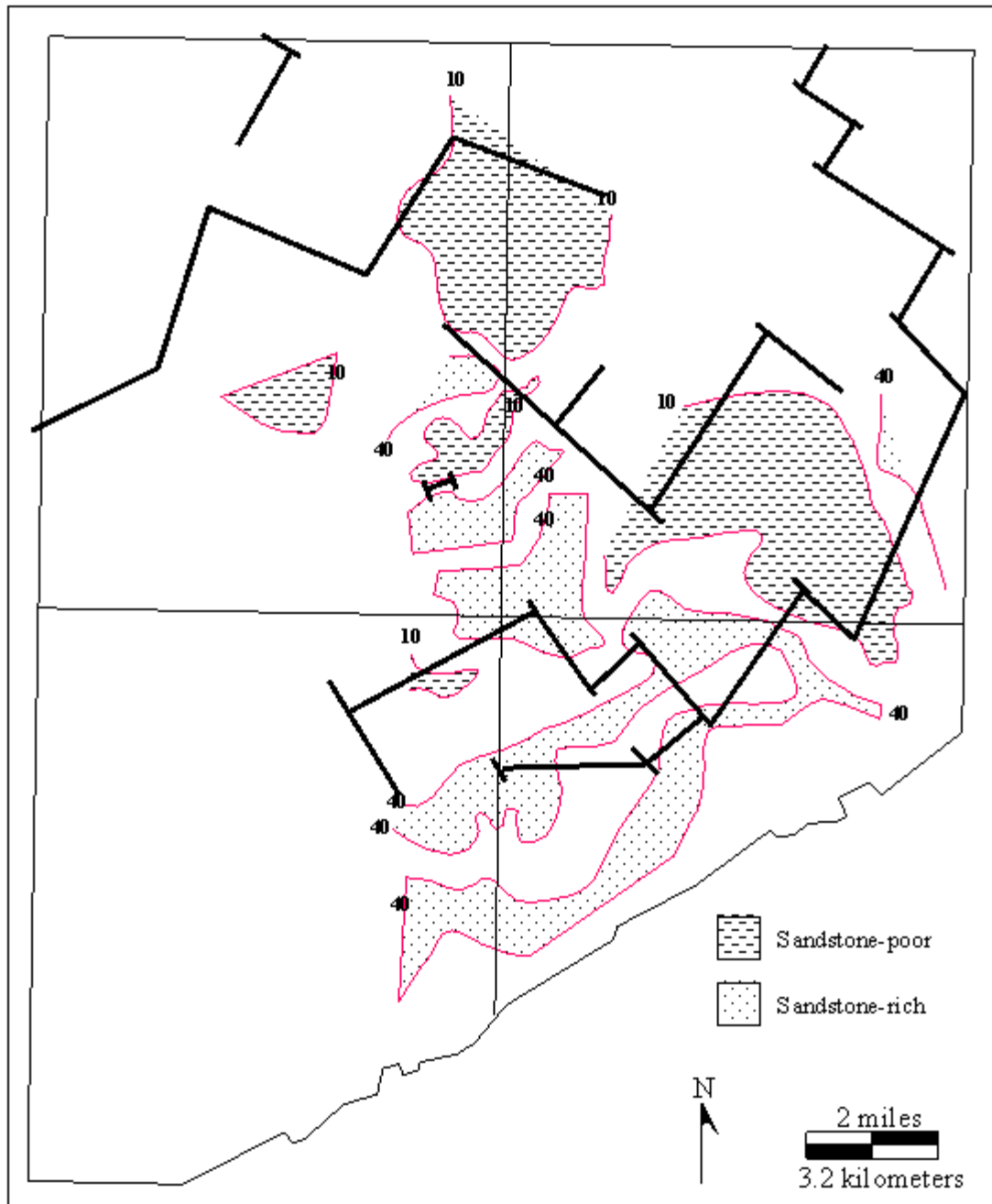


**Figure 4.32:** Lower Elkhorn/Lower Elkhorn rider interval total sandstone isolith map showing the relationship between sandstone-rich and sandstone-poor areas and inferred faults.

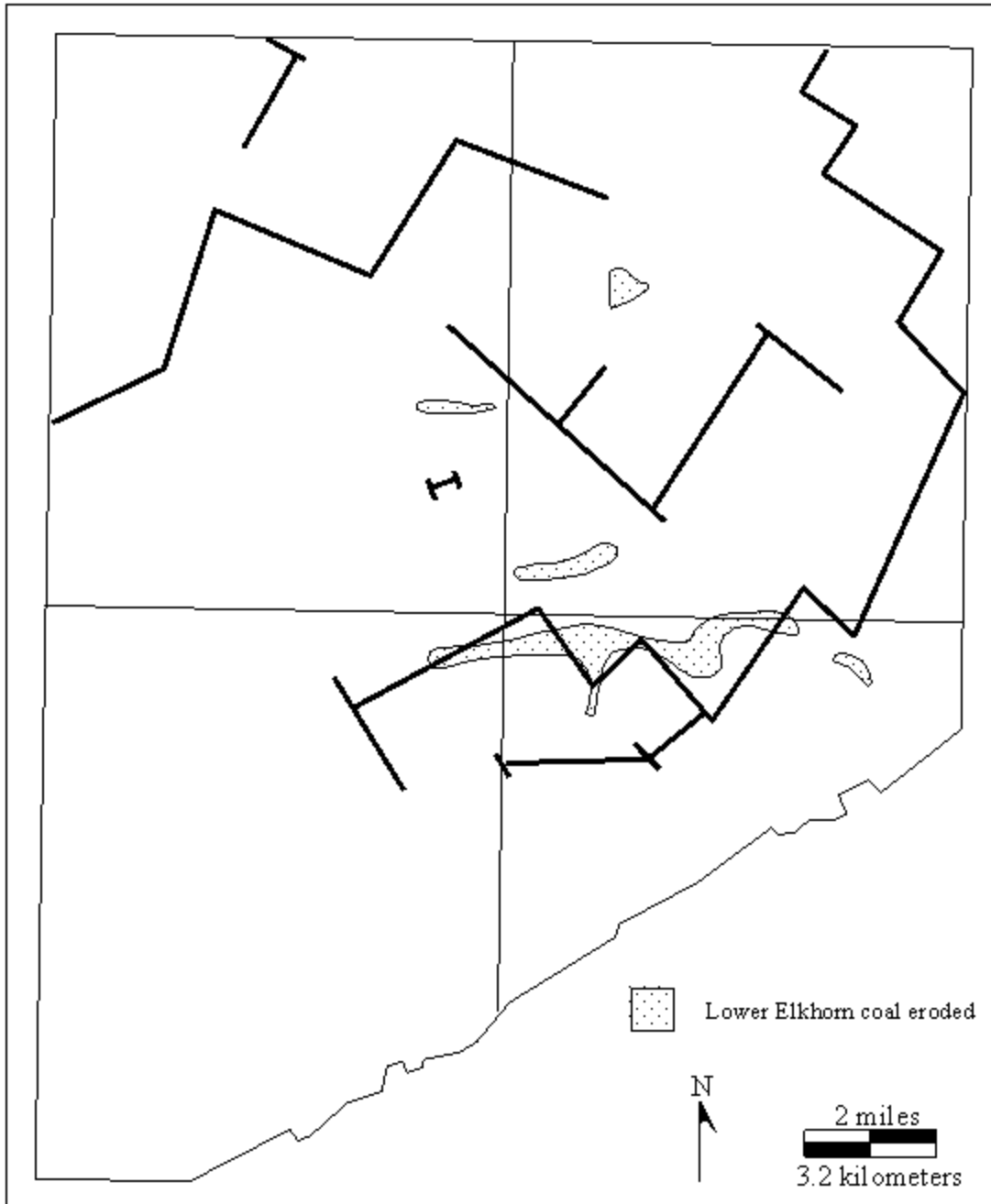


**Figure 4.33:** The relationship between the Lower Elkhorn coal seam zero coal thickness isolith contour and Newman Limestone lineaments.

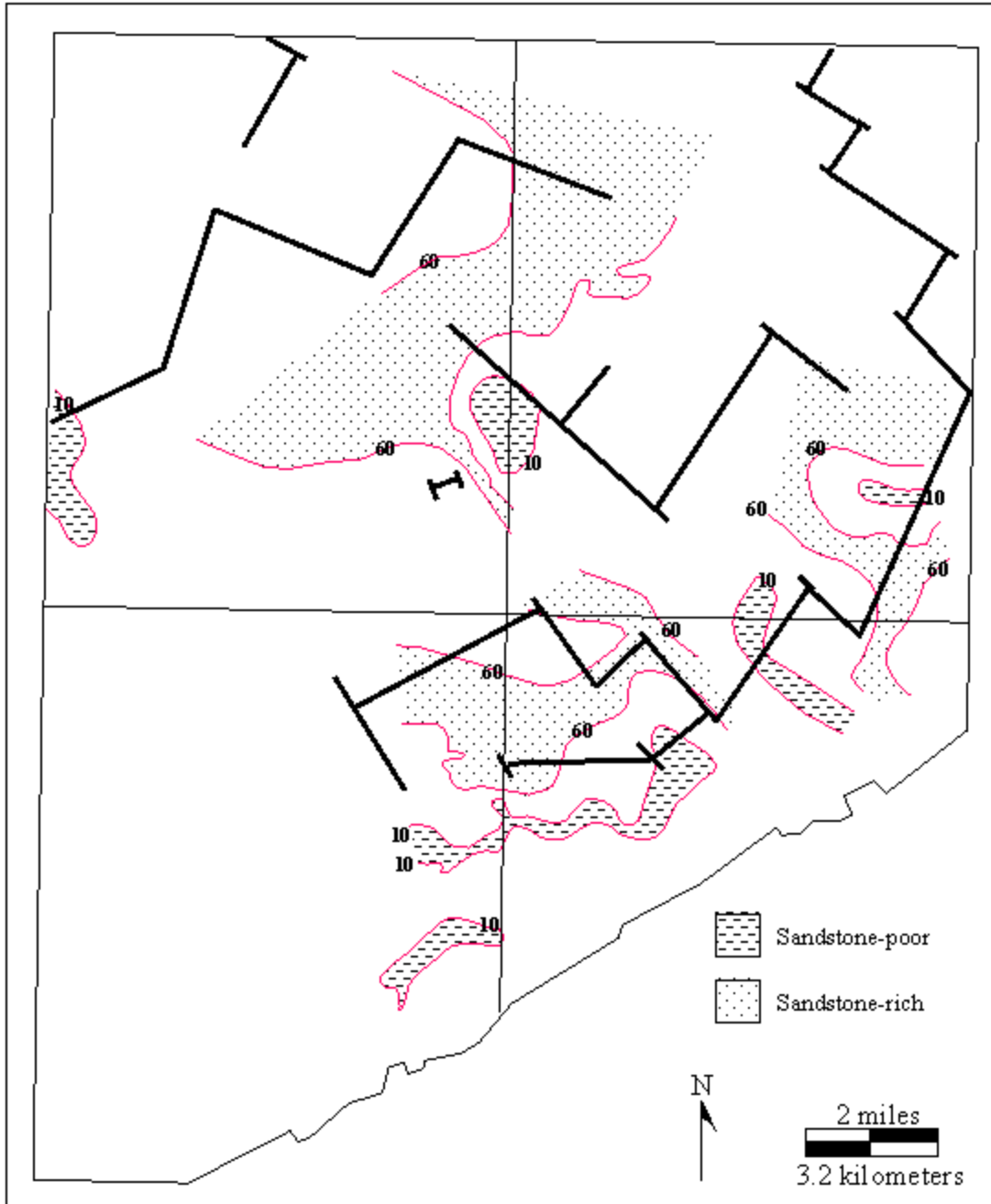


**Figure 4.34:** Total sandstone thickness isolith map for the Upper Elkhorn No. 3 zone showing the relationship between sandstone-rich and sandstone-poor areas and Newman Limestone lineaments. Contour interval is 10 feet (3 m).

## 5.0 Discussion and Conclusions

### 5.1 Objective and Methodology

The objective of this thesis is to develop models that aid in the prediction of channel-related mining problems prior to development, in areas with limited data distribution. Understanding the controlling mechanism of paleochannel development and associations with other stratigraphic parameters enhances predictability in areas of poor drill-hole density. Depositional models that explain the orientation, dimensions, and superposition of deltaic sediments were evaluated.

This thesis was conducted in two steps: (1) channel types and their characteristics were identified and (2) the controlling mechanisms of channel emplacement were inferred on the basis of stratigraphic and structural analyses. Field studies were conducted in order to identify the types of channels associated with the Lower Elkhorn coal. To identify controlling mechanisms of these channels, 506 coal exploration drill holes were divided into stratigraphic intervals, and thickness trends and orientations were analyzed using sandstone isolith maps, cross-section profiles, and second-order trend-surface residual analysis of sandstone thickness and coal-bed structure. In addition, structural elevation data from the deeper Mississippian Newman Limestone, taken from 7,189 oil and gas drill holes, was studied using structure maps and continuous grids of dip to locate faults that underlie the Pennsylvanian System.

Trend-surface residual analysis of total sandstone thickness and coal-seam structure was done to locate synsedimentary faults that may have controlled the location of paleochannels in the study area. The results of these analyses indicate that second-order trend surfaces are the most useful surface for separating out local sandstone thickness and

coal-seam structure trends. Variation in the extent of the data set was found to affect the results of trend-surface analysis. Widely distributed data sets preferentially model regional structures and trends. In order to identify more localized trends that are more useful at a mine scale, smaller subsets of data are needed. Whereas previous workers using trend surface for stratigraphic analysis used simple addition of residual maps, this study used conditional algebra prior to addition to ensure that only like residuals were calculated. This method results in better definition of stratigraphic stacking relationships for testing hypotheses of local structural controls.

An analysis of the structural dip and strike for the top of the Mississippian Newman Limestone was done to precisely locate faults that underlie the Pennsylvanian System, and to compare those faults to those identified using trend-surface residual analysis of sandstone thickness and coal-seam structure. This analysis was done in two ways: (1) structural contour analysis and (2) analysis of continuous grids of dip. Structural contour analysis revealed a dominant northeast–southwest structural component with a subordinate northwest–southeast component, which closely matched trends identified using trend-surface residual analysis. Similar trends have been noted in the Fire Clay cba (Weisenfluh and Ferm, 1991b; Greb et al., 1999a), but now can be shown to be more widespread and tested to deeper structure. Trend-surface residual analysis, however, yielded more general lineament trends and geometries. Computer-generated continuous grids show similar results as structure contour analysis, but in much greater detail.

## 5.2 Channel Types

Three types of channels are associated with the Lower Elkhorn coal within the study area: (1) regional incised channels, (2) local scours, and (3) heterolithic channels.

These channels were identified using field studies, sandstone isolith maps and profiles, and cross sections of drill-hole records.

Regional incised channels are the largest types of channels identified within the four-quadrangle study area. Regional incised channels are associated with thick (greater than 40 feet [12 m]), medium- to coarse-grained sandstone bodies. Areas of increased sandstone thickness (greater than 60 feet [18 m]) within the study area are likely a result of multistoried sandstone bodies. Furthermore, the dominant orientation of this channel type is northeast–southwest to east–west, which is normal to the inferred northwest paleoslope.

Regional incised channels are associated with northeast–southwest-trending faults in the Newman Limestone. The deviation in orientation of these channels away from the northwest paleoslope is probably because of synsedimentary faults. Regional incised channels are not consistently found on the downthrown side of a fault. The geometry of the channels, however, does parallel the geometry of adjacent faults. The lack of correspondence could be a result of (1) the manual placement of faults, (2) how the fault is manifested in the overlying sediments, (3) a change in the throw of the fault during later reactivation, or (4) channels cutting across faulted areas as the alluvial belt widened or avulsed with time.

The potential for regional incised channels within TECO’s Lower Elkhorn coal reserve is low because the current drilling information is sufficient to have detected them. Furthermore, the current projections of this channel type, using known location and fault traces, show that regional incised channels are unlikely to affect any future Lower Elkhorn coal reserves owned by TECO Coal Company.

Local scours are the smallest channel type that has been identified within the study area. Observed local scours have a maximum depth of incision of about 5 feet (1.5 m), and are in the basal part of medium- to coarse-grained sandstone bodies. Local scours are seen to truncate fine- to medium-grained sandstone and shale lithologies in the roof of the study mine and in highway exposures. The small size of local scours makes prediction impossible by any drilling program. Also, there are no relationships between observed local scours and inferred faults, or position within the sandstone body (i.e., axis, margin, etc.). Therefore, the probability of encountering local scours throughout the remainder of TECO's Lower Elkhorn coal reserve is uncertain, although they should be expected where medium- to coarse-grained sandstone occurs near the top of the coal. Also, where encountered, local scours will be narrow and unlikely to be continuous for long distances.

Heterolithic channels are intermediate in size between regional incised channels and local scours. Observed heterolithic channels are narrow (less than 1,000 feet [304 m] wide) and as much as 3,000 feet (914 m) long, although the total length may be longer. Heterolithic channels consist of inclined, interbedded sequences of sandstone and shale, inclined sandstone bedforms, and few inclined heterolithic slump blocks.

Heterolithic channels, observed on mine maps for the Lower Elkhorn coal and inferred to be associated with the Upper Elkhorn No. 3 coal, are associated with the margin and axis of sandstone-rich areas, and may have preferentially occupied the same topographic low as the underlying heterolithic channels. Observations within the Lower Elkhorn study mine suggest that these channels represent depositional events separate from the overlying sandstone-rich areas. Because of the relationship between heterolithic

channels and sandstone-rich areas, heterolithic channels should be anticipated beneath sandstone-rich areas (greater than 40-foot sandstone isolith contour for the Lower Elkhorn/Lower Elkhorn rider interval).

The relationship between heterolithic channels and inferred faults is not as clear as with regional incised channels. The heterolithic channel deposits encountered within the Lower Elkhorn study mine are found on the downthrown side of a fault, and appear to follow the geometry of the fault block in a general way. In addition, a paleochannel observed on Upper Elkhorn No. 3 mine maps, approximately 300 feet (91 m) above the Lower Elkhorn horizon, is also on the downthrown side and parallels the geometry of the same fault as the Lower Elkhorn paleochannel. The stacking and similarities in geometry of the two paleochannels suggests that synsedimentary faulting controlled their development. Hence, on the basis of the observed relationships, heterolithic channels should be anticipated to be associated with areas of increased total sandstone thickness, and to parallel the downthrown side and geometry of the inferred faults. On the basis of this criteria, there is some probability that heterolithic channels will be encountered in the remaining Lower Elkhorn coal reserves owned by TECO Coal Company. Mining operations can use the structural data to anticipate the possibility of heterolithic channels in areas of inferred faults (1) to help anticipate possible changes in roof conditions and (2) to project the likely trends of the heterolithic roof if it is encountered.

Heterolithic channels can be distinguished from regional incised channels, which also follow faults, because they generally have higher percentages of shale, inclined strata (epsilon crossbedding, lateral accretion sets, and slump blocks), and do not remove the

coal over large areas. Because of slumps and mixed rock types, roof support will be more difficult beneath heterolithic channels than beneath larger sandstone channels.

### 5.3 Depositional Setting of the Channel Types

Early work by Horne (1978) defined two types of channels for the Eastern Kentucky Coal Field: (1) lower delta plain, distributary channels and (2) upper delta plain fluvial deposits. Both types of channel deposits are linear and lenticular in geometry, are medium- to coarse-grained, and have sharp erosional basal contacts with siderite pebble conglomerates and log fossils. Though much of the identifying criteria for both channel types are the same, the defining characteristic between the two channel types is width and the presence of lateral accretion surfaces. Distributary channels, according to Horne et al. (1978), are as much as 1,000 feet (300 m) wide with few lateral accretion surfaces because distributaries do not tend to migrate laterally. In contrast, upper delta plain fluvial deposits are 1 to 7 miles (1.5 to 11 km) wide with more abundant lateral accretion and amalgamation surfaces.

An alternative explanation to the upper/lower delta plain model described in Horne et al. (1978) comes from the recent application of sequence stratigraphy to coal measure strata by Aitken and Flint (1994, 1995). The defining characteristics of incised valleys are sandstone bodies that incise deep into their substrate, show a sharp increase in grain size compared to surrounding strata, coal rafts and siderite pebble conglomerates, and numerous amalgamation surfaces. Aitken and Flint (1994) also suggested a minimum width of 3 miles (5 km) for incised channels. In this model, incised valleys develop as channels eroded into their underlying substrate during a sea-level fall.

The delta plain model and incised valley model differ in the association between channel and related strata, as well as their relationship to sea level. The upper delta plain channels have associated overbank deposits (i.e., levees, floodplain, etc.). In contrast, the incised valley model has equivalent paleosol horizons, and deposition is limited to within the valleys. Furthermore, incised valley formation is controlled by allocyclic processes (eustatic changes), whereas the delta plain development, in the sense of Horne et al. (1978), is an autocyclic process.

The defining depositional model for the three channel types is not clear. On the basis of size only, regional incised channels and associated sandstone-rich areas fit the upper delta plain model of Horne et al. (1978) or the incised valley model of Aitken and Flint (1994, 1995). Using the same criteria, heterolithic channels are similar in dimensions to the lower delta plain channels of Horne et al. (1978). The problem with using only size to classify channels is that the observed heterolithic channels have epsilon crossbedding and lateral accretion surfaces, whereas in the lower delta plain model these bedforms are not as common because lower delta plain channels generally do not migrate (Horne et al., 1978). Overbank deposits described above the Lower Elkhorn coal are not consistent with the incised valley model, but are common features in the upper and lower delta plain models. Local scours result from local areas of increased flow velocity, and are probably a feature of both incised valley and delta plain channels.

In conclusion, on the basis of lateral accretion surfaces and associated overbank deposits, the heterolithic channels were likely meandering channels (Horne et al., 1978) or possibly tidal channels (Greb and Weisenfluh, 1996). Regional incised channels and large sandstone-rich areas were not directly observed at the surface, so their relationship

to adjacent strata is not understood. However, regional incised channels may represent a later, possibly eustatic, event that incised through the heterolithic channel deposits and the Lower Elkhorn coal, thereby following Aitken and Flint's (1994, 1995) incised valley model in size and characteristics. Hence, both models may have applications for different sandstone bodies. Some sandstone bodies do represent laterally contemporaneous depositional features, while others may represent later events, which have cut through older deposits. Finally, the orientations of regional incised channels may be a result of the shoreline position, except in areas of synsedimentary faulting.

#### 5.4 Improving the Methods of Identifying Synsedimentary Faults

The analysis of the structure of the top of the Newman provided the clearest picture of synsedimentary fault location and geometry. The limitation of this data set, however, is the reduced concentration of data along the southern margin of the Q-12 data set. Though it was not done for this study, geophysical logs can be analyzed for thinning of the Newman Limestone that results from a fault cutout. By looking for areas of stratigraphic thickness reduction as a result of faulting, faults could be identified in areas with fewer data points than are needed for computer modeling of structure or dip.

Seismic reflection is another useful tool for locating faults. Seismic reflection can provide a two-dimensional cross section of a fault, and if the resolution is sharp enough, show how the fault is manifested into the overlying strata. The cost of seismic reflection methods, however, make this a less likely method for locating possible faults.

## **Appendices**

**Appendix 4.1** Mine and Highway Exposure Location Information

**Appendix 4.1.1: Myra Highway Exposure Location Information.**

**Location information:**

*Quadrangle:* Dorton

*Type:* Roadcut

*Source:* Observation

*County:* Pike

*Northing:* 4126146

*Easting:* 358404

*Zone:* UTM 17

*Elevation:* N/A

*Mapper:* M.G. Shultz

**Stratigraphic Range:**

*Top:* Upper Elkhorn No. 3

*Bottom:* Betsie Shale Member (upper boundary)

**Appendix 4.1.2: Beefhide Mine Exposure Location Information.**

**Location Information:**

*Quadrangle:* Jenkins West

*Type:* Mine exposure

*Source:* Observation

*County:* Letcher

*Northing:* 4121964

*Easting:* 355896

*Zone:* UTM 17

*Elevation:* N/A

*Mapper:* G.A. Weisenfluh

**Stratigraphic Range:**

*Top:* Crummies Shale Member

*Bottom:* Lower Elkhorn coal

**Appendix 4.1.3:** Abandoned Lower Elkhorn Mine Location Information.

**Location Information:**

*Quadrangle:* Dorton

*Type:* Mine exposure

*Source:* Observation

*County:* Pike

*Northing:* 4125615

*Easting:* 359745

*Zone:* UTM 17

*Elevation:* N/A

*Mapper:* M.G. Shultz and G.A. Weisenfluh

**Stratigraphic Range:**

*Top:* Crummies Shale Member

*Bottom:* Lower Elkhorn coal

**Appendix 4.1.4:** Branham and Baker (AEP) Mine 23 Portal (Old Portal) Location Information.

**Location Information:**

*Quadrangle:* Jenkins East

*Type:* Mine exposure

*Source:* Observation

*County:* Pike

*Northing:* 4124150

*Easting:* 362019

*Zone:* UTM 17

*Elevation:* N/A

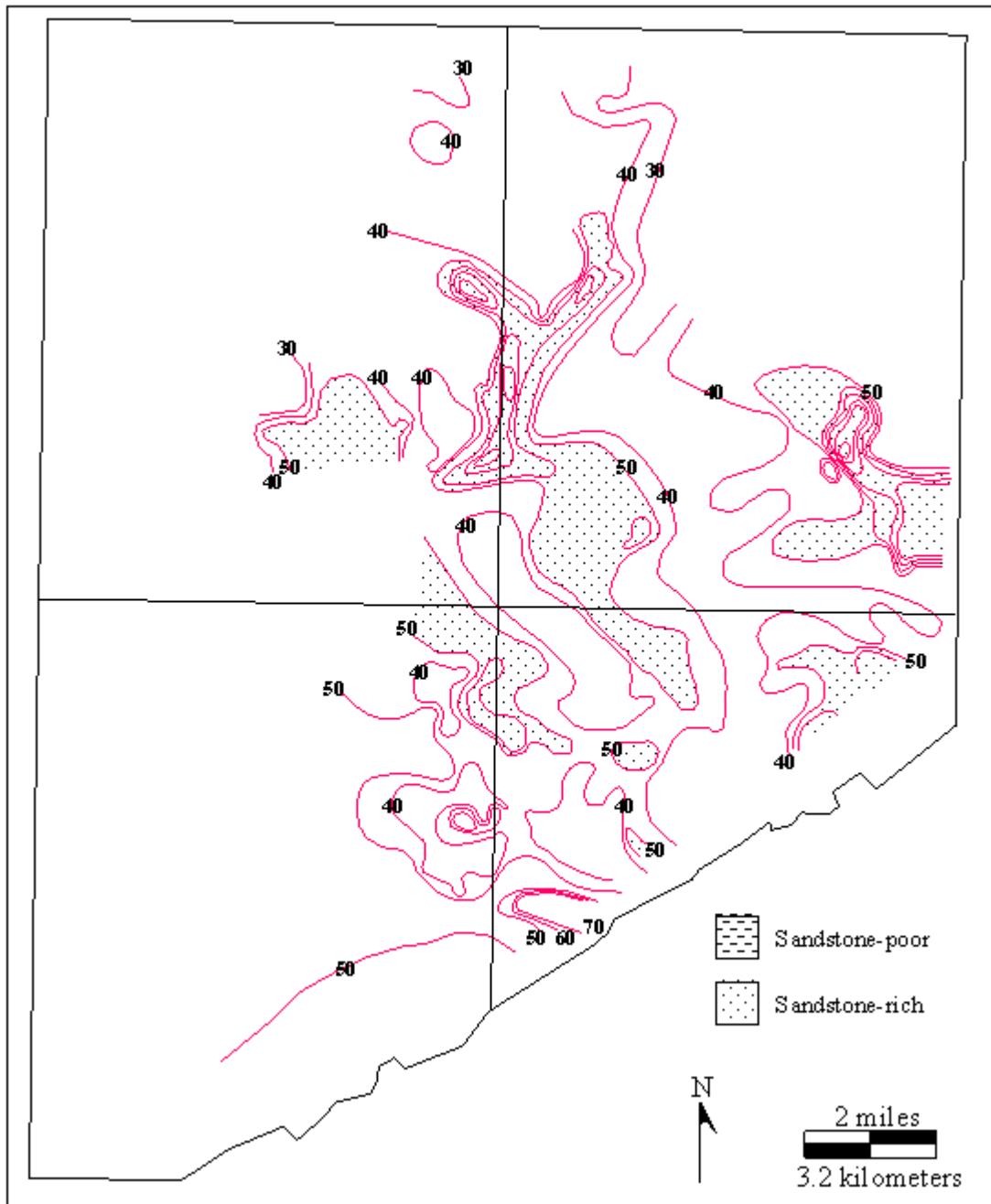
*Mapper:* M.G. Shultz and G.A. Weisenfluh

**Stratigraphic Range:**

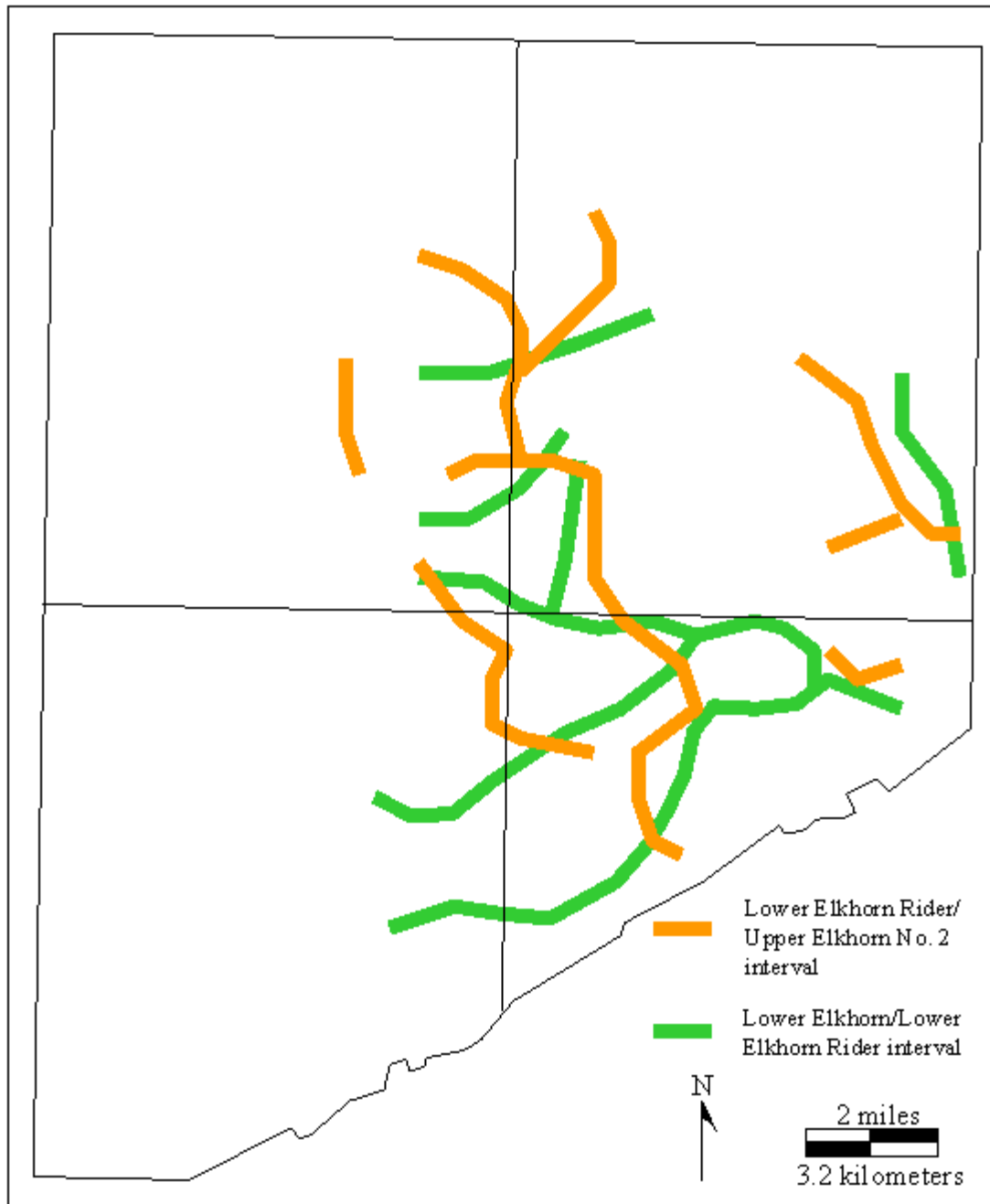
*Top:* Crummies Shale Member

*Bottom:* Lower Elkhorn coal

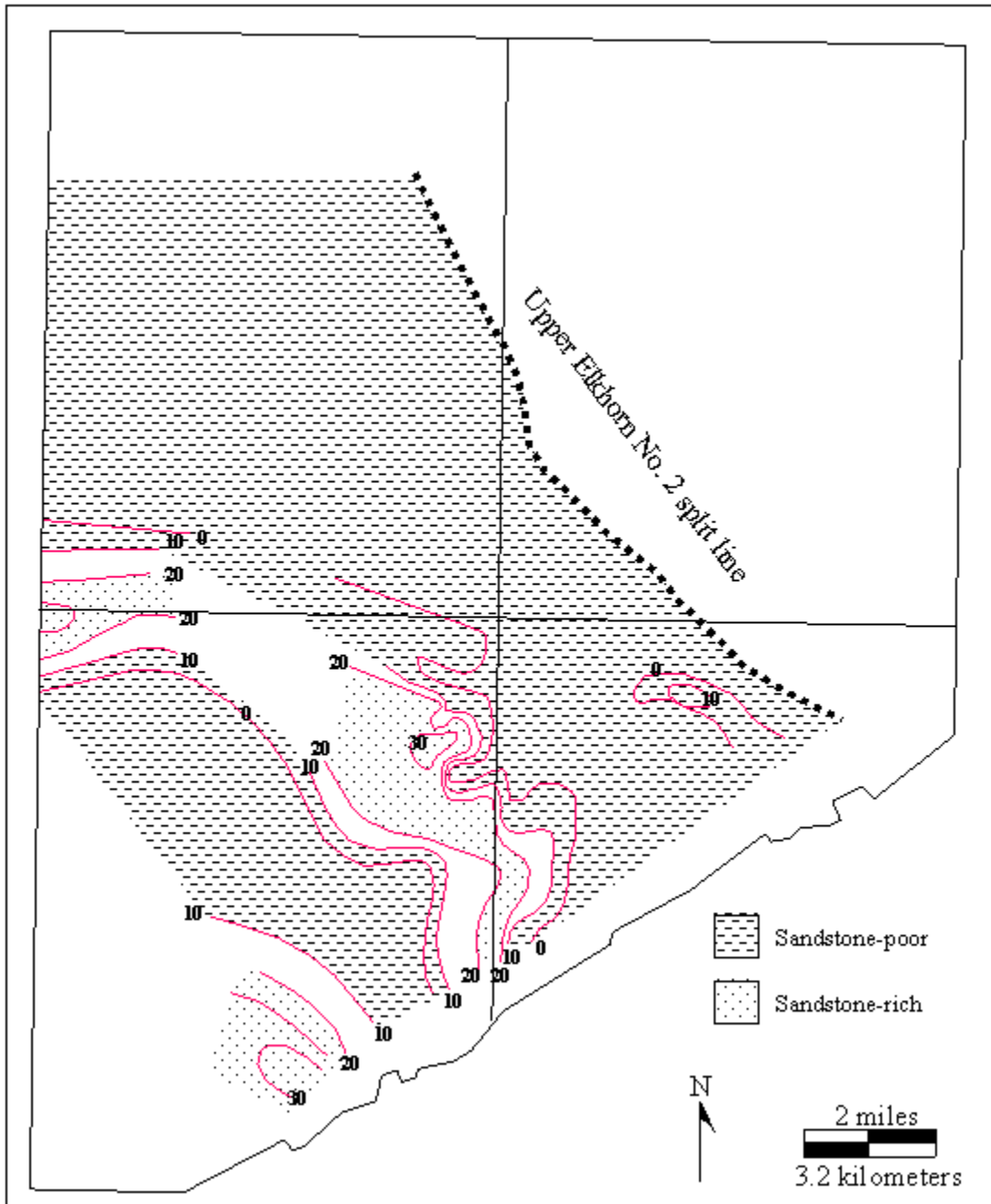
**Appendix 4.2:** Isolith Maps of the Defined Stratigraphic Intervals.



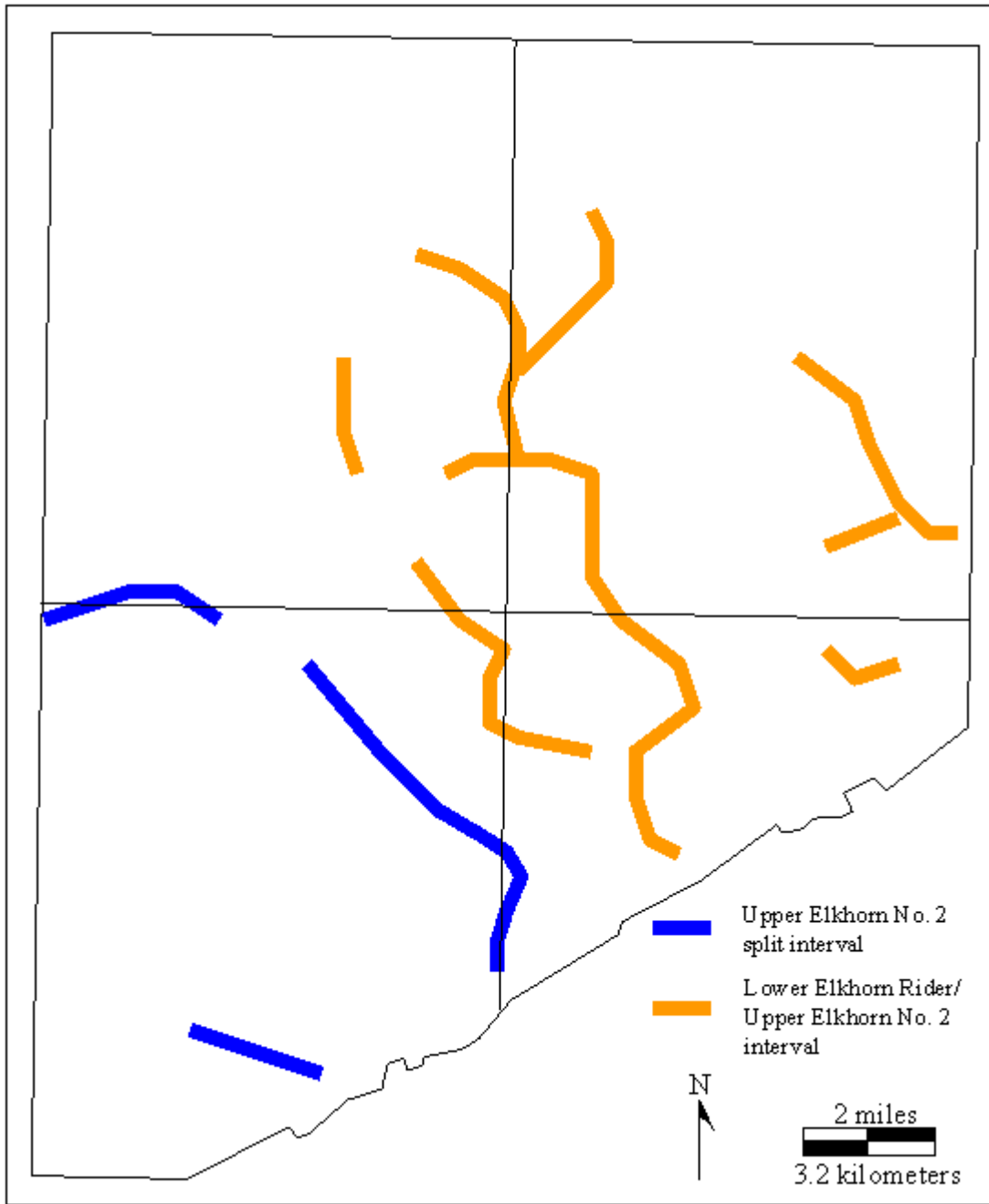
**Appendix 4.2.1:** Lower Elkhorn rider/Upper Elkhorn No. 2 total sandstone thickness isolith. Contour interval is 10 feet (3 m).



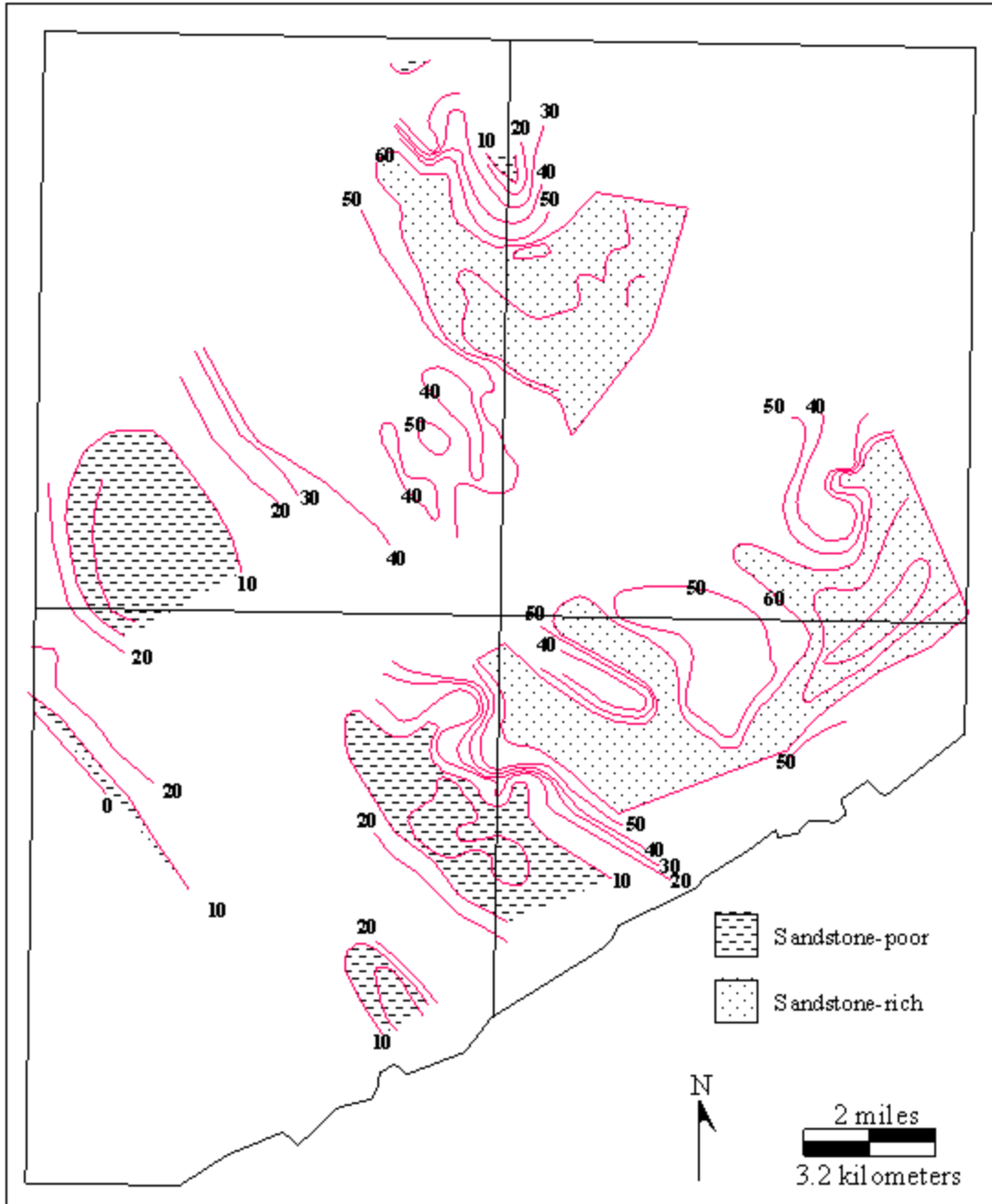
**Appendix 4.2.2:** Comparison of sandstone-rich areas between the Lower Elkhorn Lower/Lower Elkhorn rider to Lower Elkhorn rider/Upper Elkhorn No. 2 intervals.



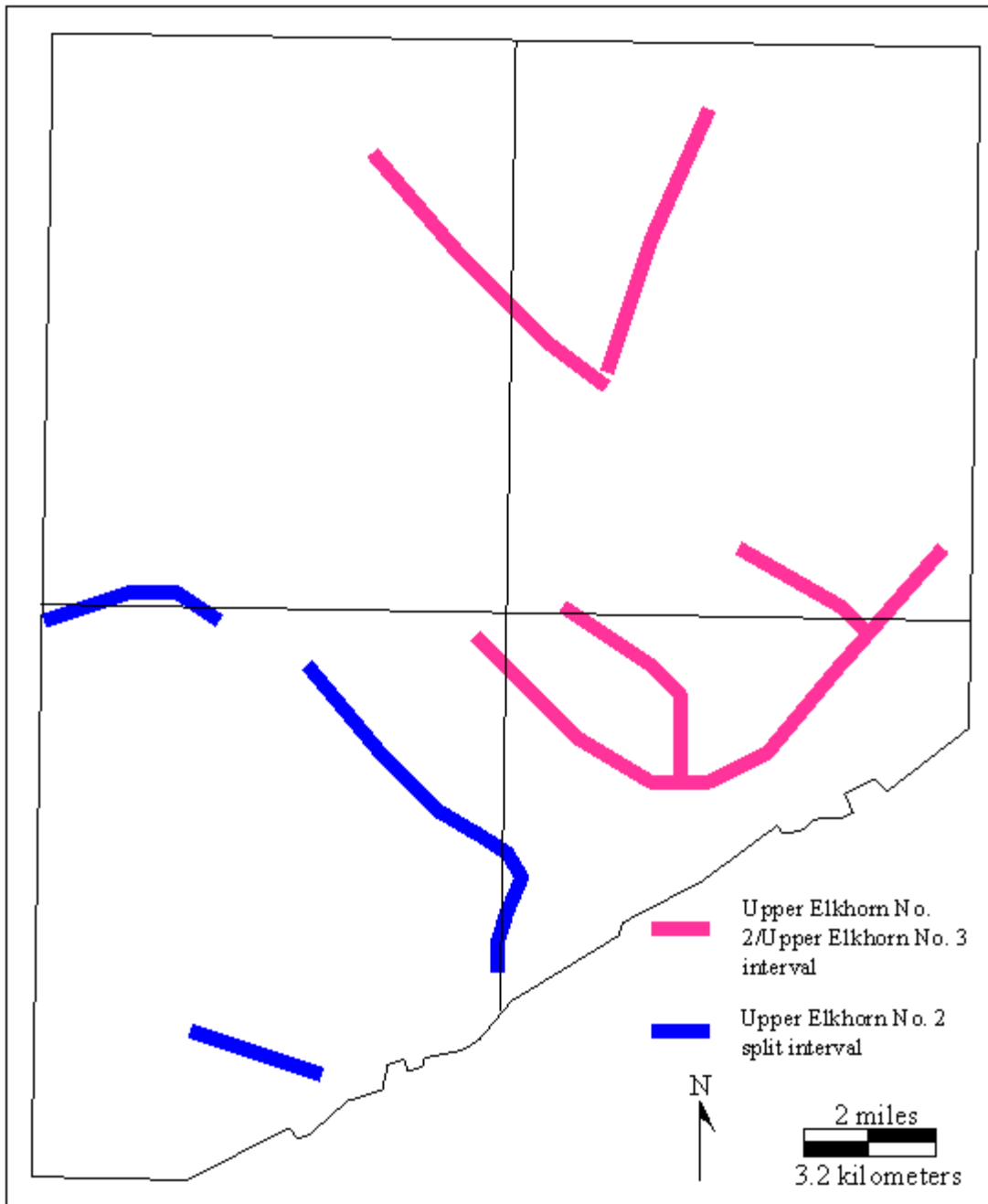
**Appendix 4.2.3:** Total sandstone thickness isolith map for the Upper Elkhorn No. 2 split interval. Contour interval is 10 feet (3 m).



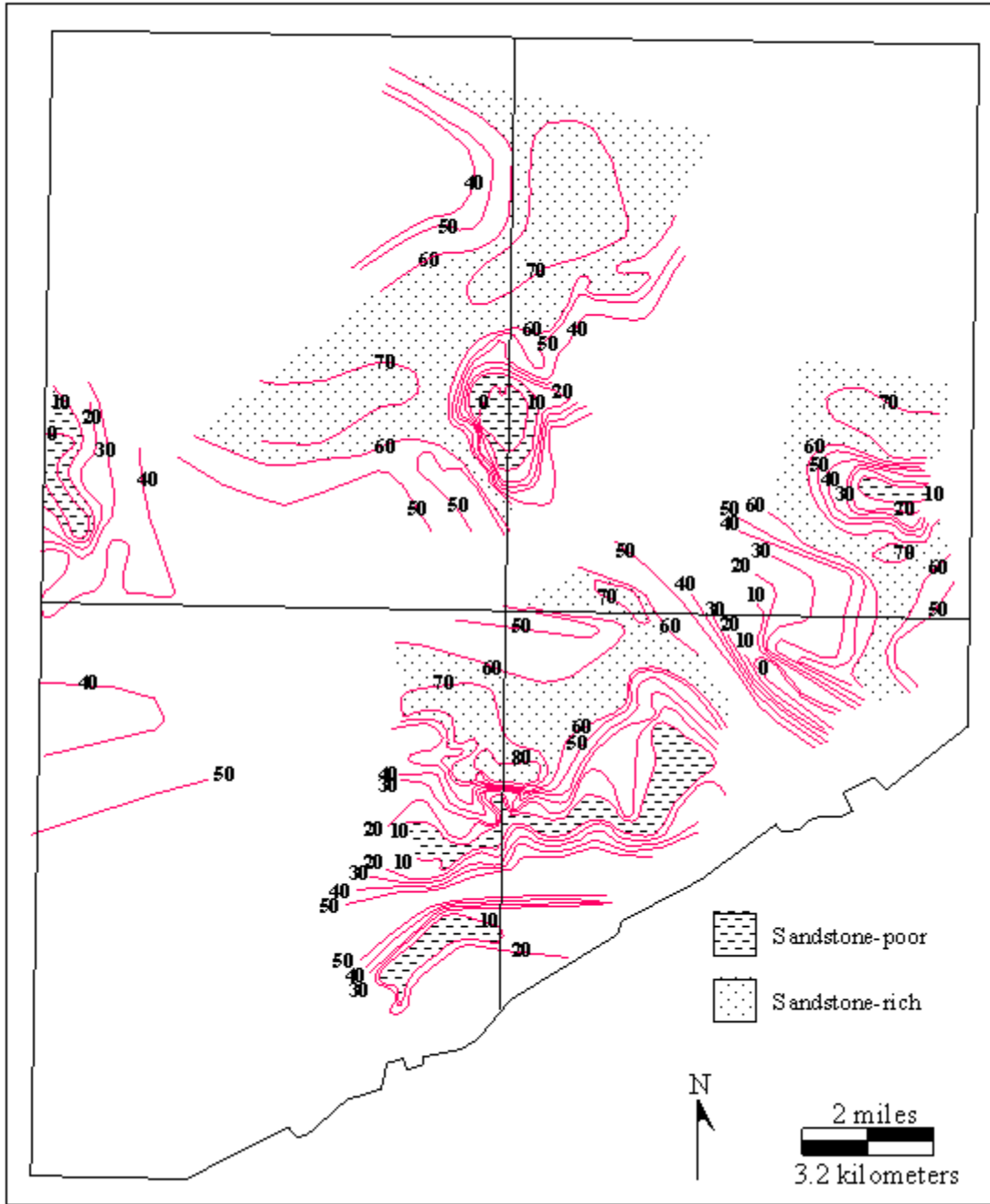
**Appendix 4.2.4:** Comparison of sandstone-rich areas between the Lower Elkhorn rider/Upper Elkhorn No. 2 and Upper Elkhorn No. 2 split intervals.



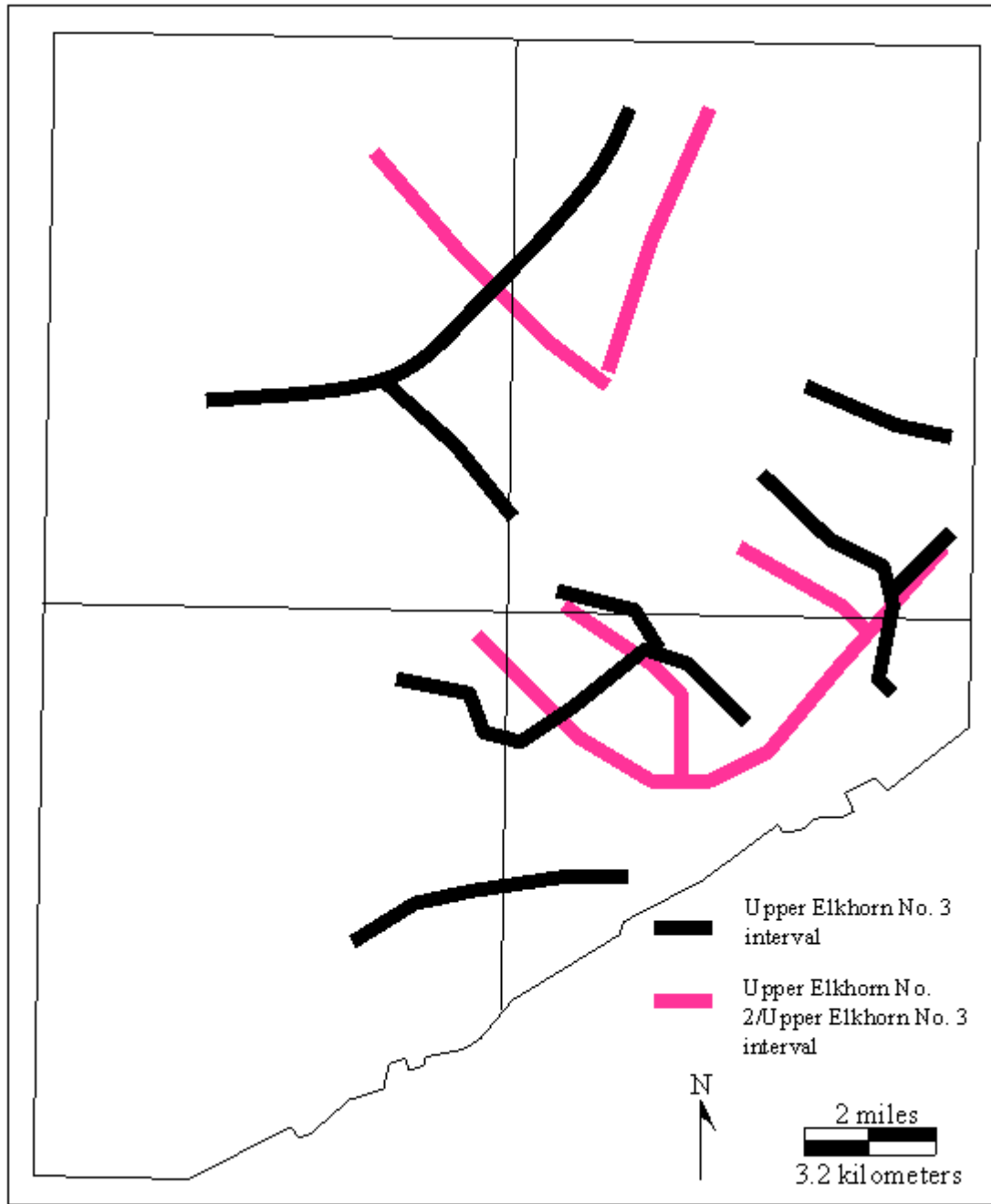
**Appendix 4.2.5:** Total sandstone thickness isolith map for the Upper Elkhorn No. 2/Upper Elkhorn No. 3 interval. Contour interval is 10 feet (3 m).



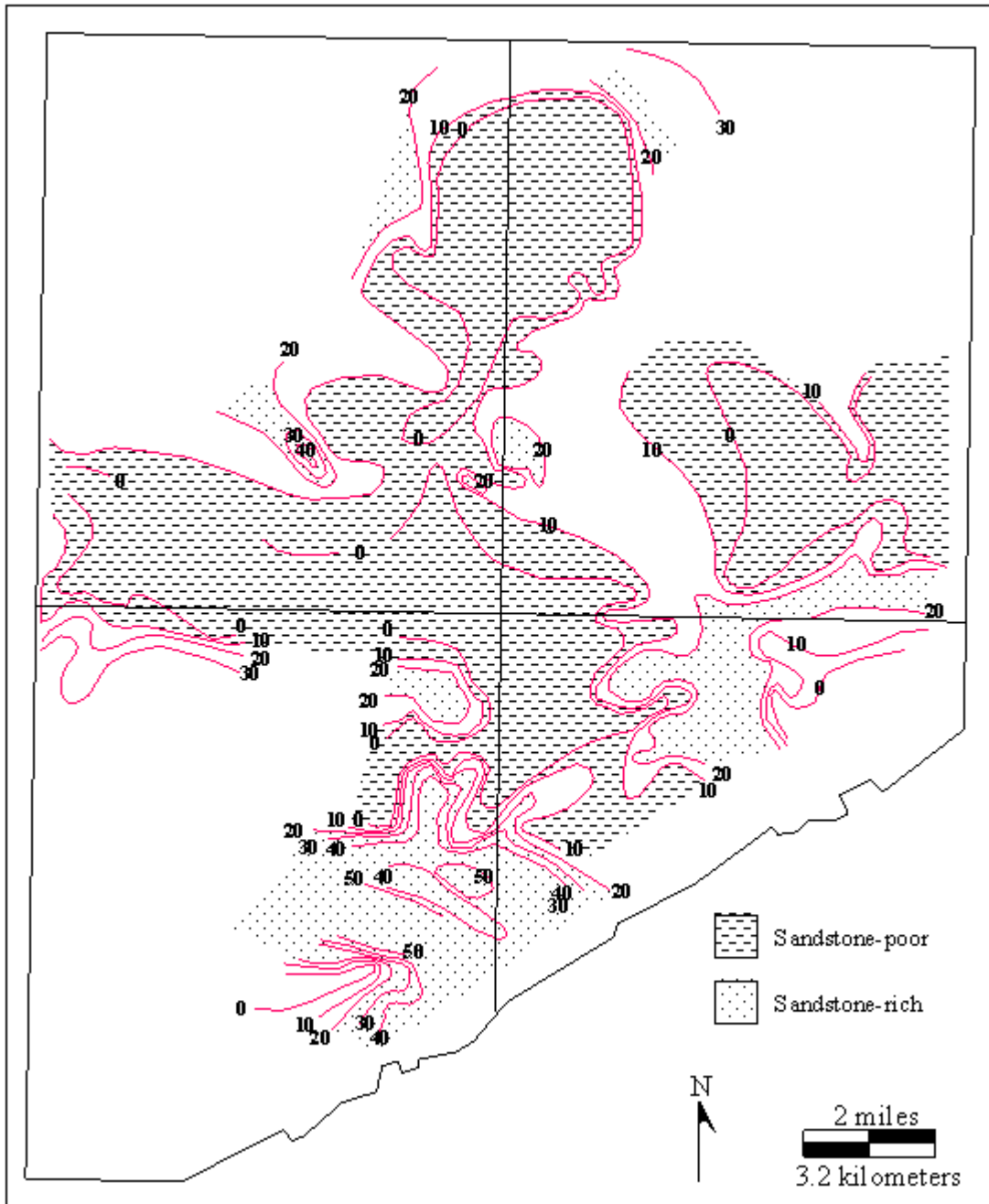
**Appendix 4.2.6:** Comparison of sandstone-rich areas between the Upper Elkhorn No. 2 split and Upper Elkhorn No. 2/Upper Elkhorn No. 3 intervals.



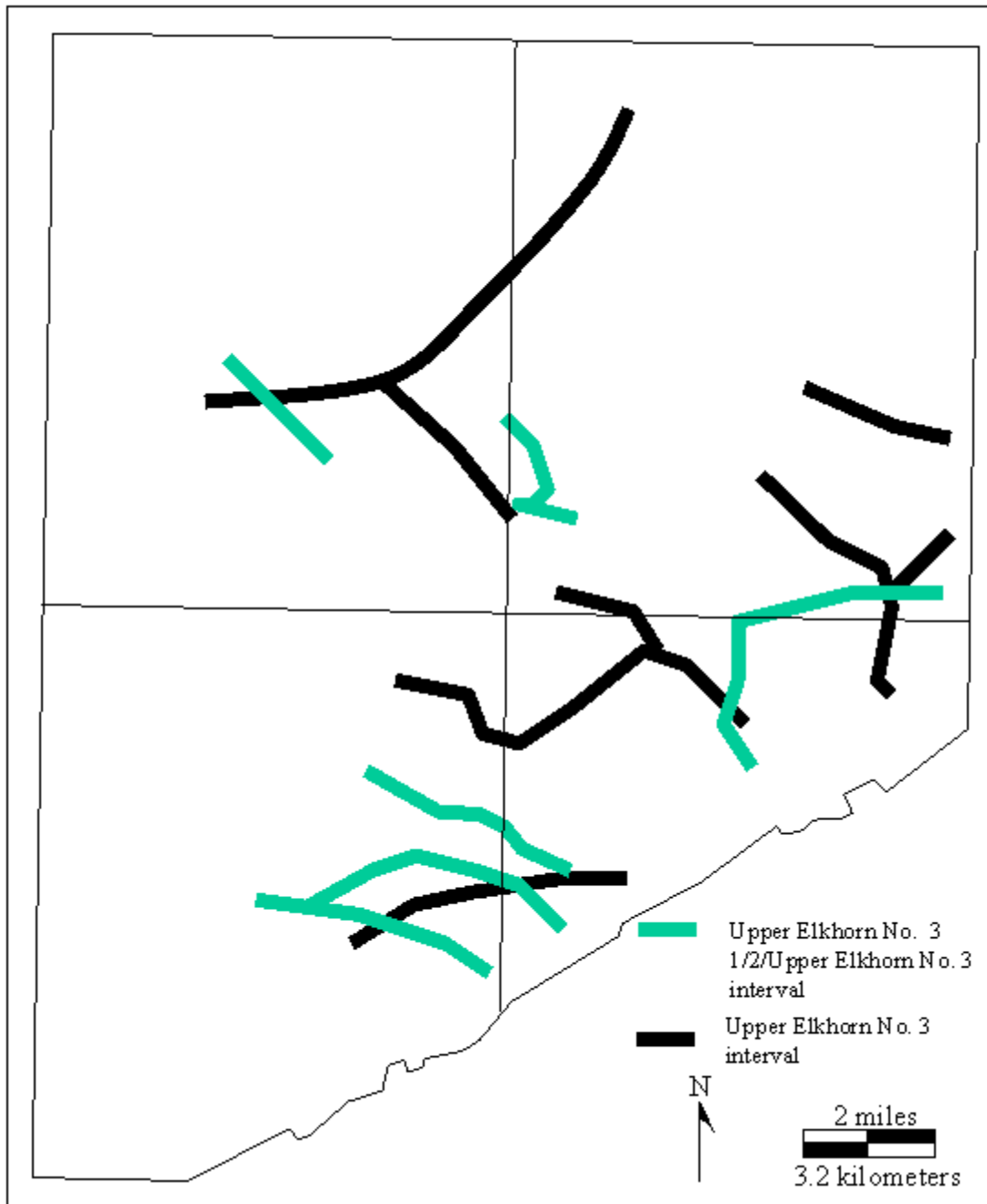
**Appendix 4.2.7:** Total sandstone thickness isolith map for the Upper Elkhorn No. 3 zone. Contour interval is 10 feet (3 m).



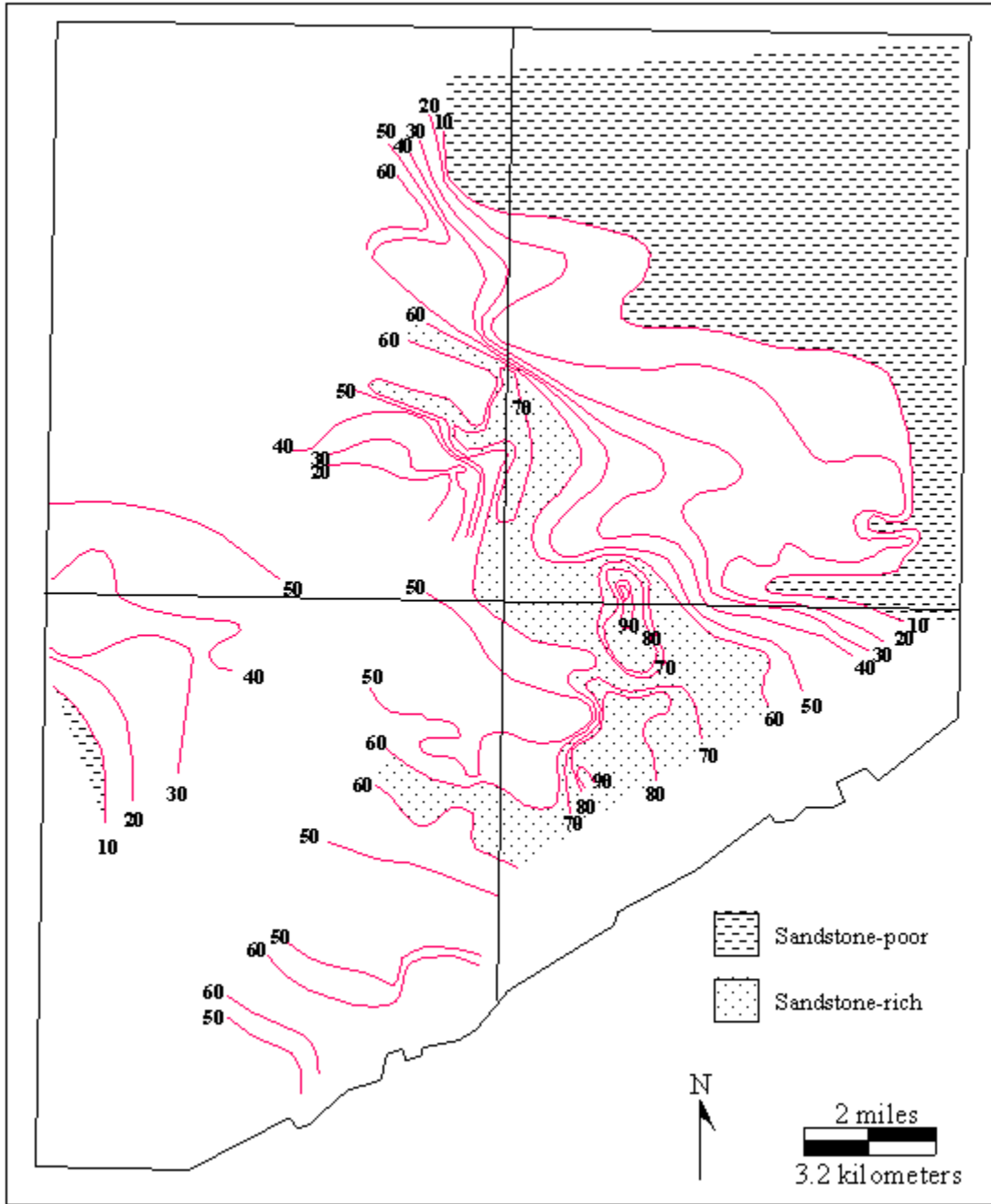
**Appendix 4.2.8:** Comparison of sandstone-rich areas between the Upper Elkhorn No. 2/Upper Elkhorn No. 3 and Upper Elkhorn No. 3 intervals.



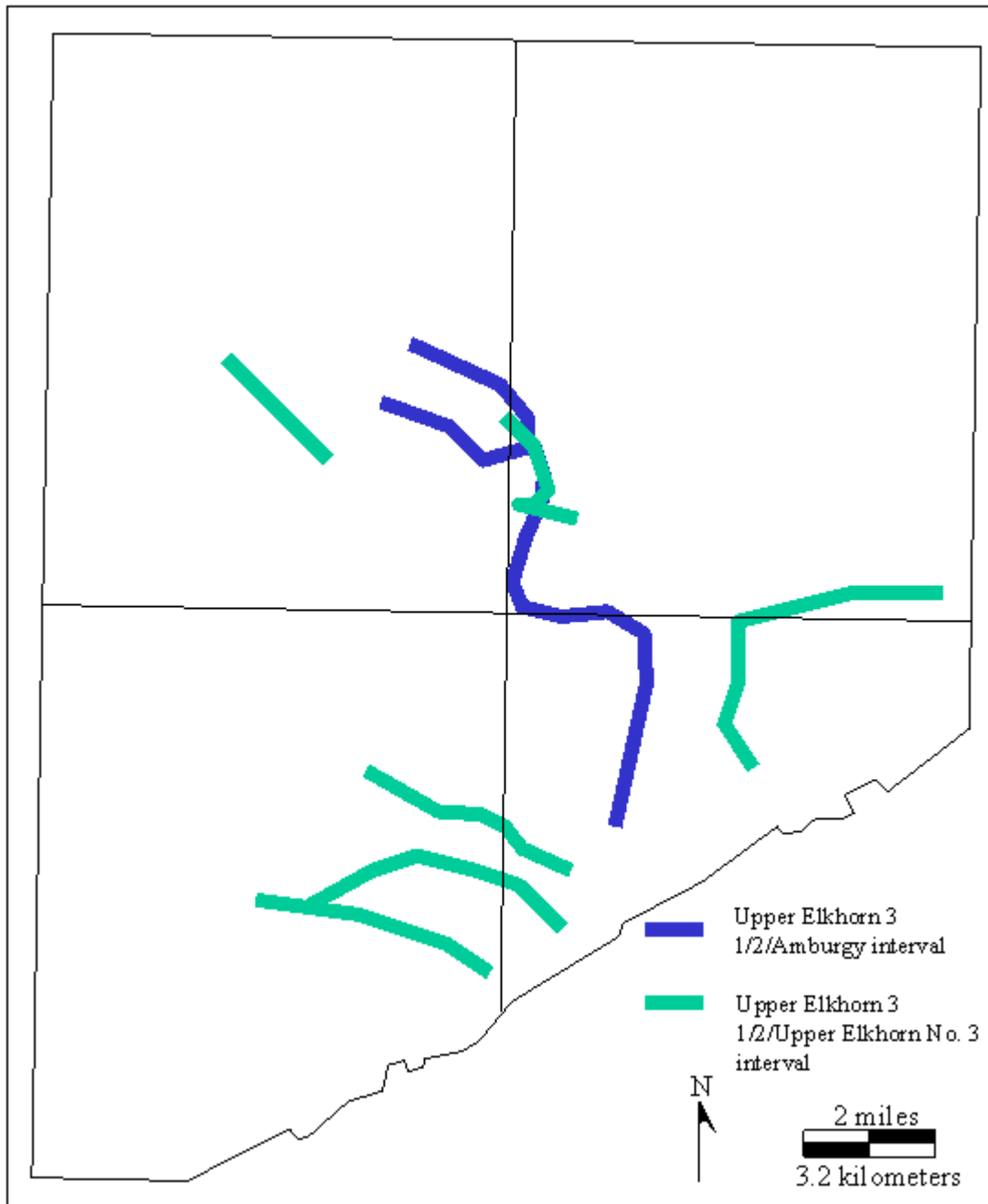
**Appendix 4.2.9:** Total sandstone thickness isolith map for the Upper Elkhorn No. 3/Upper Elkhorn No. 3 ½ interval. Contour interval is 10 feet (3 m).



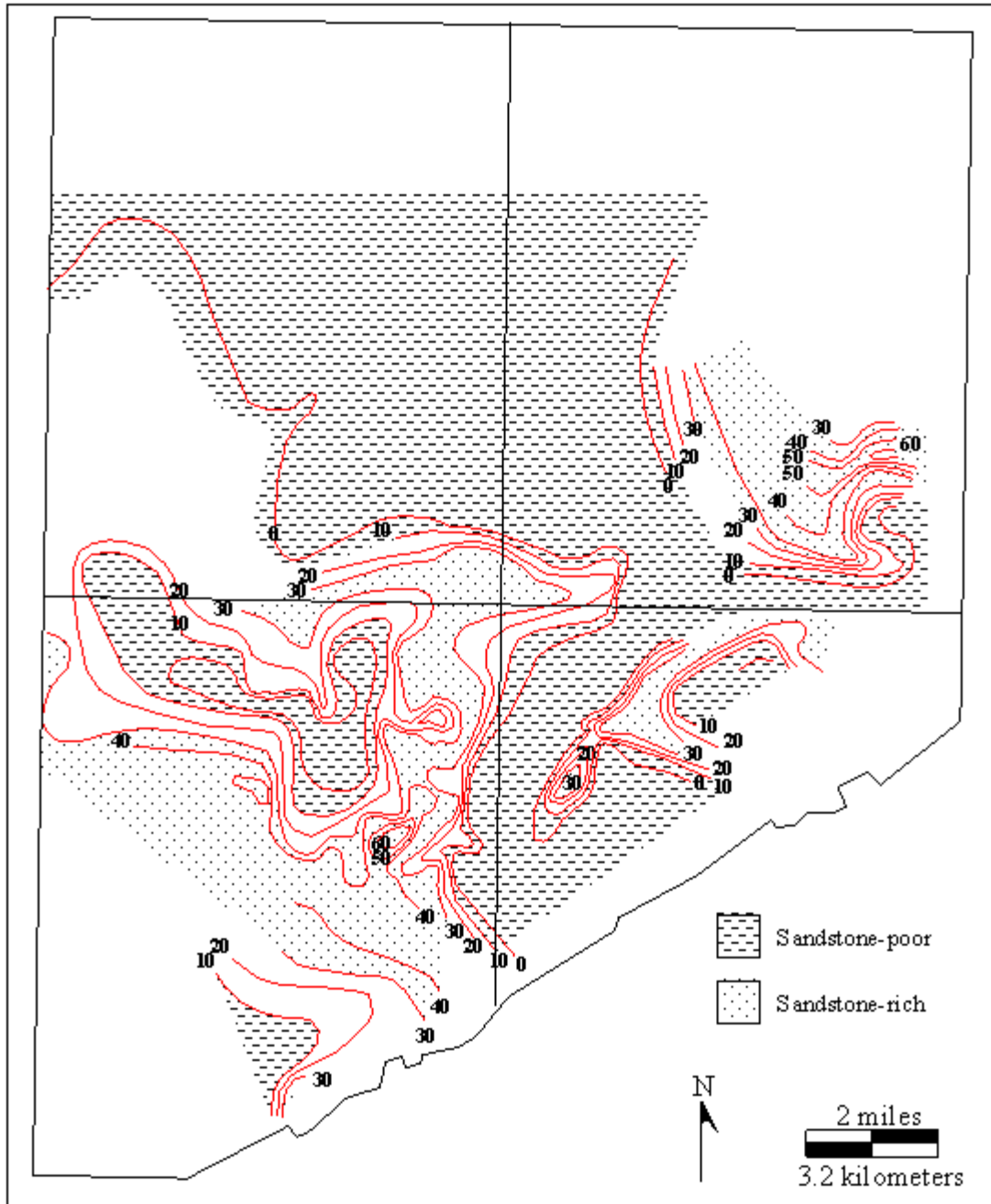
**Appendix 4.2.10:** Comparison of sandstone-rich areas between the Upper Elkhorn No. 3 zone and Upper Elkhorn No. 3/Upper Elkhorn 3 ½ intervals.



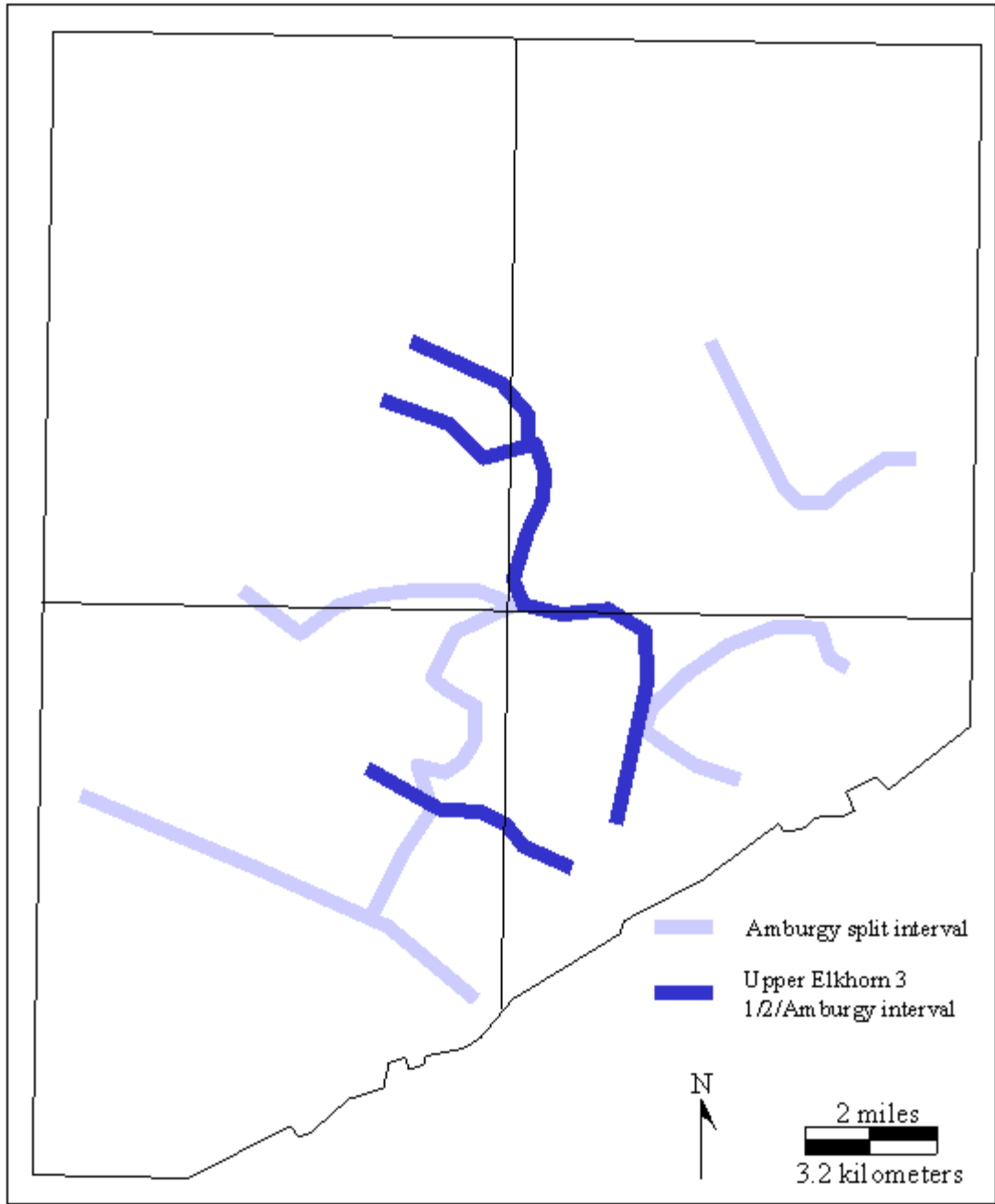
**Appendix 4.2.11:** Total sandstone thickness isolith map for the Upper Elkhorn No. 3 1/2/Amburgy interval. Contour interval is 10 feet (3 m).



**Appendix 4.2.12:** Comparison of sandstone-rich areas between the Upper Elkhorn No. 3/Upper Elkhorn 3 ½ and Upper Elkhorn 3 ½/Amburgy intervals.

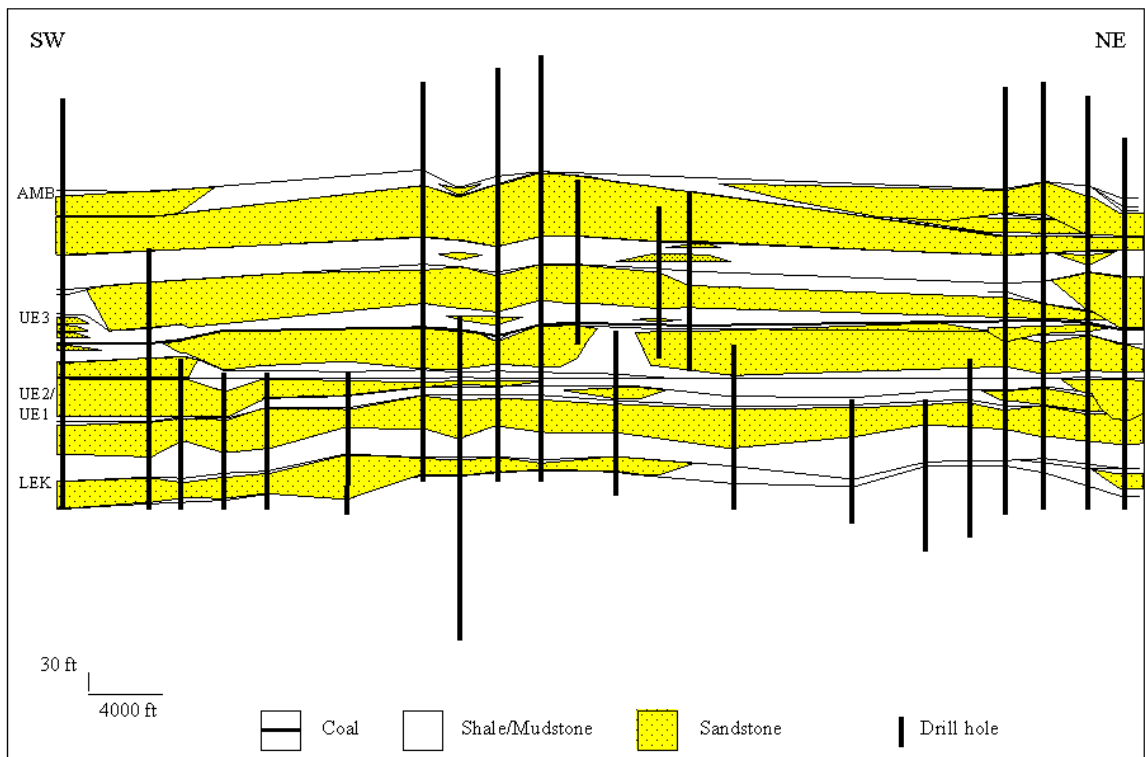


**Appendix 4.2.13:** Total sandstone thickness isolith for the Amburgy split interval. Contour interval is 10 feet (3 m).

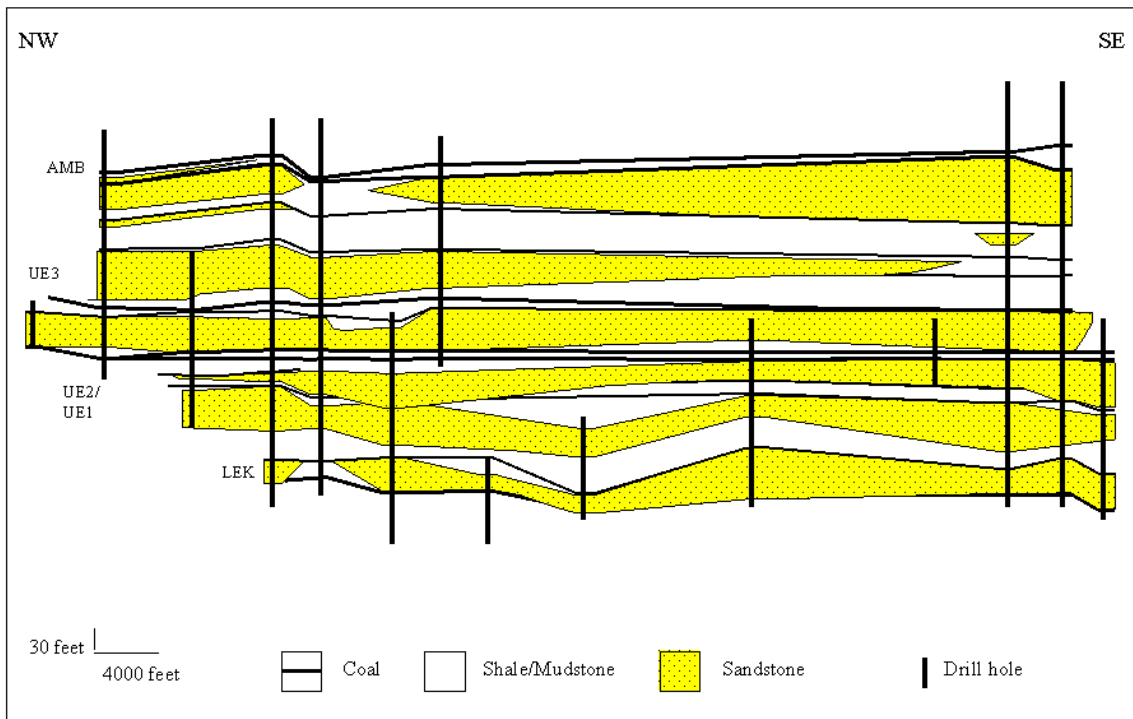


**Appendix 4.2.14:** Comparison of sandstone-rich areas between the Upper Elkhorn 3 1/2/Amburgy and Amburgy split intervals.

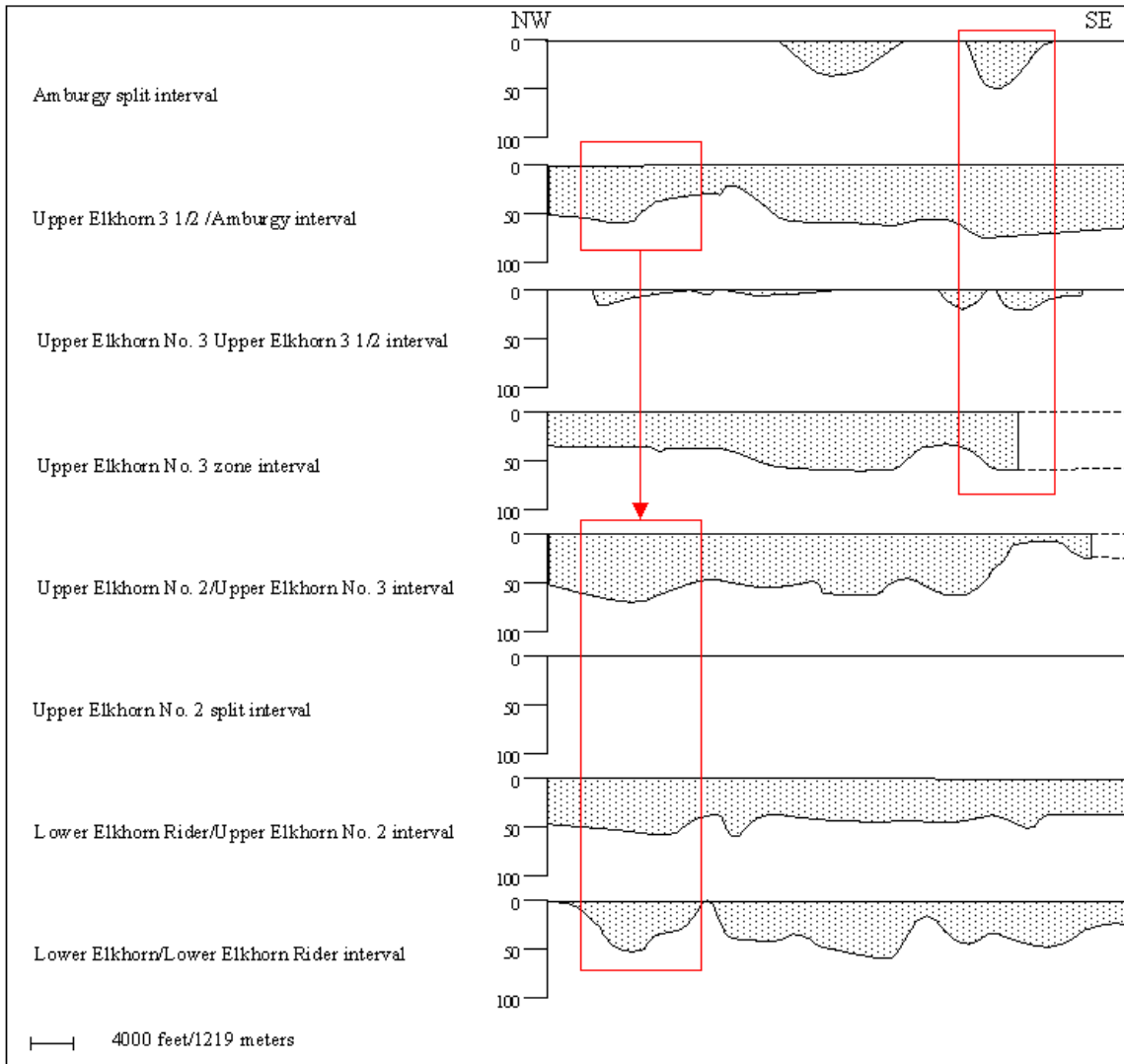
**Appendix 4.3: Cross Sections and Isolith Profiles.**



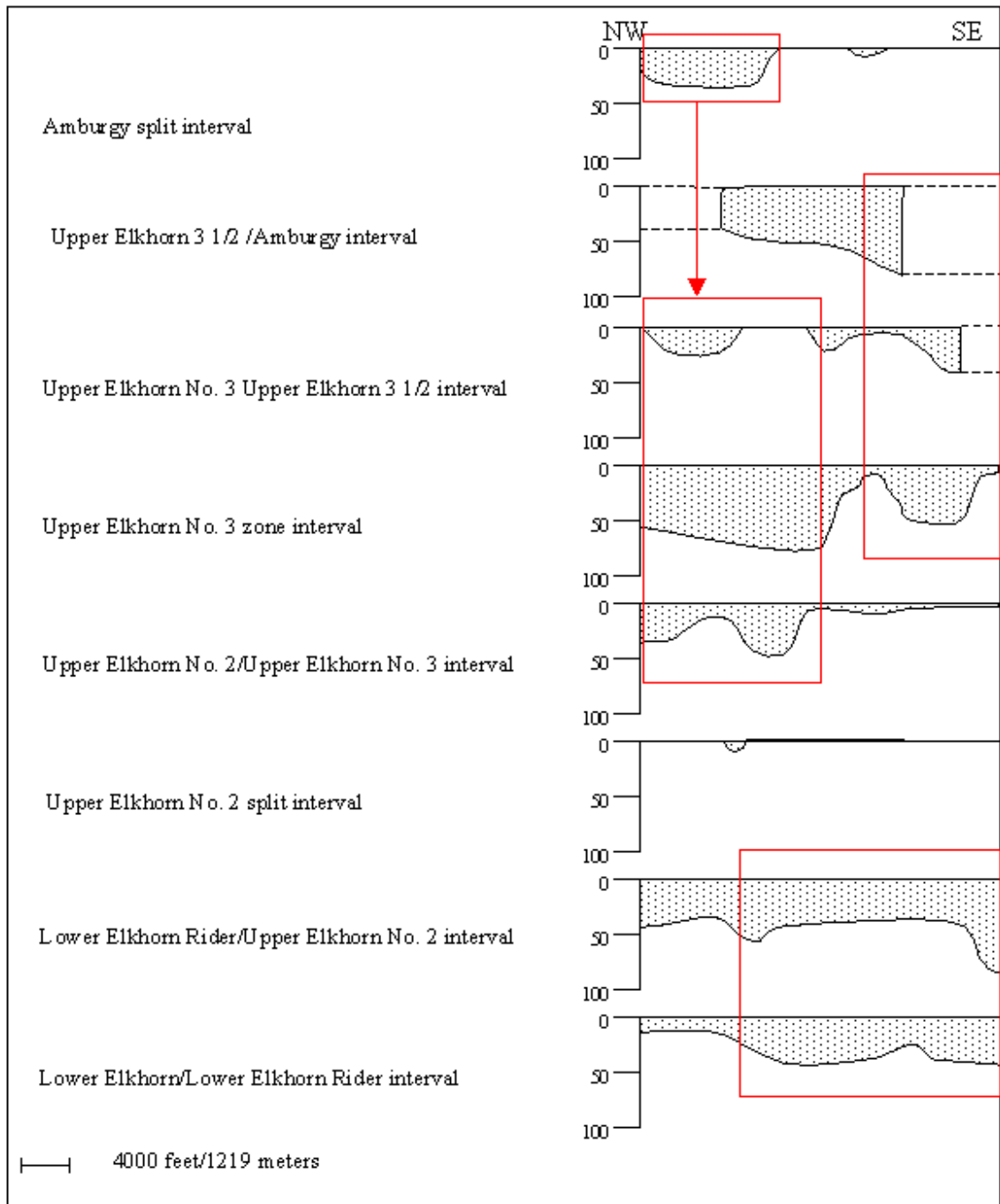
**Appendix 4.3.1:** Cross section A-A'. Location of cross section shown in Figure 4.12. Datum is the base of the Upper Elkhorn No. 2 coal.



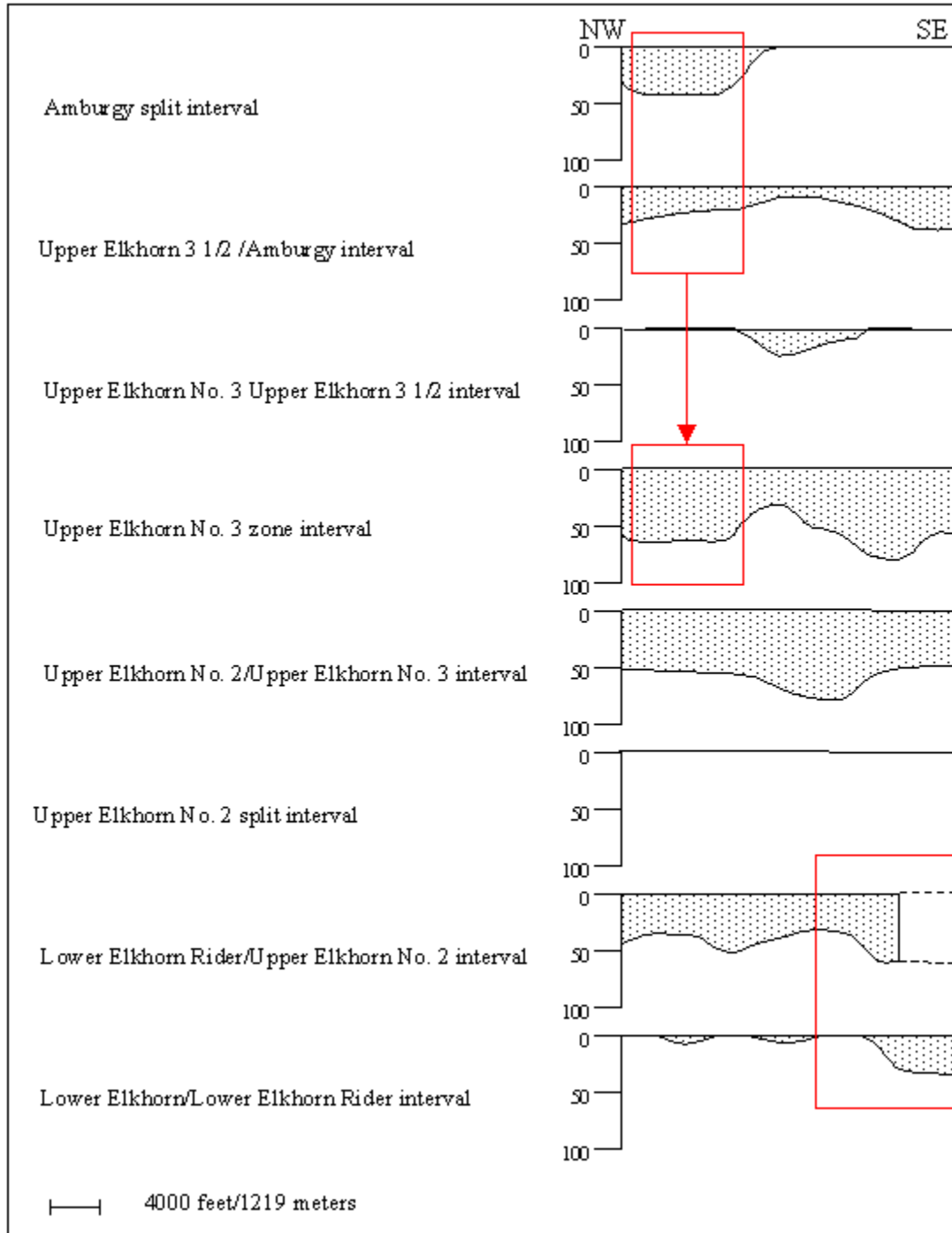
**Appendix 4.3.2:** Cross section B-B'. Location of cross section shown in Figure 4.12. Datum is the base of the Upper Elkhorn No. 2 coal.



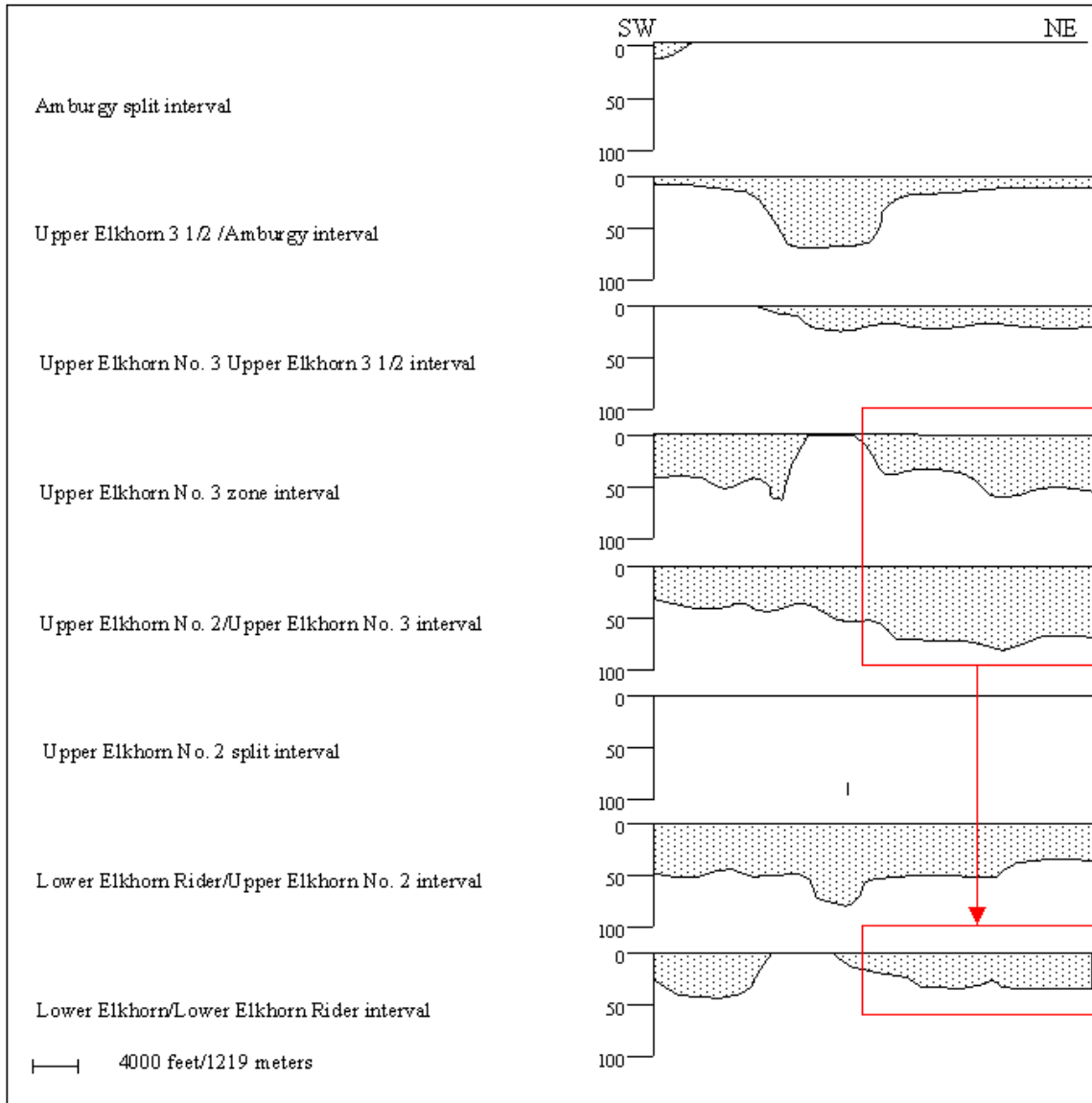
**Appendix 4.3.3:** Total sandstone thickness isolith profile B-B'. Northwest is to the left and southeast is to the right. Stacking relationships shown by the red boxes. Location of profile shown in Figure 4.12. Thickness values are in feet (e.g., 0 ft, 50 ft, 100 ft).



**Appendix 4.3.4:** Total sandstone thickness isolith profile C-C'. Northwest is to the left and southeast is to the right. Stacking relationships shown by the red boxes. Location of profile shown in Figure 4.12. Thickness values are in feet (e.g., 0 ft, 50 ft, 100 ft).



**Appendix 4.3.5:** Total sandstone thickness isolith profile D-D'. Northwest is to the left and southwest is to the right. Stacking relationships shown by the red boxes. Location of profile shown in Figure 4.12. Thickness values are in feet (e.g., 0 ft, 50 ft, 100 ft).



**Appendix 4.3.6:** Total sandstone thickness isolith profile E-E'. Southwest is to the left and northeast is to the right. Stacking relationships shown by the red boxes. Location of profile shown in Figure 4.12. Thickness values are in feet (e.g., 0 ft, 50 ft, 100 ft).

## References:

- Aitken, J.F., and Flint, S.S., 1994, High-frequency sequences and the nature of incised-valley fills in fluvial systems of the Breathitt Group (Pennsylvanian), Appalachian foreland basin, eastern Kentucky, *in* Dalrymple, R.W., Boyd, R., and Zaitlin, B.A., *Incised-valley systems; origin and sedimentary sequences*: SEPM Special Publication 51, p. 353–368.
- Aitken, J.F., and Flint, S.S., 1995, The application of high-resolution sequence stratigraphy to fluvial systems: A case study from the upper Carboniferous Breathitt Group, eastern Kentucky, U.S.A.: *Sedimentology*, v. 42, p. 3–30.
- Andrews, W.M., Hower, J.C., Ferm, J.C., Evans, S.D., Sirek, N.S., Warrell, M., and Eble, C.F., 1996, A depositional model for the Taylor coal bed, Martin and Johnson Counties, eastern Kentucky: *International Journal of Coal Geology*, v. 31, p. 151–167.
- Bradley, D.C., Kidd, W.S.F., 1991, Flexural extension of the upper continental crust in collisional foredeeps: *Geological Society of America Bulletin*, v. 103, p. 1416–1438.
- Carver, R.E., 1968, Differential compaction as a cause of regional contemporaneous faults: *American Association of Petroleum Geologists Bulletin*, v. 52, no. 3, p. 414–419.
- Chesnut, D.R., Jr., 1992, Stratigraphic and structural framework of the Carboniferous rocks of the Central Appalachian Basin in Kentucky: *Kentucky Geological Survey*, ser. 11, Bulletin 3, 42 p.
- Cloos, E., 1968, Experimental analysis of Gulf Coast fracture patterns: *American Association of Petroleum Geologists Bulletin*, v. 52, no. 3, p. 420–444.
- Cornett, G.C., 2002, Penecontemporaneous faulting within the Pennsylvanian Pikeville to Four Corners Formations, Breathitt Group, southeastern Kentucky: Unpublished M.S. thesis, University of Kentucky, Lexington, Ky., 244 p.
- Davis, M.W., and Ehrlich, R., 1974, Late Paleozoic crustal composition and dynamics in the southeastern United States, *in* Briggs, G., ed., *Carboniferous of the southeastern United States*: *Geological Society of America Special Paper* 148, p. 171–185.
- Drahovzal, J.A., and Noger, M.C., 1995, Preliminary map of the structure of the Precambrian surface in eastern Kentucky: *Kentucky Geological Survey*, ser. 11, Map and Chart 8, 9 p. plus 1 sheet.

- Ferm, J.C., 1974, Carboniferous paleogeography and continental drift: Seventh International Congress of Stratigraphy and Geology of the Carboniferous, Krefeld, *Compte Rendus*, p. 9–25.
- Ferm, J.C., and Cavaroc, V.V., 1979, A nonmarine sedimentary model for the Allegheny rocks of West Virginia, *in* Klein, G., and deVires, eds., Late Paleozoic and Mesozoic continental sedimentation, northeastern North America: Geological Society of America Special Paper 106, p. 1–19.
- Golden Software Inc., 2002, Surfer 8 user's guide: Golden, Colo., 619 p.
- Greb, S.F., 1991, Roof falls and hazard prediction in eastern Kentucky coal mines, *in* Peters, D.C., ed., Geology in coal resource utilization: American Association of Petroleum Geologists, Energy Minerals Division. Techbooks Publishing, Fairfax, Va., p. 189–201.
- Greb, S.F., and Weisenfluh, G.A., 1996, Paleoslumps in coal-bearing strata of the Breathitt Group (Pennsylvanian), Eastern Kentucky Coal Field, U.S.A.: *International Journal of Coal Geology*, v. 31, p. 115–134.
- Greb, S.F., Eble, C.F., and Hower, J.C., 1999a, Depositional history of the Fire Clay coal bed (Late Duckmantian), eastern Kentucky, U.S.A: *International Journal of Coal Geology* v. 40, p. 255–280.
- Greb, S.F., Hiatt, J.K., Weisenfluh, G.A., Andrews, R.E., and Sergeant, R.E., 1999b, Geology of the Fire Clay coal in part of the Eastern Kentucky Coal Field: Kentucky Geological Survey, ser. 12, Report of Investigations 2, 37 p.
- Greb, S.F., and Popp, J.T., 1999, Mining geology of the Pond Creek seam, Pikeville Formation, Middle Pennsylvanian, in part of the Eastern Kentucky Coal Field, U.S.A.: *International Journal of Coal Geology*, v. 41, p. 25–50.
- Greb, S.F., Eble, C.F., Williams, D.A., and Nelson, W.J., 2001, Dips, ramps and rolls—Evidence for paleotopographic and syn-depositional control on the Western Kentucky No. 4 coal bed, Tradewater Formation (Bolsovian), Illinois Basin: *International Journal of Coal Geology*, v. 45, p. 227–246.
- Hardin , F.R., and Hardin, G.C., 1961, Contemporaneous normal faults of Gulf Coast and their relation to flexures: *American Association of Petroleum Geologists Bulletin*, v. 45, p. 238–248.
- Hook, R.W., and Ferm, J.C., 1988, Paleoenvironmental controls on vertebrate-bearing abandoned channels in the upper Carboniferous: *Palaeogeography, Palaeoclimatology, Palaeoecology*, v. 63, p 159–181.

- Horne, J.C., Ferm, J.C., Caruccio, F.T., and Baganz, B.P., 1978, Depositional models in coal exploration and mine planning in the Appalachian region: American Association of Petroleum Geologists Bulletin, v. 62, p. 2379–2411.
- Horne, J.C., 1976 Sedimentary responses to contemporaneous tectonism, *in* Ferm, J.C., and Horne, J.C., eds., Carboniferous depositional environments in the Appalachian region: University of South Carolina Department of Geology, Carolina Coal Group, Columbia, S.C., United States p. 259–265.
- Houseknecht, D.W., 1986, Evolution from passive margin to foreland basin: The Atoka Formation of the Arkoma Basin, south-central U.S.A.: Special Publication of the International Association of Sedimentologists, v. 8, p. 327–345.
- Hower, J.C., Pollock, J.D., and Griswold, T.B., 1991, Structural controls on the petrology and geochemistry of the Pond Creek coal seam, Pike and Martin Counties, eastern Kentucky, *in* Peters, D.C., ed., Geology in coal resource utilization: American Association of Petroleum Geologists, Energy Minerals Division, Techbooks Publishing, Fairfax, Va., p. 413–425.
- Liu, Y., 1992, A quantitative analysis of vertical and horizontal lithic variation in some coal-bearing rocks in southeastern Kentucky: Unpublished M.S. thesis, University of Kentucky, Lexington, Ky., 381 p.
- Miall, A. D., 1992, Alluvial deposits, *in* Walker, R.G., and James, N.P., eds., Facies models, response to sea level change: Geological Association of Canada, p. 119–142.
- Raione, R.P., Hower, J.C., and Wild, G.D., 1991, Influence of regional structure on the development and quality of the Upper Elkhorn No. 2 coal bed, eastern Kentucky: International Journal of Coal Geology, v. 18, p. 305–325.
- Root, S.I., and MacWilliams, R.H., 1986, The Suffield Fault, Stark County, Ohio: Ohio Journal of Science, v. 86, no. 4, p. 161–163.
- Shelton, J.W., 1968, Role of contemporaneous faulting during basinal subsidence: American Association of Petroleum Geologists Bulletin, v. 52, no. 3, p. 399–413.
- Swan, A.R.H., and Sandilands, M., 1995, Introduction to geological data analysis: Oxford, Blackwell, 446 p.
- Thomas, W.A., 1968, Contemporaneous normal faults on flanks of Birmingham Anticlinorium, central Alabama: American Association of Petroleum Geologists Bulletin, v. 52, no. 11, p. 2123–2136.

Weisenfluh, G.A., 1982, Controls on deposition of the Pratt seam, Black Warrior Basin, Alabama: Unpublished Ph.D. dissertation, University of South Carolina, Columbia, S.C., 75 p.

Weisenfluh, G.A., and Ferm, J.C., 1991a, Application of depositional models to mining problems, in Peters, D.C., Ed., *Geology in coal utilization*: American Association of Petroleum Geologists, Energy Minerals Division. Techbooks Publishing, Fairfax, Va., p. 189–201.

Weisenfluh, G.A., and Ferm, J.C., 1991b, Roof control in the Fireclay Coal Group, southeastern Kentucky: *Journal of Coal Quality*, v. 10, no. 3, p. 67–74.

Weisenfluh, G.A., and Ferm, J.C., 1998, Kentucky's coal industry: Historical trends and future opportunities: Kentucky Geological Survey, ser. 11, *Information Circular* 59, 9 p.

## VITA

Michael Garry Shultz was born on August 21, 1978, in Steubenville, Ohio. In November of 2000, he received his Bachelor of Science with departmental honor, majoring in geology, at Ohio University in Athens, Ohio. During the course of his studies at Ohio University, and upon graduation, he worked as a geologist for the East Fairfield Coal Company.

Michael Garry Shultz

4-28-03